New molecular insights into sperm epigenetics: Regulation of LINE-1 elements by CpG methylation and histone-modifications, and its impacts on sperm quality

Inaugural Dissertation

submitted to the

Faculty of Medicine

in fulfillment of the requirements

for the PhD-Degree

of the Faculties of Veterinary Medicine and Medicine

of the Justus Liebig University Giessen

by

Gies, Sabrina Elisabeth

of

Frankfurt am Main

Giessen (2019)

From the Department of Urology, Pediatric Urology and Andrology

Working group “Epigenetics of the Urogenital System”

Head of the working group: Prof. Dr. rer. nat. Undraga Schagdarsurengin

of the Faculty of Medicine of the Justus Liebig University Giessen

First Supervisor and Committee Member:

Prof. Dr. rer. nat. Undraga Schagdarsurengin

Second Supervisor and Committee Member:

Prof. Dr. med. vet. Christine Wrenzycki

Committee Members:

Prof. Dr. med. Thomas Haaf

Date of Doctoral Defense:

November 5th, 2019

Table of contents

1. Introduction

According to the World Health Organisation (WHO), up to 15 % of couples worldwide are infertile.[1] This means these couples are unable to achieve within one year a pregnancy on a natural way without prevention. The reasons for infertility can be detected in similar parts either on the male or female side (30 %, respectively). But also, reasons on both sides of a couple can accumulate to infertility (25 %). For the remaining 15 % of the couples no reason for their infertility can be found.[2] This is referred to as unexplained or idiopathic infertility.

1.1 Male infertility and possible treatments for couples

Male infertility affects around 7 %[3] of all men and is mainly induced by varicocele (17 %), hypogonadism (10 %) or urogenital infections (9 %).[4] More causes of male infertility are illustrated in Figure 1. Very eye-catching is that for approximately one third of the cases the reason for male infertility remains unexplained (idiopathic) and is therefore challenging to treat. Associated reproductive technologies (ART), like intrauterine insemination (IUI), intracyto-plasmic sperm injection (ICSI) or in vitro fertilization (IVF) can help couples to overcome their infertility. In the first case a prepared sperm sample from the male partner is transferred to the uterus of the female partner on the day of ovulation to enable pregnancy. The other two cases are mainly performed in an embryological laboratory, where an egg is either incubated with a prepared sperm sample (IVF) or directly fertilized with a single sperm (ICSI). Afterwards an embryo transfer (ET) of one or more embryos to the uterus of the hormone-pretreated woman is done to initiate pregnancy. Fertilization and life birth rates are not as high as desired and cause additional emotional stress on the couples besides the financial pressure of the costly ART treatments (2000-8000€).[4] In Germany, ICSI is the most commonly used ART to treat severe male infertility (75 %)[5] and its fertilization rates are between 50 % and 80 %.[6,7]According to the German IVF Registry (DIR) live birth rates with IVF or ICSI are ranging from 30.4 to 31.3 % in young women (age 25-29 years) and decrease to 15.1-14.0 % in older women (age ≥ 40 years).[8] So, there is a need to reveal and treat the infertility causes not

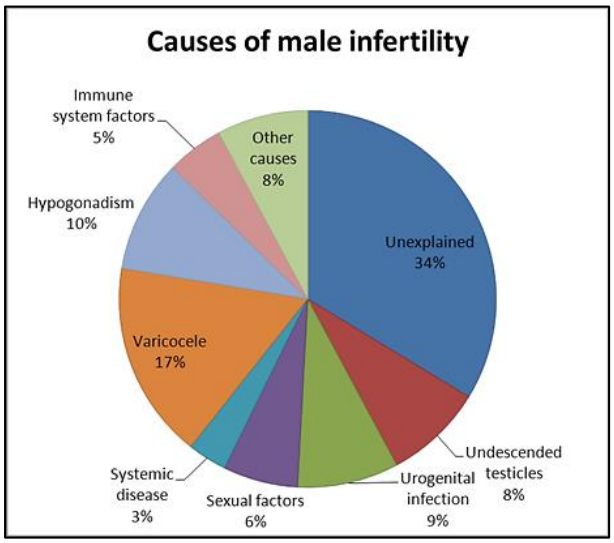

Figure 1: Causes of male infertility.[4]

only on the male but also on the female side to increase baby-take-home-rates. Many studies indicate that aberrations in the sperm epigenome can lead to male infertility, due to lifestyles and environmental exposures and can also impair offspring health.[9–11]

1.2 Spermatogenesis

Male fertility is ensured by the production of mature spermatozoa and starts with spermatogenesis. Spermatogenesis is a well-structured and continuous process (Figure 2), which starts in the young male at puberty, on the surface of somatic Sertoli cells within the germ epithelium of the seminiferous tubules. Because of the steady proliferation and differentiation steps, germ cells occur as different cell groups and migrate from the basement membrane to the luminal area. During this time, the germ cells go through three characteristic developmental phases. At first, the mitotic proliferation, a spermatogonium type A divides into type B through mitosis, whereby one cell persists as stem cell. Then a spermatogonium type B differentiates through several mitoses into one primary spermatocyte and doubles during that time its DNA content (2n). At the second developmental phase, the first meiotic division of a primary spermatocyte yields two secondary spermatocytes and these multiplicate during the second meiotic division into four round spermatids (1n). At the third developmental phase, spermiogenesis, the differentiation of four round spermatids into elongated spermatids takes place, in which the nuclear chromatin is condensed, the acrosome is formed, and the flagellum is developed. Finally, maturing spermatozoa are released into the lumen and further transported to the epididymis, where they acquire motility and become fertile.[12,13]

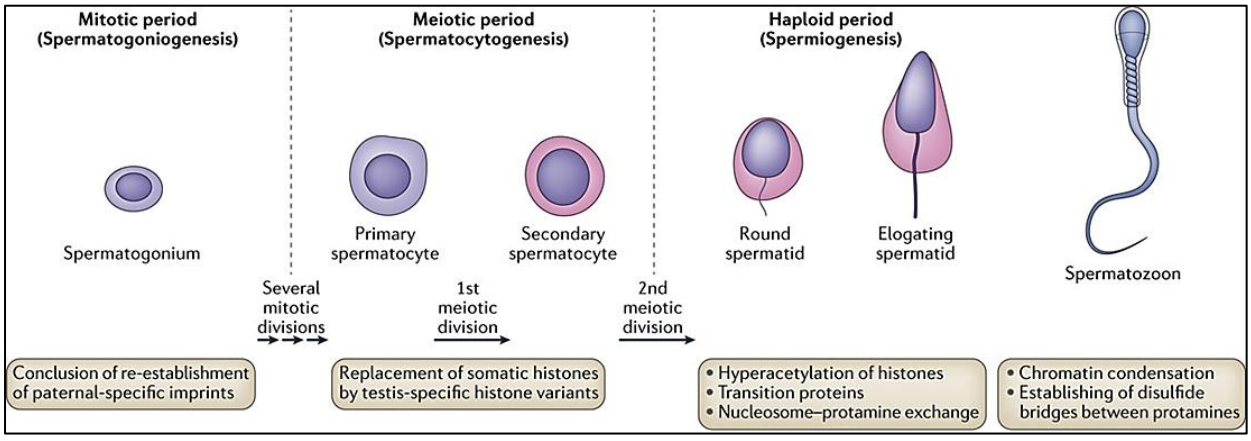

Figure 2: Spermatogenesis in human and epigenetic processes.[9]

The whole process of spermatogenesis in healthy men requires 64 days, with a new cycle starting every 16 days, plus a 2-week epididymal maturation period.[9,14] During all this time epigenetic processes have to be strictly regulated to ensure the production of feature complete spermatozoa, which are able to inseminate an egg cell and provide full development capacity. Therefore, it is necessary for males to monitor their environmental health at least two months earlier before they want to father a child.[15]

1.3 Components and modifiers of the sperm epigenome

The epigenome represents the total amount of all heritable epigenetic elements that determine the targeted expression of a gene and thus the development of a cell without modifying its DNA sequence.[15] Especially the components of the sperm epigenome (Figure 3), like the DNA methylation profile, non-coding RNAs and post-translational histone modifications (PHTMs) are highly vulnerable to alterations and must be precisely regulated to ensure male fertility.[16,17] As mentioned above, aberrations in the sperm epigenome, due to lifestyle (e. g. smoking, alcohol consume, diet or overweight) and environmental exposures, can harm offspring health and lead to male infertility.[9–11] In a meta-regression analysis was shown, that in the last 40 years (1973-2011) sperm concentration and total sperm count have declined over 50-60 % in human.[18] This decline may be due, for instance, to the susceptibility of the sperm epigenome to modifiers such as parabens in cosmetic products[19] or bisphenol A in drinking bottles[20], which both negatively affect male fertility by lowering testosterone levels and sperm production. In order to examine and identify aberrations in the sperm epigenome, an understanding of the chromatin structure is essential.

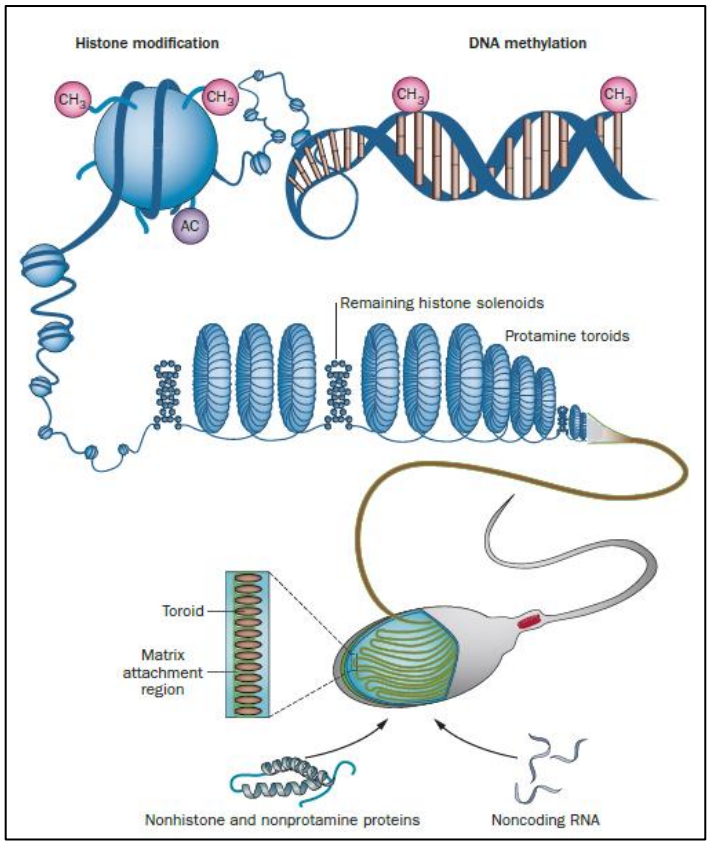

Figure 3: The components of the sperm epigenome.[17]

In somatic cells, DNA is packaged in so called nucleosomes in which about 147 bp of DNA is wrapped around a histone octamer, consisting of four core histones, with two copies of each (H2A, H2B, H3, and H4). During spermiogenesis, these histones are replaced by the roughly ten times smaller protamines in order to not only shut down transcription and protect the paternal DNA against harmful substances, but also to condense the sperm head and simplify its motility.[21]

1.3.1 DNA methylation: regulators and epigenetic reprogramming in human germ line

The best analyzed epigenetic modification, also in sperm cells, is the DNA methylation. DNA methylation (Fig. 4) takes place by the addition of a methyl group of S-adenosyl-1-methionine (SAM) to carbon five of a cytosine residue (5mC) at cytosine-phosphate-guanine dinucleotides (CpGs).[22] This process is mediated by DNA methyltransferases (DNMTs), namely DNMT1/2/3A/3B or 3L, and can be established in two different manners. After cell division hemi-methylated CpGs attract DNMT1, the maintenance methyltransferase, which methylates the newly replicated DNA strand. In contrast, DNMT3A and DNMT3B, *de novo* methyltransferases, can methylate completely unmethylated DNA on both strands during development.[23] DNMT2 methylates RNA instead of DNA and DNMT3L, which has no catalytic activity itself, assists the *de novo* methyltransferases by increasing their binding affinity to SAM.[23,24] DNA demethylation (Fig. 4) is initiated by Ten-Eleven Translocation (TET) enzymes 1-3, which demethylate stepwise 5mC into 5-hydroxylmethyl- (5hmC), 5-formyl- (5fC), and 5-carboxylcytosine (5caC). Finally unmodified cytosines are regenerated by thymine-DNA glycosylase (TDG) and base excision repair (BER) mechanisms.[11,25] DNMTs and TET proteins are shown to be expressed throughout human spermatogenesis, with stage specific levels. DNMTs are increasingly present in earlier stages of spermatogenesis, while TETs are more likely to be found in later stages.[25,26]

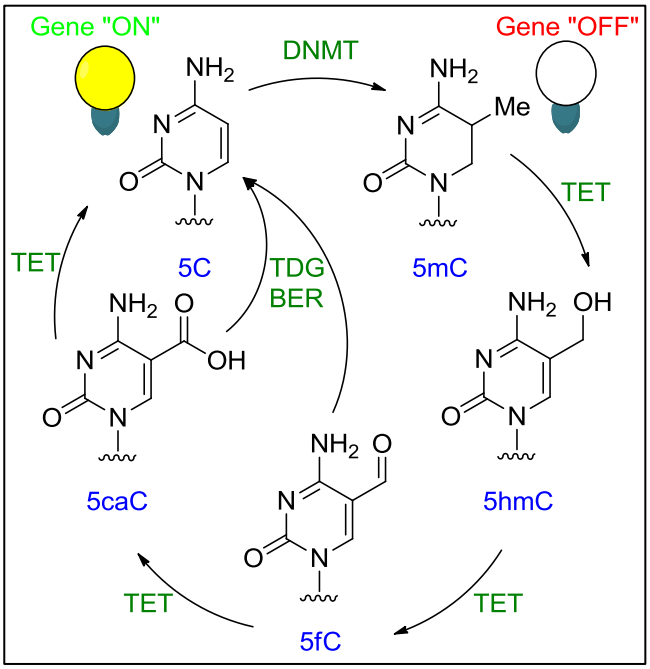

Figure 4: Methylation (Me) and demethylation cycle of a cytosine residue mediated by DNMT/TET enzymes and repair mechanisms (TDG/BER).

The establishment and regulation of DNA methylation patterns is essential for a normal cell function and plays distinct roles in transcriptional gene regulation, genomic imprinting, X-chromosome inactivation and embryonic development.[27,28]

Global DNA methylation levels in the human germline change dynamically in two waves to ensure correct embryonic development (Figure 5). The first wave of DNA demethylation starts shortly after fertilization, where the male genome is rapidly and actively demethylated, to generate a toti-potent zygote with full development capacity.[27] Then the maternal genome is passively and slower demethylated. Meanwhile the first wave methylation levels of imprinted genes are conserved, as these marks will be given to the next generation.[29] Reaching the stage of blastocyst implantation, DNA methylation patterns become re-established by *de novo* methyltransferases in a cell lineage-specific manner.

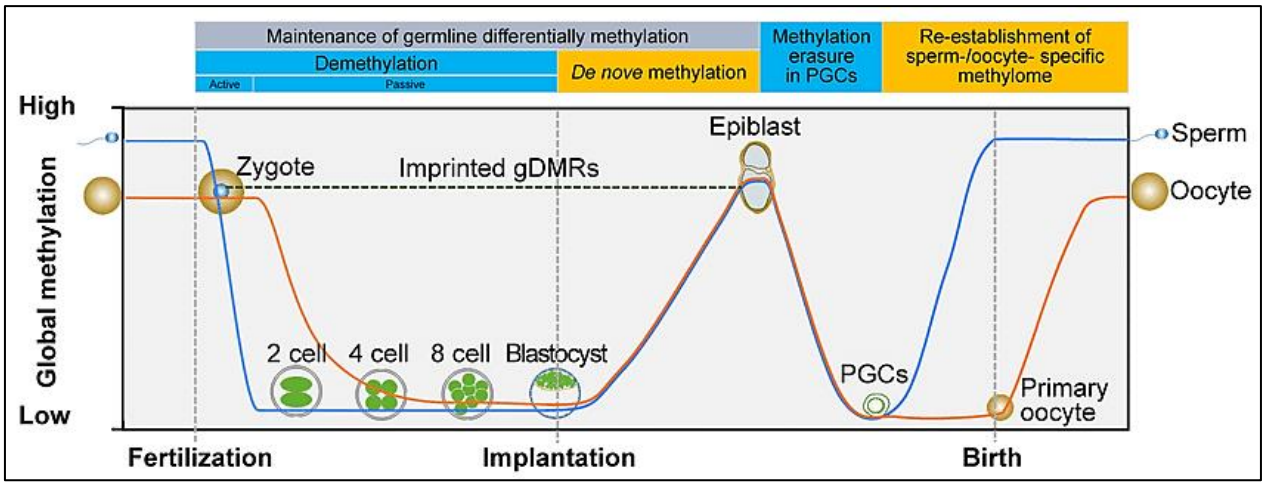

Figure 5: Epigenetic reprogramming of the global DNA methylation patterns in the human germ line.[29]

The second wave of demethylation occurs in primordial germ cells (PGCs), where also the methylation status of imprinted genes is erased. Afterwards sex-specific *de novo* methylation starts, where the sperm-specific imprints will be re-established in prespermatogonia before birth and the oocyte-specific methylome will be completed after birth.[29,30] It is worth noting, that there are many time windows during epigenetic reprogramming, in which errors in establishing the correct germline-specific DNA methylation patterns can arise and affect the new generation later in life.[11,27]

In general, DNA methylation patterns in male germ cells are much lower compared to somatic cells, but are similar to those of embryonic stem cells.[11,28,31] DNA methylation in mature human sperm is a direct reflection of the spermatogonial stem cell landscape.[32]

1.3.2 Post-translational Histone modifications (PTHMs) in spermatozoa

In humans, the histone-to-protamine exchange occurs during the last step of spermatogenesis and affects reportedly 85 % to 97 % of the genome.[33,34] Initially regarded as remnants of an incomplete replacement, the remaining histones and their PTHMs of the N-terminal tails, mostly methylation (me), acetylation (ac) or phosphorylation (ph), are now considered to have essential roles for gene activation and repression in embryogenesis and beyond.[22,27] Many studies revealed that retained histones, where less condensed paternal DNA is more accessible for transcription, are not randomly distributed and mark genes and chromosomal regions (e. g. HOX/miRNA clusters, bivalent histone modifications [H3K4me3/K27me3] or imprinted loci), and are important for male fertility and proper embryo development.[30,35,36] Additionally, post-translational modifications (PTMs) of human sperm proteins, like AKAP, CABYR and PA200,[37–39] are shown to be fundamental for the regulation of cellular processes required for human spermatogenesis and sperm function, including sperm compaction and maturation.[40,41]

In 2016 a comprehensive analysis of histone PTHMs in mouse, human male germ cells and human spermatozoa was performed using nanoliquid chromatography–tandem mass spectrometry (nano-LC-MS/MS).[42] In mouse, a total of 61 PTHMs and in human 103 PTHMs were found on the four core histone H2A, H2B, H3 and H4. A strong conservation of PTHMs on histone H3 (17/20) and H4 (10/12) could be observed in mouse and human germ cells, but not for the other two histones H2A and H2B. In Figure 6 the PTHMs found on histones H3 and H4 are displayed for mouse and human sperm cells.

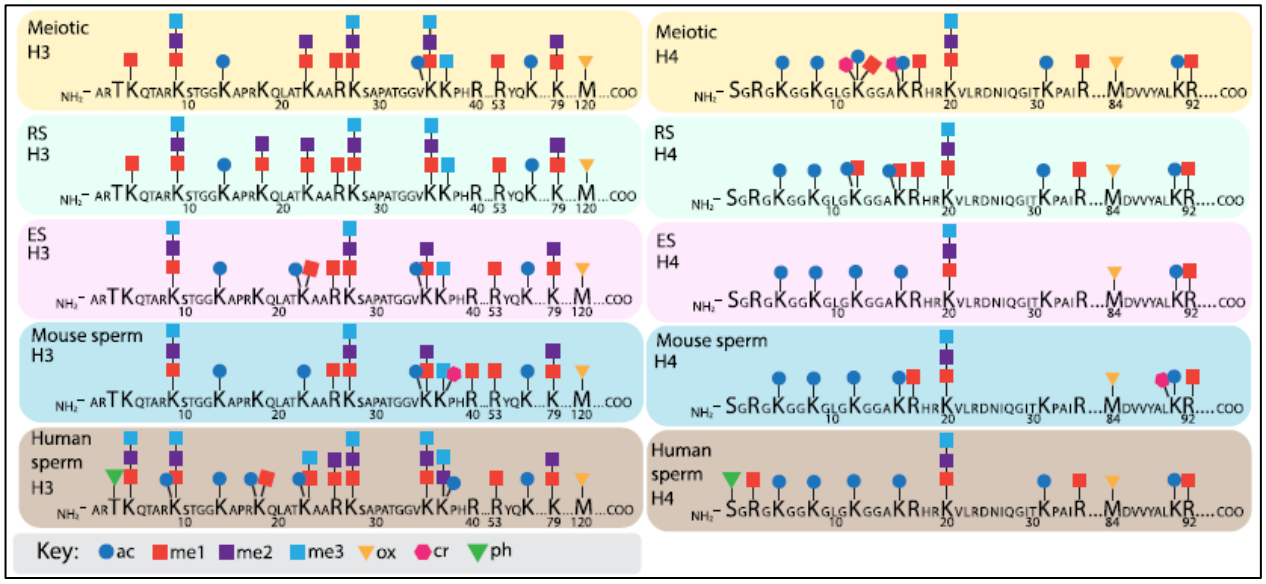

Figure 6: The post-translational histone modifications in mouse and human sperm cells displayed as a scheme.[42]

Among the conserved PTHMs in human and mouse sperm cells H3K9me1/2/3, H3K27me1/2/3 and H4K20me1/2/3 can be found.[42] Mono- or dimethylation of lysine residues of peptides on histones residues are associated both with open and active chromatin regions, whereas trimethylation represents a hallmark of constitutive heterochromatin and often appears at silenced genes.[43–45]

In human sperm cells, among H3, H3K9me3 (27.9 %) was found to be the most abundant PTHM on peptide amino acids (aa) 9-17 followed by H3K27me1/H3K36me2 on peptide aa 27-40. Regarding H4 aa 4-17, H4K16ac (22.5 %) was the most common PTHM, while the remaining residues were unmodified (40.3 %). Among H4 peptide aa 20-23, high proportion of H4K20me2 (80.9 %), H4K20me3 (9.8 %) and H4K20me1 (7.9 %) were found.[42] Interestingly, the gain in H4K20me3 level from round to elongated spermatids was the highest.[42]

The methylation of H4K20 has been identified as key player of the genomic integrity, having crucial roles in DNA damage repair, DNA replication and chromatin compaction.[46] In particular, H4K20me3 is a proven repressor of repetitive DNA elements and transposons in somatic cells.[47,48] Methylation of H4K20 is mediated by specific histone methyltransferases, namely SET8 (alias KMT5A), SUV4-20 H1 (alias KMT5B) and SUV4-20 H2 (alias KMT5C), which each mono-, di- and trimethylate H4K20 in a cell cycle specific manner.[46] The regulation of these histone methyl-transferases and the resulting H4K20 methylation states are not fully unraveled. Figure 7 shows in a scheme the currently known enzymes that induce H4K20 methylation in human. SET8 specifically mono-methylates H4K20 and demethylation of H4K20me1 is performed by PHF8, which is also responsible for H3K9me1/me2 and H3K27me2 demethylation.[49,50] H4K20me2 is generated by SUV4-20 H1, which can also produce H4K20me3.[51] The main portion of H4K20me3 is generated by SUV4-20 H2, whereas both SUV4-20 H1 and SUV4-20 H2 prefer H4K20me1 as substrate.[46] The exact erasure mechanisms of H4K20me2 and H4K20me3 in mammals are still unknown. Histone lysine demethylases closely related to PHF8 (H4K20me1 demethylase), such as PHF2 and JMJD2A have been suggested to target H4K20me2 and H4K20me3. The demethylase activity of PHF2, produced in bacterial cell extracts, was investigated in an *in vitro* histone demethylation assay, but no catalytic activity was recorded for H4K20me3.[52]

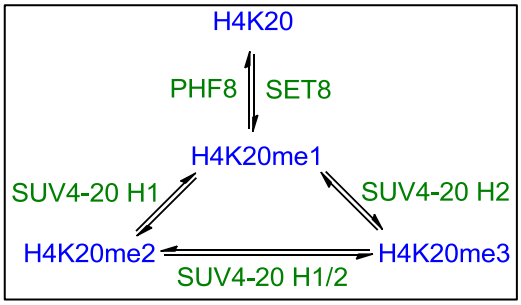

Figure 7: Methylation and demethylation cycle of H4K20 by its histone methyltransferases.

In a comparative molecular dynamics simulations study the molecular recognition of H4K20me2 and H4K20me3 by JMJD2A was investigated.[53] In this simulation JMJD2A binds with high affinity to both PTHMs (H4K20me2 > H4K20me3). In another study the crystal structure of human JMJD2A alone and in complex with H4K20me3 was resolved, but no change in the conformation of JMJD2A could be observed in both structures.[54] Further research on the regulation of H4K20 methylation is necessary to understand, why especially these PTHMs are highly enriched and conserved in mouse and human sperm cells. H4K20 methylation in human sperm has not yet been analysed and genome-wide localized. In order to demonstrate that heterochromatin must also be correctly labelled with epigenetic markers in human sperm, the methylation state of H4K20 was investigated in this thesis.

1.4 Long interspersed nuclear element 1: LINE-1 (L1)

The human genome consists of about 45 % transposable elements (TE) with repetitive character (Fig. 8).[55] TEs can be subdivided into two subclasses based on their transposition mechanism. Class I TEs, the retrotransposons, like long and short interspersed nuclear elements (LINEs, SINEs [alias ALUs]) and retrotransposons containing long terminal repeats (LTRs), need an RNA intermediate for their transposition mechanism ("copy and paste"). In contrast, class II TEs, the DNA transposons, need an DNA intermediate for their transposition mechanism ("cut and paste").[56,57]

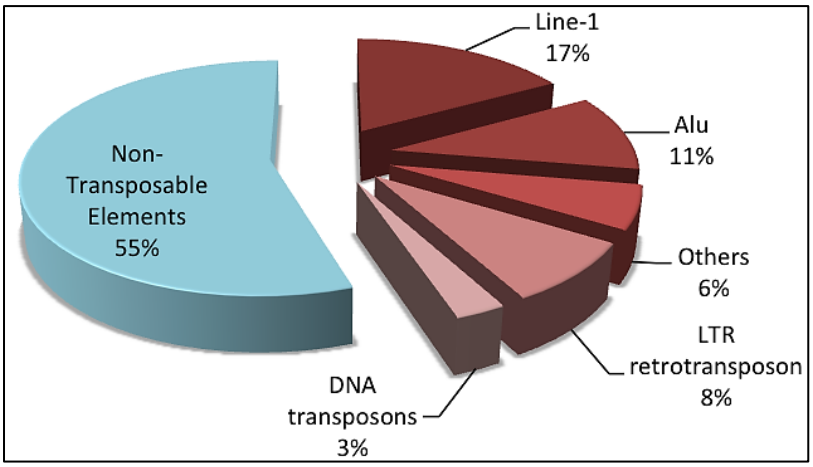

Figure 8: Scheme of the human genome consisting of 55 % non-transposable and 45 % transposable elements. Class I TEs: L1, ALU (SINEs), LTR. Class II TEs: DNA transposons.[55]

LINE-1 elements (L1) are the only active class I transposons, which account for up to 17.0 % of the human genome with a copy number of nearly 500.000.[57,58] These elements, derived from an ancient retrovirus, are the evolutionary youngest class of TEs that emerged about five million years ago, when chimpanzees diverged to humans.[59,60]

Most L1 elements are inactive through their truncation at the 5` or 3`-untranslated region (UTR) and were considered long time as "junk" DNA since they apparently had no important function. Various studies have shown that 80-100 full-length copies of these elements are still active in the human genome, playing crucial roles in cell differentiation and generation of alternative transcription start sites.[57,61,62]

1.4.1 L1 structure and its retrotransposition cycle

Human L1 elements are around 6 kb in full length and consist of a 5`UTR, two open reading frames (ORF1, ORF2) and a 3`UTR ending in a poly(A) tail (Figure 9, top). ORF1 encodes a 40 kDa RNA binding protein with nucleic acid chaperone activity and ORF2 encodes a 150 kDa protein with reverse transcriptase (RT) and endonuclease activities. The complete L1 retrotransposition cycle can be described in six steps (Fig. 9, bottom).

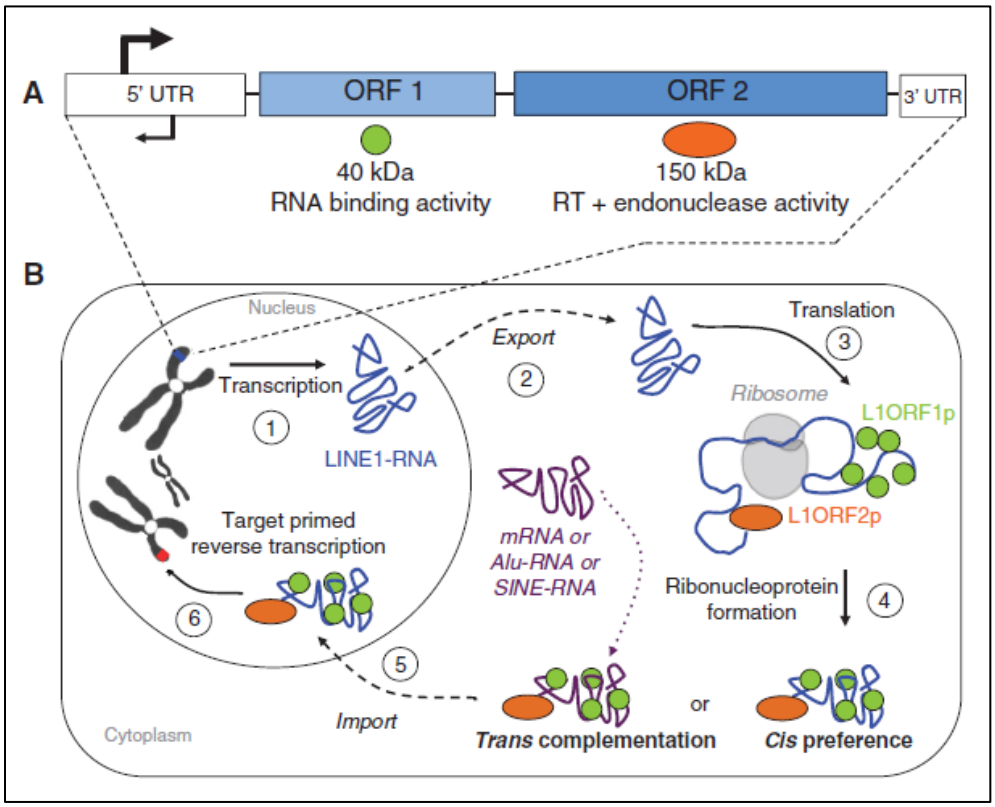

Figure 9: General structure of a L1 element (top) plus its six-step retrotransposition cycle (bottom).[56]

In the first step L1 RNA is transcribed by RNA polymerase II from the internal L1 promoter located at its 5`UTR and is exported from the nucleus into the cytoplasm of the cell in the second step. Then in the third step L1 RNA is translated into two ORF proteins, namely ORF1p and ORF2p. Both proteins will form in the fourth step a ribonucleoprotein (RNP) complex with L1 RNA in *cis*

preference or *trans* complementation with other RNAs (like mRNA or class I/II TEs RNA) is possible. In the fifth step these RNP complexes are transferred back into the nucleus, where they can integrate themselves in their final sixth step at new genomic locations through target primed reverse transcription (TPRT) leading to mutations.[56,63]

L1 retrotransposition is reported in the germ line, human embryonic stem cells (hESCs) and in somatic cells.[64–66] There, L1 mutations can influence its activity positively and negatively.[65] On the one hand, L1 element activity in the early mouse embryo ensures precise global chromatin accessibility and genomic stability, since the highest levels of L1 transcripts were found in the 2-cell mouse embryo and these level were significantly lowered in the 8-cell stage.[62] On the other hand, a prolonged or shorted L1 activity leads to delays in chromatin reorganization and thus to impairments in the further development of the early mouse embryo.[62] In epithelial cancers (like prostate and ovarian) tumorigenesis is promoted by L1 insertions at cancer-specific DNA hypo-methylation sites, while in breast and bladder cancers insertions of L1 at cancer-specific genes reduced tumorigenesis.[63,67] Also, higher L1 transcript levels are reported in testicular germ cells in men suffering from hypospermatogenesis.[68] Hence, it is necessary that L1 elements are strictly regulated so that harmful effects are prevented.

1.4.2 Association of remaining sperm nucleosomes with repetitive elements

Initial studies of sperm nucleosomes and histones, respectively, remaining in sperm chromatin after histone-to-protamine exchange revealed, that these are enriched at developmental promoters, miRNA genes and some imprinted loci.[27,30,36] Additionally, our group and others have shown that nucleosomes are also remaining in gene-poor regions and, at the genome-wide scale, they are rather depleted from gene-rich regions. As shown in Figure 10 the nucleosome-rich regions include frequently repetitive DNA elements like L1 and SINEs, and are also characteristic for introns, few promoter regions (e.g. that of RNA processing genes) and, genes important for pre-implantation development.[34,69]

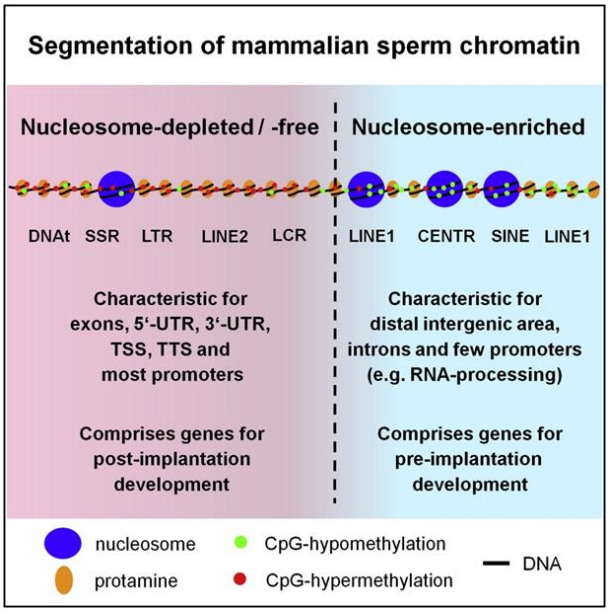

Figure 10: Nucleosome retention patterns in mammalian sperm chromatin.[34]

Further examinations of retained nucleosomes and PTHMs in human sperm cells and their genomic localization, respectively, are needed to understand the association of L1s and sperm nucleosomes and to clarify the partially contradicting observations reported in different papers. Moreover, epigenetic mechanisms regulating L1 in sperm and spermatogenesis are not well studied yet and need to be investigated further. Hence, in the present thesis, the epigenetic tagging of L1 and L1 regulators, well known from studies on somatic cells, were analyzed.

1.4.2.1 CpG methylation

DNA hypermethylation of a gene promoter is associated with its suppression, as it inhibits the transcription machinery from binding to the promoter region (Fig. 11).[70] In many cancer types, such as breast, brain and prostate, DNA hypermethylation in promoter regions of e.g. tumor suppressor genes is a frequently observed feature. For instance, hypermethylation of GHSR (growth hormone secretagogue receptor) can be used as an epigenetic marker in human to distinguish cancer (e.g. breast, lung, prostate) from non-cancer samples.[71] In contrast, DNA hypomethylation of a gene promoter is linked to gene activation, as the chromatin is more open to the transcriptional machinery.[24,27] Loss of DNMT proteins leads to a strong demethylation of the whole genome and to severe implications. For example, knockout of *Dnmt1* as well as *DNMT3A/3B* in mice induced aberrant paternal imprinting during spermatogenesis and embryonic lethality.[28,72] In human ejaculated spermatozoa high mRNA levels of *DNMT1* and *DNMT3A* are reported but not of *DNMT3B*.[26]

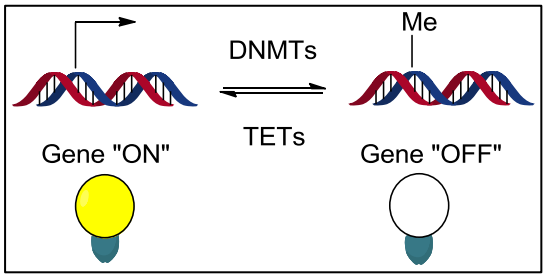

Figure 11: DNA hypermethylation of a gene promoter leads to its suppression.

As already mentioned, L1 comprises about one fifth of the human genome and is proven to serve as surrogate measure for the global DNA methylation level due to this high number.[73] DNA hypermethylation of L1 promoters is an epigenetic suppression mechanism of L1 retrotransposition that can often be observed in normal somatic tissues.[74] Particularly DNA hypomethylation of L1 promoters along with its increased expression are hallmarks in various cancer types and is linked to a number of diseases such as hemophilia A, schizophrenia and bipolar disorder.[74–76] Aberrations in global DNA methylation and imprinting genes are associated with poor sperm quality and male infertility.[31,77,78] For the causal diagnosis of idiopathic male infertility, the global DNA methylation state (5-mC, *L1*) and DNA methyltransferase activities (*DNMT1*, *DNMT3A*) were determined here.

1.4.2.2 Post-translational Histone modifications (PTHMs) as L1 regulators

As noted, in human sperm cells the highest conservation of PTHMs was detected on H3 (31 PTHMs) and H4 (14 PTHMs), using mass spectrometry.[42] Moreover, on histone H4 peptide aa 20-23 the most abundant PTHMs were H4K20me2 (80.9 %) and H4K20me3 (9.8 %).[42] H4K20me2 plays distinct roles for DNA replication, by marking places of origin for the Orc (origin of replication) complex and DNA double-strand break repair, by recruiting repair enzymes like 53BPI to damage sites.[46,79]

H4K20me3 is described as heterochromatin marker, repressor of transcription when present at promoters and silencer of repetitive DNA elements in somatic cells.[47,48,80] In a study on human colorectal cancer (CRC), reduced H4K20me3 levels were found in CRC patients compared to healthy controls, whereby H4K20me3 was localized in both cohorts at repetitive DNA elements like L1 and SINE elements. In the same study, another heterochromatin marker, H3K9me3, was also localized at repetitive DNA elements, but in smaller amounts (60.6 %) compared to H4K20me3 (74.8 %).[81] It is postulated, that retrotransposons have regulatory functions for their host genome, by acting as a template for the transcription factor binding repertoire.[82] Moreover, it is possible that retained histones in spermatozoa are transferred to the egg cell and participate in the establishment of gene expression in the early embryo, as highest L1 activity is reported in the 2-cell mouse embryo and decreases with its further development.[62,83] The knockdown of histone methyltransferases KMT5B and KMT5C led to a reduction of H4K20me3 and in particular to an upregulation of L1 elements, which induced the death of mouse embryos at morula stage.[84,85]

In regard of the high numbers of idiopathic infertile males, H4K20me2 and H4K20me3 and their histone methyltransferases (KMT5A, KMT5B and KMT5C) were investigated here in human sperm cells, to see if these factors were also associated with L1 regulation and have the potential to affect male fertility.

1.4.2.3 Transcription factors (TFs) of L1

Transcription factors are proteins which bind alone or together with others to a specific DNA sequence in the promoter region of a gene and can either promote or inhibit its transcription. Gene promoters are typically located near the transcription start site (TSS) upstream of a gene (5`UTR). The 5`UTR is an essential component for the retrotransposition cycle of a L1 element. However, the 3`UTR, which contains a polypurine tract, is not critical for L1 retrotransposition.[86,87] Human L1 elements contain in their 5`UTR multiple promoter binding sites for transcription factors such as YY1, RUN3 and SOX (Fig. 12).[86]

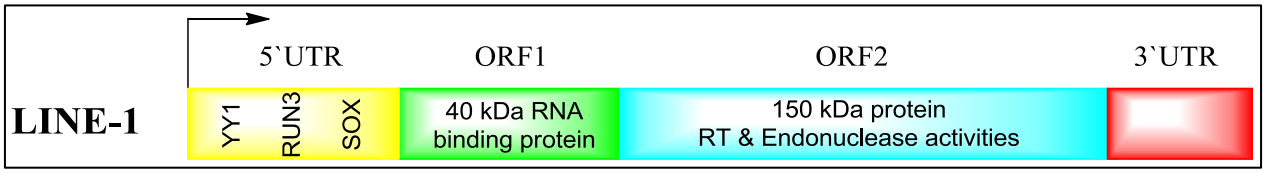

Figure 12: General structure of a L1 element, including transcription factor binding sites (YY1, RUN2, SOX). RT= reverse transcriptase.

YY1 (Yin Yang 1) is a transcription factor binding on the antisense strand of the L1 5`UTR between position +13 and +21. Mutations in the YY1 binding site show weak effects on L1 retrotransposition, but this site is required for the precise initiation of L1 retrotransposition in cultured human cells.[60,88] L1 elements lacking a YY1 binding site are predicted to shorten over time until they are incapable of retrotransposition.[86]

The transcription factor RUN3 (runt-domain transcription factor 3) has three binding sites, one antisense (+526 to +508) and two in sense strand direction (+83 to +101 and +389 to +407), on human L1 5`UTR. SOX (SRY-related HMG box containing) has two binding sites on the sense strand on human L1 5`UTR (+472 to +477; +572 to +577). Both SOX binding sites and only one RUN3 binding site (+83 and +101) induce *in vitro* L1 retrotransposition in cultured cells. On the one hand, mutations in these binding sites diminish L1 retrotransposition events. On the other hand, overexpression of RUN3 or SOX led to a nearly tenfold increase of L1 retrotransposition activity in human cervical carcinoma (HeLa) or human embryonic kidney cells (HEK), respectively.[60,86,88]

Recently SIRT6 (sirtuin 6), a histone methyltransferase and heterochromatin regulator, was discovered as a L1 suppressor in human dermal fibroblasts (HDF).[89] SIRT6 binds to the 5`UTR of L1 elements and ribosylates the nuclear corepressor protein KAP1, which is then able to interact with the heterochromatin factor HP1α and packages L1 into transcriptionally inactive heterochromatin (Fig. 13).[89] During aging and oxidative stress, SIRT6 disappears from L1 5`UTRs and relocalizes at DNA damage sites such as DNA double strand breaks, whereby L1 5`UTRs are loosened and L1 retrotransposition is reactivated.[89]

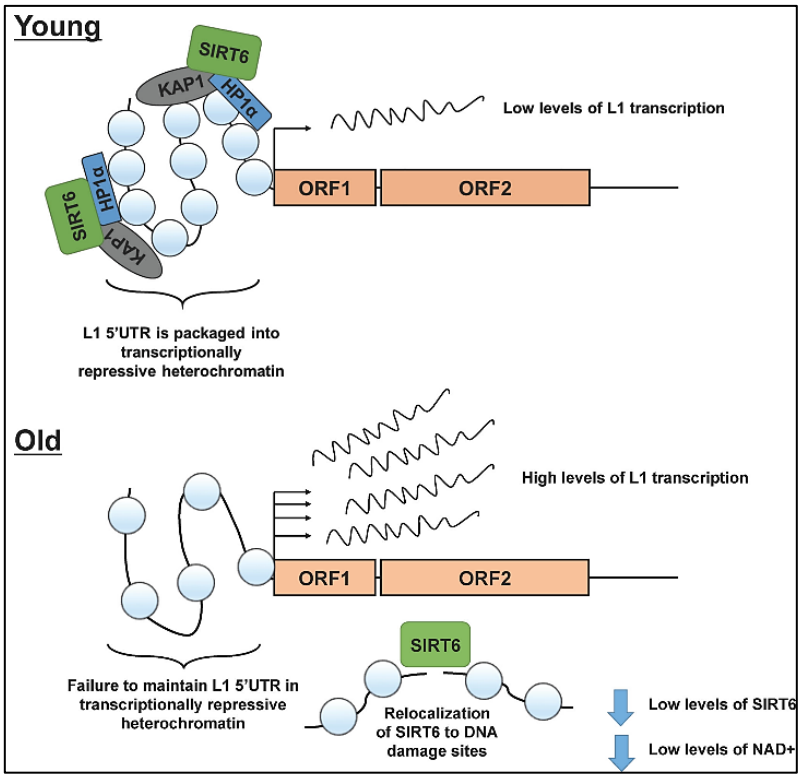

Figure 13: Model of L1 suppression by SIRT6. In young cells SIRT6 is able to keep L1 elements in their silent state, but this capability decreases with increasing age.[89]

Sirtuins are proven lifespan regulators in different organisms, such as yeast, nematodes and fruitflies through deacetylation of critical transcription factors.[90,91] Premature aging and a shortened lifespan are observed in *Sirt6* knockout mice, while overexpression of *Sirt6* led to an extended lifespan exclusively in male mice.[90] Moreover, *SIRT6* gene promoter methylation increases with age in human lymphocytes, but no significant correlation to gender or longevity was observed in that study.[91] According to the human protein atlas SIRT6 protein is highly expressed in human testis tissue, which allows the hypothesis that SIRT6 is also responsible for L1 regulation there.[92]

A genome-wide screen in 2018 revealed more L1 regulators in two human cell lines, namely human chronic myeloid leukemia K562 and human embryonic stem cells (hESC).[93] MORC2 (microrchidia 2) and human silencing hub (HUSH) complex subunits MPP8 (M-Phase Phosphoprotein 8) and TASOR (Transgene Activation Suppressor Protein) are able to bind and repress young full-length L1 elements in euchromatic environment (Fig. 14). In neuronal cells, MORC2 and HUSH-complex interactions were demonstrated and in addition, the bundled localization of these components at H3K9me3 promotes the formation of heterochromatin and L1 suppression.[93,94] In mouse germ cells *Morc1* is repressing retrotransposons and its knockout leads to loss of germ cells and infertility in males.[95]

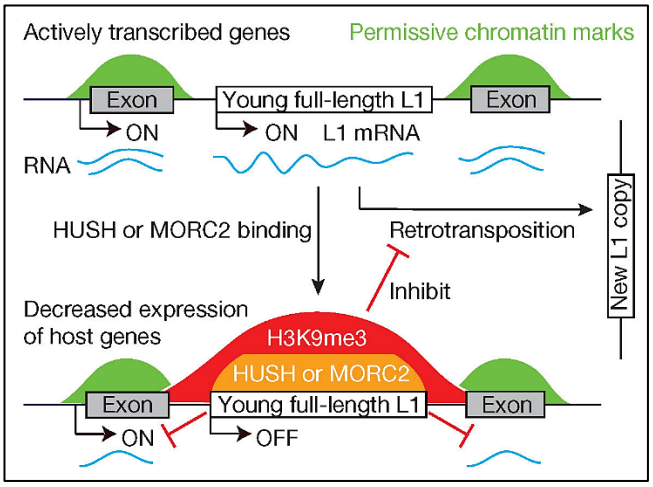

Figure 14: Model of L1 suppression by HUSH/MORC2 complex. HUSH/MORC2 bind to young full-length L1s, promote H3K9me3 deposition and thus inhibit L1 retrotransposition.[93]

In this thesis, some L1 transcription factors known from somatic cells (YY1, SIRT6 and MORC2) were analyzed in human spermatozoa and testicular tissues, to uncover L1 regulatory mechanisms and to properly address possible causes and treatment options for the factor male idiopathic infertility.

1.5 Aims of this work

It is likely that epigenetic aberrations in sperm are responsible for idiopathic forms of male factor infertility and/or reflect this situation. Available studies focused mostly on aberrations of the methylome and some PTHMs characteristic for gene regions.

The working hypothesis of this thesis was, that aberrations in sperm epigenome, specifically those leading to dysregulation of retrotransposons, are associated with idiopathic male infertility. L1 dysregulation during human spermatogenesis and its incorrect epigenetic tagging in mature spermatozoa could lead to errors in pre-implantation development and thus contribute to the triggering of sub- and infertility in men.

Epigenetic regulation of L1 in spermatogenesis and in mature sperm is largely unknown. In order to first identify and then investigate different factors of the sperm epigenome potentially controlling L1 regulation, the following components were analyzed in both motile and immotile spermatozoa of healthy males (donors/controls) and in motile spermatozoa of idiopathic infertile males (subfertile patients) used for ART. Also, human, mouse and bull testis tissues were utilized in order to get information about the expression pattern of some selected factors:

- Analyzes of *L1*-mRNA and *L1*-methylation levels in mature motile versus immotile spermatozoa, to find out whether L1 is differentially regulated, using RT-qPCR, ELISA based assays and pyrosequencing;
- Determination of global 5mC, 5hmC DNA and m6A RNA methylation and *DNMT1/3A* mRNA levels in mature human spermatozoa by ELISA and RT-qPCR, to see if differences exist between the cohorts;
- Investigation of potential L1 regulating PTHMs, like H4K20me2 and H4K20me3, and HMTs, like KMT5A, KMT5B and KMT5C, in mammalian testis tissues and mature human spermatozoa, to analyze their abundance and regulation, utilizing immunohistochemistry (IHC), immunocytochemistry (ICC), RT-qPCR and western blot (WB);
- Analyzes of L1 transcription factors known from somatic cells, YY1, MORC2 and SIRT6, to unravel L1 regulations in mature human spermatozoa and testis tissue, using IHC, RT-qPCR and pyrosequencing.

2. Materials and Methods

2.1 Materials

2.1.1 Chemicals

AppliChem, Darmstadt	NaAc solution 3 mol/l (3 M, pH 5.2)
Biorad, München	Acrylamide solution (30 %); APS;
Biozym Scientific, Oldendorf	Agarose
Merck, Darmstadt	Citric acid; Orange G; PFA; Tri-sodium citrate
PeqLab, Erlangen	PeqGold TriFast
Roth, Karlsruhe	Acetic acid; chloroform; DTT; Glycine; Glycogen; HCl; Milk dry, non-fat; NaCl; NaOH; SDS; Phenol/Chloroform/Isoamyl-alcohol; Proteinase K; Roti®-Phenol; TEMED; Tris; Triton X-100
Sigma-Aldrich, Steinheim	BSA; DEPC; EDTA; EtOH; H_2O_2; Isopropa-nol; Lithium 3,5-diiodosalicylate; MeOH; β-mercaptoethanol; PMSF; PBS; Protease inhibitor cocktail Tablets (S8820)
VWR, Darmstadt	Xylol

2.1.2 Reagents, buffers and kits

2.1.2.1 DNA, RNA and protein extraction

Thermo Scientific, Darmstadt	DNase I (50-375 U/µL, 20000 U), DNase I 10x buffer
Somatic cell lysis buffer	0.1 % SDS, 0.5 % Triton X-100 in DEPC-H_2O
Proteinase K buffer	50 mM Tris-HCl pH 8.0, 50 mM EDTA, 0.5 % NP-40, 0.5 % SDS

2.1.2.2 CpG methylation and mRNA analysis

2 % agarose gel	2 g Agarose in 100 mL 1 x TAE
10x TAE buffer (pH 8.0)	2.5 mM Tris, 17.4 M acetic acid, 11 mM EDTA ad 1 L ddH_2O
Active Motif, La Hulpe, BG	Global DNA Methylation - L1 Kit (Cat. No. 55017)
Bioline, Luckenwalde	2x My Taq HS Mix
Biotium, Fremont	GelRed Nucleic acid gel stain
GE Healthcare, Freiburg	Streptavidin sepharose high performance
Gentaur	MethylFlash™ Global DNA Methylation & Hydroxymethylation ELISA Easy Kit (Cat. No. P-1030/1032), EpiQuik RNA Methylation Quantification Kit (Cat. No. P-9005)
Promega, Mannheim	Recombinant RNasin® Ribonuclease Inhibitor (40 U/µL); dNTP mix (dATP/dCTP/cGTP/ dTTP), 10 mM
Qiagen, Hilden	PyroMark binding / denaturation / annealing / wash buffers; PyroMark Gold Q24 reagents; Rotor-Gene SYBR Green PCR Master mix; L1/SIRT6 pyrosequencing kits (Cat. No. 970012/978746)
Thermo Scientific, Darmstadt	GeneRuler DNA Ladder Mix, RiboLock RNase Inhibitor (40 U/µL)
Zymo Research, Freiburg	EZ DNA Methylation Kit

2.1.2.3 Immunohistochemistry

10x Tris-HCl Puffer, pH 7.4	1 M Tris-HCl, 1 M NaCl ad 1 L ddH_2O
1x Tris-HCl-Puffer	1/10 volume 10 x Tris-HCl, 0.1 % Triton in ddH_2O
Citrate buffer, pH 6.0	18 mM citric acid monohydrate, 82 mM sodium citrate in ddH_2O
3 % H_2O_2 / Methanol	63 mL ice cold MeOH, 7 mL 30 % H_2O_2
5 % BSA	3.5 g BSA in 70 mL 1x Tris-HCl buffer
Dako, Glostrup, DK	AEC+ high sensitivity substrate chromogen, Faramount Mounting Medium
Merck, Darmstadt	Mayer`s Haemalaun
Waldeck GmbH und Co. KG, Münster	Haemalaun, acidic
Vector, Peterborough, UK	Vectastain Elite ABC-Peroxidase Staining Kit

2.1.2.4 Western blot

10 % APS	50 mg APS in 500 µL ddH_2O
10 x SDS running buffer, pH 8.3	25 mM Tris, 192 mM glycine, 0.1 % SDS in ddH_2O
1 x PBS, pH 7.4	5 PBS Tablets in 1 L ddH_2O
1x PBST, pH 7.4	1 x PBS, 0.1 % Tween 20 in ddH_2O
BioRad, München	Laemmli buffer (4x); Extra Thick Blot Filter Paper, Precut, 7 x 8.4 cm
Coomassie destaining solution	40 % MeOH, 10 % acetic acid in ddH_2O
Coomassie staining solution	0.1 % Coomassie Brilliant blue R250, 50 % MeOH, 10 % acetic acid in ddH_2O

Laemmli loading buffer, 1 mL	900 µL Laemmli buffer, 100 µL β-Mercaptoethanol
LI-COR Biosciences, Bad Homburg	Odyssey Blocking Buffer TBS/PBS (1:3 in 1xPBS, REVERT™ Total Protein Stain Kit
Merck, Darmstadt	Immobilon-FL PVDF, 0.45 µm, 26,5 cm x 3,75 m roll
RIPA buffer	50 mM Tris-HCl (pH 7.5), 150 mM NaCl, 1 % Triton X-100, 0.1 % SDS, 0.5 % sodium deoxycholate, 1 mM PMSF, 1 mM EDTA, 4 mM sodium fluoride, 1 mM DTT, 1x Protease Inhibitor Cocktail (1 Tablet/ 100 mL)
Running gel buffer; pH, 8.8	1.5 M Tris in ddH_2O
Stacking gel buffer; pH 6.8	1.5 M Tris in ddH_2O
Transfer buffer, pH 8.0-8.5	48 mM Tris, 38 mM glycine, 20 % MeOH, 0.0375 % SDS in ddH_2O
Tris-Urea buffer	8 M Urea, 2 % SDS, 50 mM Tris (pH 8.0), 105 mM NaCl, 1 mM PMSF, 10 mM DTT, 1x Protease Inhibitor Cocktail (1 Tablet/ 100 mL)
SERVA Electrophoresis, Heidelberg	Coomassie Brilliant blue, R250
Thermo Scientific, Darmstadt	Page Ruler^{TM} prestained protein ladder 10-180 kDa

2.1.3 Antibodies

Abcam, Cambridge	Rabbit polyclonal primary antibodies: H4K20me3 (ab9053), 1:100 IHC/ICC, 1:500 WB; H4K20me2 (ab9052), 1:100 IHC/ICC, 1:500 WB; YY1 (ab109237), 1:200 IHC; SIRT6 (ab62739/ab176345), 1:2000/ 1:500 WB, KMT5C (ab91224), 1:50 WB; GAPDH (ab9485), 1:2500 WB
Dako, Glostrup, DK	Goat anti rabbit IgG biotynilated (E0432), 1:200 IHC
LI-COR Biosciences, Bad Homburg	IRDye® 800CW Goat anti-Rabbit IgG (H + L), 1:10000 WB; IRDye® 680LT Goat anti-Rabbit IgG (H + L), 1:10000 WB

2.1.4 Equipments

Biometra, Göttingen	Gel documentation system, BioDocAnalyze
Bioblock Scientific	Vibracell 75022, ultrasonic processor, 130 W
Bio-Rad, München	Mini-PROTEAN Tetra Cell; Power PAC 200 + 300; Thermocycler T100 + C1000 Touch; Trans-Blot SD Semi-dry transfer cell
BOSCH, Stuttgart	Fridge; Freezer Economic GSL 1202 + 3601
BRAUN, Schwalbach am Taunus	Gourmet cooker
Eppendorf, Germany	Thermo Mixer; Mastercycler; Pipettes; tubes
Fisherbrand, Schwerte	Mini centrifuge
Helmut Hund GmbH, Wetzlar	Microscope H 600 LL
Heidolph, Schwabach	Shaker Reax 2000; Vortex mixer REAX 2000
Heraeus, Hanau	Incubator Kelvitron T

Hettich, Frankenberg	Centrifuge (MIKRO 220R)
IKA, Staufen	Shaker VIBRAX-VXR; Magnetic Stirrer (BLSH0007)
LI-COR Biosciences, Bad Homburg	LI-COR Odyssey Fc
LG, Ratingen	Microwave Untellowave
Merck, Darmstadt	MilliQ direct water purification system
Mettler Toledo, Giessen	Fine balance Mettler AE 240; pH meter (S20K)
Nerbe plus, Winsen + Biozym, Oldendorf	Pipette tips
Olympus, Tokio, JPN	Microscope BX43
PeqLab, Erlangen	Gel chamber; NanoDrop ND-1000
Qiagen, Hilden	Stainless steel beads (ball), 5 mm; Pyromark Q24 system and supplies; Rotor Gene Q PCR cycler; TissueLyzer LT
R. Langenbrinck GmbH, Emmendingen	Cover plates; Glass plates superfrost
Roth, Karlsruhe	Neubauer-improved counting chamber
Störktronic, Stuttgart	Heating plate Präzitherm 28-1
Thermo Scientific, Darmstadt	Centrifuge (Heraeus Fresco 21); HERA-freeze™ HFU T Series -86°C Freezer; Invitrogen Power Ease® 500 Power Supply; Multiscan Go Photometer; Tube Revolver
VLM, Bielefeld	Heating block LS 2

2.2 Methods

2.2.1 Collection and preparation of human semen samples

From the Division of Gynecological Endocrinology and Reproductive Medicine, Department of Gynecology and Obstetrics, Clinical Centre of the Ludwig-Maximilians-University Munich motile sperm samples of 48 subfertile men (patients) were obtained, who underwent an ART (assisted reproductive technology), like ICSI (intracytoplasmic sperm injection) or IVF (in vitro fertilization). In this study the term "subfertile men" is used to describe the condition, when a couple was unable to conceive a child naturally within one year without contraception. The use of an ART could improve the pregnancy rates of these couples.

Semen samples from 112 healthy volunteers (donors) were collected at the Department of Urology, Pediatric Urology and Andrology of the Justus-Liebig-University Giessen. In sum 15 donors with asthenozoospermia (< 32 % mot. spermatozoa, n=10) and/or oligozoospermia (< 15 Mio/mL sperm cells, n=7) were excluded from this study. Every participant was informed and gave a written consent to this study, which was approved by the Ethics Commission of the Medical Faculty of the Justus-Liebig-University of Giessen (approval from 15.12.10 in the frame of the Clinical Research Unit KFO181/Period 2 'Mechanisms of male factor infertility', confirmed on 17.12.14) and is funded by a DFG grant to Schagdarsurengin U. (SCHA 1531/2-1).

All semen samples were collected and analyzed according to the WHO guidelines of 2010. Freshly ejaculated semen samples from donors were obtained by masturbation after at least 3 days of sexual abstinence and collected into sterile containers. After liquidation at 37 °C for 15-30 min, semen samples were separated into motile and immotile sperm cell fractions, using the swim-up technique, for further individual analysis. Briefly, liquefied semen was placed on the bottom of a round tube containing 1.2 mL sperm wash medium (HTF-Medium/2 % HSA) and put at an 45° angle for 60 min at 37 °C. During this incubation motile (M) sperm cells "swim-up" into the wash medium, which can be aspirated afterwards, whereas immotile (I) sperm cells stay at the bottom of the tube. Sperm concentration and motility were determined for both fractions. Then sperm samples were centrifuged at 500 g for 10 min at 4 °C and washed twice with PBS. Afterwards sperm samples were frozen in liquid nitrogen and stored at -80 °C until further processing. Spermiogram parameters and ages of collected donors and patients, including the ages of the female partners of the patients, are summarized in Table 1. Further patient and donor data can be found in the supplement (Tables 16-21).

Table 1: Spermiogram parameters (median, range; p-values calculated by Mann-Whitney *U*-test: *p ≤ 0.05, **p ≤ 0.01) and ages of collected donors and patients, including female ICSI/IVF-partners.

Spermiogram parameter	Donors	Patients
Number	97	48
Age (years)	29.0 (20.0-49.0)	39.0** (29.0-50.0)
Partner Age (years)	-	35.3 (27.0-44.0)
Sperm concentration (Mio/mL)	63.6 (15.4-282)	17.7** (1.00-155)
Total sperm count (Mio)	194 (30.8-930)	128** (5.12-491)
Vitality (%)	86.0 (54.0-95.0)	-
Progressive motility (%)	61.0 (33.0-85.0)	39.5** (9.00-62.0)
Total motility (%)	70.0 (42.0-89.0)	61.0** (25.0-83.0)

2.2.2 Human cancer cell line cultures

Cervix carcinoma cell line HeLa and prostate cancer cell lines (LNCaP, DU145 and PC3) were used as positive controls to test PCR primers and antibodies for investigations in human sperms. These cell lines were cultured in an appropriate culture media (Dulbecco's modified Eagle's medium and cell culture medium developed at the Roswell Park Memorial Institute supplemented with 10 % fetal calf serum and 1 % penicillin/streptomycin, Life Technologies GmbH)[96] at 90 % confluency, 5 % CO_2 and 37 °C. Cell lines were washed twice with PBS and finally scraped in PBS. After centrifugation (5 min, 1500 g at 4 °C) the supernatants were removed and the cell pellets were either resolved in PBS buffer (for DNA/RNA extraction, see 2.2.3) or in RIPA buffer (for protein extraction). HeLa protein pellets, resuspended in 300 µL RIPA buffer supplemented with protease inhibitor cocktail, were left on ice for 30 min with vortexing each 5 min. Sonication was performed with ultrasonic processor Vibra Cell for three cycles, each 10 s (Amplitude 30 %, max. pulse), until pellets were completely solubilized. After centrifugation (5 min, 13000 rpm, 4 °C) protein extracts were taken into a new tube, concentrations were determined (NanoDrop) and kept frozen at -80 °C.

2.2.3 DNA & RNA extraction

Motile and immotile sperm cell fractions, separated after swim-up procedure, were thawed on ice, 4 Mio sperm cells were taken out and washed twice with PBS (in DEPC-H_2O). Instantly motile sperm cells were equally divided for further DNA and RNA extraction. Immotile sperm cells were

treated for 15 min on ice with 250 µL somatic cell lysis buffer (0.1 % SDS, 0.5 % Triton X-100 in DEPC-H_2O) prior division, to ensure the analysis of a pure spermatozoa population.[97,98]

RNA was isolated with the Trifast reagent, then separated from the DNA with chloroform and precipitated with alcohol. Initially semen samples were resuspended in 150 µL Trifast and lysed on TissueLyser LT for 5 min at 4 °C and 50 osc/sec. Foams were removed by short centrifugation (30 s, 13000 rpm, 4 °C), 350 µL Trifast (total 500 µL Trifast) and subsequently 100 µL chloroform were added and mixed thoroughly per Hand. After incubation for 5 min at RT samples were centrifuged at 4 °C and 13000 rpm for 10 min. The upper aqueous phase containing RNA was put into a new tube and precipitated overnight at -20 °C by addition of one volume isopropanol (500 µL) and 5 µL glycogen (20 mg/mL). Afterwards RNA was pelletized at 13000 rpm and 4 °C for 30 min, washed twice with 500 µL Ethanol (75 % in DEPC-H_2O) and air-dried at RT. To exclude DNA contamination in following RT-qPCRs, RNA was subsequently DNase I digested. Therefore, RNA was dissolved in 16 µL DEPC-H_2O, 2 µL of DNase I and 2 µL of DNase I 10x-buffer were added and the mixture was incubated for 30 min at 37 °C. DNase I heat inactivation occurred at 65 °C for 10 min after 2 µL EDTA (50 mM) were added. RNA concentration was measured (NanoDrop) and samples were stored at -80 °C.

DNA isolation started with Proteinase K digestion, followed by phenol/chloroform extraction and alcohol precipitation. Therefore, a semen sample was resuspended in 120 µL Proteinase K buffer, 80 µL DTT (0.1 M) and lysed on TissueLyser LT for 5 min at 4 °C and 50 osc/sec. After short centrifugation (30 s, 13000 rpm, 4 °C) foams were removed and overnight protein digestion at 56 °C was initiated by the addition of 10 µL Proteinase K (20 mg/mL in PBS). Next the aqueous phase was increased with 300 µL of Tris buffer (10 mM, pH 8.0) to facilitate handling. 500 µL of phenol/chloroform solution were added, well mixed per hand shaking and centrifuged for 10 min at 13000 rpm at RT. The DNA containing upper aqueous phase was supplemented with 500 µL chloroform, well mixed per hand shaking and centrifuged again for 10 min at 13000 rpm at RT. DNA was precipitated overnight at -20 °C through the addition of one volume isopropanol, 1/10 volume NaAc solution (3 M, pH 5.2) and 5 µL glycogen (20 mg/mL) to the aqueous phase. Centrifugation at 13.000 rpm and 4 °C for 30 min pelletized DNA, which was washed twice with 500 µL Ethanol (75 % in ddH_2O) and air-dried at RT. DNA was resuspended in 30 µL Tris EDTA buffer (10 mM, pH 8.0), concentration was measured (NanoDrop) and samples were stored at -80 °C.

2.2.4 CpG methylation analysis

For L1 methylation analysis DNA was either bisulfite treated prior pyrosequencing or directly used for ELISA. SIRT6 methylation was analyzed using pyrosequencing, and global 5-mC/5-hmC DNA and m6A RNA methylation levels were determined using ELISA.

2.2.4.1 Bisulfite treatment and pyrosequencing

Bisulfite treatment was done using the EZ DNA Methylation Kit (Zymo Research) according to the manufacturer`s protocol. 500 ng DNA were treated overnight at 50 °C with 100 µL CT Conversion reagent (reconstituted in 750 µL ddH_2O and 210 µL M-Dilution Buffer). Then samples were cooled for 10 min on ice, mixed with 400 µL M-Binding-Buffer and transferred on a Zymo-Spin™ IC Column. After centrifugation at 13000 rpm for 1 min, the flow-through was loaded onto the column a second time to increase DNA binding and centrifuged again. The column was washed with 100 µL M-Wash Buffer and treated with 200 µL M-Desulphonation Buffer at RT for 30 min to remove incomplete converted cytosines. Subsequent centrifugation at 13000 rpm for 1 min and washing with 200 µL M-Wash-Buffer (twice) was done. Bisulfite converted DNA was eluted in 15 µL Tris buffer, concentration was measured (NanoDrop) and samples were stored at -80 °C.

10-20 ng BS-DNA were used per pyrosequencing reaction. Pyrosequencing uses a real-time and sequence-based working method to quantify methylation level of CpGs from a gene region of interest using the pyrosequencing instrument and PyroMark Q24 Software. According to the manufacturer`s protocol, a PCR amplification of the desired gene region with the provided forward and reverse PCR primers of a PyroMark Q24 Kit (Qiagen, Table 2) was done. Then, PCR products were immobilized to streptavidin sepharose beads (GE Healthcare) and incubated in denaturation buffer to get single-stranded DNA, to which the provided sequencing primer anneals. Through sequencing by synthesis, a light emission proportional to the amount of the correctly incorporated nucleotide is measured. Light signals are displayed as peaks in a pyrogram and the methylation of the examined CpGs is indicated in percent. Bisulfite treated prostate cancer cell line DNA (LNCaP) was used as positive methylation control during pyrosequencing.

Table 2: Pyrosequencing Kits used from Qiagen, including general information.

Gene	Cat. no.	Sequence to analyze	PCR product size (bp)	Number of CpGs
L1	970012	GCTCGTGTAGTCAGTCG	145	3
SIRT6	978746	AACATGTC**G**CCTGC**G**GC**G**T CAGCAAGAGGC**G**CATGC**G**C	205	5

2.2.4.2 ELISA

L1 methylation was also investigated using the Global DNA Methylation Assay-L1 Kit (ELISA, 12 CpGs, Active Motif, Cat. No. 55017) according to the product manual instructions. Shortly, 800 ng DNA were MseI digested, hybridized to the provided L1 probe and immobilized onto a streptavidin-coated plate. Methylated fragments were detected using a 5-Methylcytosine primary and a horseradish peroxidase secondary antibody. Global methylation was quantified by OD measurements at 450 nm and the generation of a DNA standard curve fit, by the methylated and non-methylated DNA standards provided.

The DNA 5-mC/5-hmC levels were analyzed using the MethylFlash^{TM} Global DNA Methylation/ Hydroxymethylation ELISA Easy Kits (Cat. No. P-1030/1032, Gentaur) and the m6A RNA methylation level was analyzed using the EpiQuik RNA Methylation Quantification Kit (Cat. No. P-9005, Gentaur) according to the product manuals instructions. Briefly, 100 ng DNA/RNA were bound to an assay plate and incubated with the respective primary antibody solution. A color developer solution was then added to measure the absorbance of 5-mC/5-hmC DNA and m6A RNA at an OD of 450 nm. The global DNA and RNA methylation levels were quantified by generating a standard curve fit using the methylated and non-methylated standards provided.

2.2.5 RT-qPCR analysis

Synthesis of cDNA was performed using DNase I digested RNA of human sperm and M-MLV reverse transcriptase (Promega) according to the manufacturer`s protocol with minor deviations or LunaScript RT SuperMix Kit. In the first case 300 ng of RNA were incubated with 200 units of the M-MLV reverse transcriptase with the provided 5x M-MLV reaction buffer. Additionally, 2 µL dNTP mix (10 mM, Promega), 2 µL random Hexamere (10 mM), 2 µL Poly dT primer mix (10 mM) and 20 units of RNase Inhibitor (0.5 µL of 40 U/µL) were added with DEPC-H_2O to a final volume of 20 µL. For reverse transcription this mixture was incubated for 10 min/25 °C, 60 min/42 °C and 5 min/ 85 °C. The resulting cDNAs were purified with the QIAquick Nucleotide Removal Kit (Qiagen) and stored at -80 °C until PCR analysis. In the other case 300 ng RNA were reverse transcribed with the ready-to-use LunaScript RT SuperMix, containing random hexamer and oligo-dT primers, dNTPs, Murine RNase Inhibitor, and Luna Reverse Transcriptase. 4 µL of LunaScript RT SuperMix (5x) were added to 300 ng RNA and the final volume was adjusted with DEPC-H_2O to 20 µL. Reverse transcription was performed at 25 °C/2 min, 55 °C/10 min and 95 °C/1 min. The resulting cDNAs synthesized with this kit needed no further purification steps

and were directly stored at -80 °C until PCR analysis. Specific qPCR primer sets were either designed with the Primer 3 online tool (v. 0.4.0) or taken from literature to analyze *DNMT1*, *DNMT3A*, *L1*, *KMT5A/B/C*, *SIRT6*, *MORC2*, *GAPDH* and *ß-Actin* (Table 3) mRNA levels in samples. Amplification of cDNA (~15 ng/reaction) was performed for 45 cycles (initial denaturation 95 °C/5 min, cycling: 95 °C/30 s, 60 °C/30 s, 72 °C/30 s, final elongation 72 °C/ 3 min) on the CFX96 Touch Real-Time PCR Detection System (Biorad). All PCR reactions were performed in duplicates and relative values for all mRNA levels were calculated using cDNA from prostate cancer cell lines (LNCaP/DU145/PC3) as calibrator and positive control. Differences in mRNA levels between groups were identified using the double delta CT (ΔΔCT) method. PCR product sizes were verified on a 2 % agarose gel.

Table 3: Primer sets used for mRNA level quantification in motile and immotile sperm cells.

Gene	Primer sequences (5`-3`)	PCR product size (bp)
DNMT1	FWD: GAACGGTGCTCATGCTTACAA REV: TCTCCATCGGACTTGCTCCT	159
DNMT3A	FWD: CCTGCAGAAGCGGGTGAG REV: ATATGCGCAGGCTGCATC	183
L1[65]	FWD: GAATGATTTTGACGAGCTGAGAGAA REV: GTCCTCCCGTAGCTCAGAGTAATT	67
KMT5A	FWD: GGGAACTGCCAAACCAAAC REV: TTCAATGGAAGCCTTGCTG	127
KMT5B	FWD: AATTCCAGCTTCTTCCAACTC REV: GCATTCTTTTGCTCCAGCC	147
KMT5C	FWD: AGATGAACGTCAGCCCTGTG REV: CCGCTGCCTCAGGAAAGTT	80
	FWD: GCCCGCTACTTCCAGAGC REV: GGAGGTAGCGATAGACGTGG	70
	FWD: AGGTGACATGCTTCTACGG REV: CTGGTTCGGAAAGCTCCTTC	100
SIRT6[99–101]	FWD: GAGGAGCTGGAGCGGAAGGTGTG REV: GGCCAGACCTCGCTCCTCCATGG	156
	FWD: CTCCTCCGCTTCCTGGTC REV: CGTCTTACACTTGGCACATTCTT	123
	FWD: CTGGTCAGCCAGAACGTGGA REV: CACGACTGTGTCTCGGACGTA	135
MORC2	FWD: TCGGAAGCGGAGTGTC REV: CGTGCAGCCCTTTATCT	191
GAPDH[25]	FWD: TGGAGAAGGCTGGGGCTCAT REV: GACCTTGGCCAGGGGTGCTA	176
ß-Actin	FWD: CGAGAAGATGACCCAGATCA REV: ATAGCACAGCCTGGATAGCA	74

2.2.6 Statistical analysis and Figure preparations

Data calculations were performed with Microsoft Excel (Microsoft Corporation, Redmond, WA, USA) and the statistical significance was determined with the SPSS 24.0 software (IBM, Chicago, USA) by setting $p<0.05$ as significant and $p<0.01$ as highly significant. Mean and median values including ranges (lowest to highest) and standard deviations were calculated for all parameters of interest. Differences between variables within two groups (non-normally distribution) were analyzed using Mann-Whitney *U* test (two-tailed). Relationships between variables were calculated with Pearson`s and/or Spearman`s rank correlation. Correlation directions (positive [+], negative [-]) and strengths were assumed with the correlation coefficient r (range: 0.50-1.00 strong, 0.30.-0.49 medium, 0.10-0.29 weak, 0.00-0.09 no correlation).[102,103] ChemDrawBio Ultra 12.0 Software was used to design Figures manually.

2.2.7 Protein extraction and western blot analysis of sperm nucleoproteins

Swim-up semen samples (motile and immotile fractions) were defrozen on ice, at least 20 x 10^6 sperm cells were taken and washed with PBS (in DEPC-H_2O). Sperm cells were resuspended in Tris-Urea buffer (8 M Urea, 2 % SDS, 50 mM Tris (pH 8.0), 105 mM NaCl, 1 mM PMSF, 10 mM DTT, 1x Proteinase Inhibitor Cocktail) and incubated at RT for 30 min under frequent vortexing. Then sperm cells were sonicated with ultrasonic processor Vibra Cell for three cycles, each 10 s (Amplitude 30 %, max. pulse). Removal of cell debris was performed by centrifugation (10 min, 13.000 rpm, RT) and whole protein extracts were taken into a new tube. Protein concentrations were measured (Nanodrop) and extracts were kept at -80 °C until further processing.

25-50 µg protein were mixed with 4x Laemmli loading buffer and put on a SDS Gel. This consisted of a 15 % running gel (2.3 mL ddH_2O, 5 mL acrylamide, 2.5 mL running gel buffer, 100 µL SDS [10 %], 100 µL APS [10 %], 4 µL TEMED) and a 4 % stacking gel (2.1 mL ddH_2O, 500 µL acrylamide, 380 µL stacking gel buffer, 30 µL SDS [10 %], 30 µL APS [10 %], 3 µL TEMED). Protein separation was started at 100V for ~20 min, until the proteins reached the running gel and continued at 140 V for ~100 min until the proteins reached the bottom of the gel. Gels were equilibrated for 15 min in transfer buffer. In the meantime, a PVDF membrane (0.45 µM) was activated in 100 % for 5 min, washed for 2 min in ddH_2O and equilibrated 5 min in transfer buffer. Semi-dry was used as protein transfer technique for 30 min at 150 mA and 25 V (max). After protein transfer the membranes were dried at 37 °C for 15 min to bind proteins irreversible.

Subsequent to renewed activation of the membrane the whole protein content, which was transferred onto the membrane, was analyzed with the REVERT^{TM} Total Protein Stain Kit. Images of these stainings were documented with the Odyssey Fc system for later normalization. After that the membrane was blocked in Odyssey blocking buffer (1:3 in PBS) for 1 h at RT. Primary antibodies (H4K20me3 [ab9053], 1:500; H4K20me2 [ab9052], 1:500; GAPDH [ab9485], 1:2500; SIRT6 [ab62739/ab176345], 1:2000/1:500; KMT5C [ab91224], 1:100) diluted in Odyssey blocking buffer (1:3 in PBS, 0.1 % Tween-20) were added to the membrane and incubated overnight at 4 °C on a rotator (15 rpm). Hereafter the membranes were washed three times with PBST buffer for 5 min (20 rpm) and incubated for 1 h (15 rpm) with secondary antibody (IRDye® 800CW/680LT Goat anti-Rabbit IgG, 1:10000) diluted in Odyssey blocking buffer (1:3 in PBS, 0.1 % Tween-20, 0.01 % SDS). After three times washing in PBST buffer for 5 min (20 rpm), membranes were rinsed three times with PBS and fluorescence signals were detected with the Odyssey Fc system (2 min acquisition).

2.2.8 IHC on human/bull/mouse testis tissues and ICC with human spermatozoa

Immunohistochemical (IHC) stainings were performed to analyze H4K20me3 (ab9053), H4K20me2 (ab9053) and YY1 (ab109237) on human testis tissues, obtained for TESE (testicular sperm extraction) and on wildtype mouse/bull testis tissues, all exhibiting normal spermatogenesis. Immunocytochemical (ICC) stainings for H4K20me3 (ab9053), H4K20me2 (ab9053) and YY1 (ab109237) were performed with human spermatozoa (motile fractions) from healthy donors.

At the start formalin-fixed and paraffin-embedded human testis tissue samples on microscope slides (R. Langenbrinck) were deparaffinated stepwise in Xylol (3 x 10 min) and Ethanol (2 x 5 min in 100 % EtOH, 2 x 5 min in 96 % EtOH and 2 x 5 min in 70 % EtOH) and cooked for 20 min in citrate buffer (18 mM citric acid monohydrate, 82 mM sodium citrate) to improve primary antibody binding. After cooling down for 30 min at RT, peroxidase activity was inhibited by blocking in ice cold hydrogen peroxide solution in methanol (3 % H_2O_2 in MeOH). Then the slides were washed three times for 5 min in Tris-HCl buffer (0.1 M Tris-HCl, 0.1 M NaCl) and blocked for 20 min in BSA solution (5 % in Tris-HCl) to prevent non-specific antibody binding. Primary antibodies (H4K20me3, ab9053, 1:100; H4K20me2, ab9053, 1:100; YY1, ab109237, 1:200) diluted in BSA solution were dropped onto one side of the slides and incubated overnight at 4 °C. As negative control BSA solution without antibody was dropped onto the other side of each slide. The slides were washed three times for 5 min in Tris-HCl buffer and incubated at RT

for 1 h with secondary antibody (goat anti-rabbit IgG, 1:200, Dako). After repeated washing in Tris-HCl buffer (3 x 5 min) slides were developed for 10-30 min with ABC-Peroxidase Staining Kit. Development was stopped through washing in ddH_2O (3 x 5 min) and counterstaining was performed for 5 s in Mayer`s Haemalaun with final washing in dH_2O (3 x 5 min). Slides were mounted with Dako Faramount and covered with glass plates followed by microscopic examination and documentation of the antibody staining pattern.

ICC slides were prepared by scratching out at least one million sperm cells (motile swim-up fraction) onto a glass plate. After drying, sperm cells were decondensed for 10 min in DTT (10 mM in Tris-HCl buffer) and further 2 h in Lithium diiodo salicylate solution (10 mM LIS in 1 mM DTT Tris-HCl buffer). Then sperm cells were fixed with 4 % PFA (in PBS, pH 7.4) and blocked for 15 min in BSA/Triton solution (0.1 % BSA, 2 % Triton X-100 in PBS). Primary and secondary antibody incubation, as well as ABC system, Dako reagents and documentation were performed as described above for human testis tissue.

2.2.9 ChIP and ChIP-qPCR with human spermatozoa

Chromatin Immunoprecipitation (ChIP) was performed with H4K20me3 (ab9053) and ChIP-IT High Sensitivity Kit (Active Motif, Cat. No. 53040) on 10-20 Mio motile and immotile human sperm cells of four healthy donors to analyze DNA loci, which are interacting with this histone modification. According to the manufacturer`s protocol, with following modifications, sperm cells were first fixed with formaldehyde, to cross-link protein/DNA complexes. Then sperm cells were sonicated, using ultrasonic processor Vibra Cell ten times for 30 s on and 30 s off at an 40 % amplitude (total 10 min), to generate the desired DNA fragmentation (200-1200 bp). After centrifugation (10 min, 13000 rpm, 4°C) 10 % of the supernatant were abstracted as input and another 10 % for a chromatin check on 2 % agarose gel. The remaining supernatant (80 %) of each sample was incubated with 8 µg H4K20me3 (ab9053) overnight at 4°C for immunoprecipitation. Antibody-bound protein/DNA complexes were captured with Protein G agarose beads and washed using the provided ChIP filtration columns. After elution of the complexes from these columns reverse cross-linking and Proteinase K digestion was performed, to separate protein/DNA complexes. Finally, DNA was purified using the provided DNA purification columns and concentration of double stranded DNA (dsDNA) was determined using Qubit 2.0 Fluorometer (Cat. No. Q328669).

Recently, our group (Ozturk *et al*., 2019 in preparation) identified through an MNase followed by genome-wide ChIP-sequencing of motile human sperm fractions (three healthy volunteers) the genome/gene loci, which are highly enriched with H4K20me3. Based on these results, ChIP-qPCR primer sets (Table 4) in promoter regions of five selected genes enriched for H4K20me3 were designed or chosen from literature.

Table 4: Primer sets used for H4K20me3-ChIP-qPCR in motile and immotile human sperm cells.

Gene	Primer sequences (5`-3`)	PCR product size (bp)
CXCL8	FWD: TGGCTGGCTTATCTTCACCA REV: AGTGGCAGGTGTTAGAACAAGA	107
TNSFS13B	FWD: GCAGGAACTTTCAGCTGCTTTT REV: AGCCCACCCTTAAGTGTAGCAA	90
IFNW1	FWD: TGGTTCTAAAGAGCTTATTTGCTGC REV: AGCCTCCATTTTTACCCTCCT	110
CST8	FWD: TTTAGACCAAAGGCCGGAGG REV: TGCAGGGAGGTTACGCTTTG	95
***L1-*ORF1**[104]	FWD: TAACCAATACAGAGAAGTGC REV: GATAATATCCTGCAGAGTGT	298
***L1-*5`UTR**[65]	FWD: GAATGATTTTGACGAGCTGAGAGAA REV: GTCCTCCCGTAGCTCAGAGTAATT	67

An intra- and inter-individual comparison of H4K20me3 enrichments in motile and immotile sperm cells was performed. Therefore, relative binding of H4K20me3 was calculated using the ChIP-qPCR signals (CTs generated with H4K20me3-precipitated DNA and respective input DNAs). Relative binding of H4K20me3 was calculated as enrichments over the input signals.

3. Results

3.1 In fertile men, *DNMT1* and *DNMT3A* mRNAs are stored at high levels in motile spermatozoa and are strongly correlated to each other

Here, the gene expression levels of the DNA methyltransferase *DNMT1* (maintenance) and *DNMT3A* (*de novo*) were measured in human spermatozoa. Total sperm RNA from motile human spermatozoa of 96 donors (donors` M) and 48 subfertile patients (patients` M) were extracted and reverse transcribed into cDNA. Specific qPCR primer sets for *DNMT1* and *DNMT3A* (Table 3) were used to quantify and compare the mRNA levels in donors` and patients` M using RT-qPCR. Figure 15 displays the relative and logarithmic mRNA levels as box plots (dark blue: DNMT1, light blue: DNMT3A) for the cohorts after normalization to the housekeeping gene *GAPDH* (Table 3).

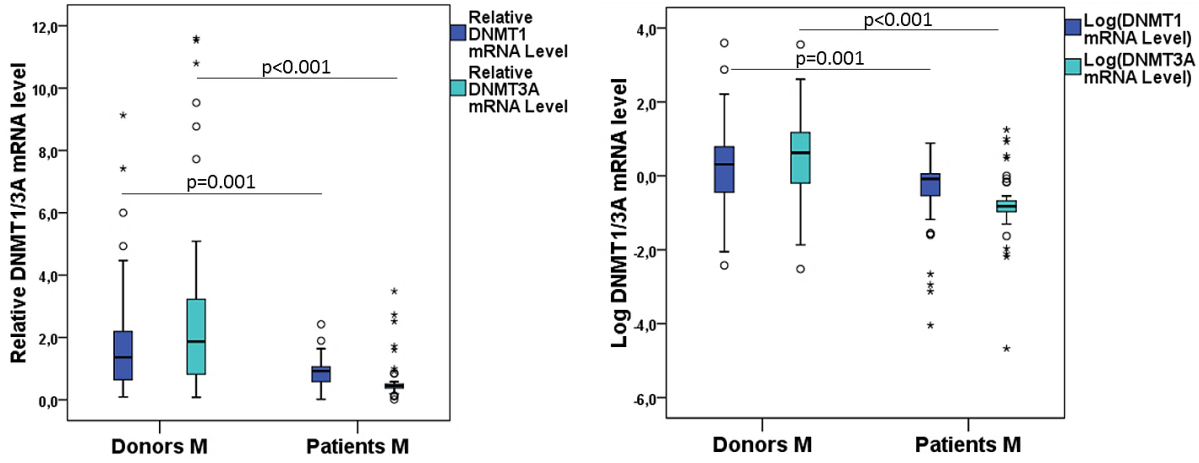

Figure 15: *DNMT1/DNMT3A* mRNA levels of donors` and patients` M (left: relative scale; right: log scale). Both transcript levels were significantly decreased in patients` M compared to donors` M (p=0.001/p<0.001, n=144/143).

Both the *DNMT1* and *DNMT3A* mRNA levels in patients` M were significantly decreased (p=0.001/p<0.001, n=144/143) compared to the healthy donors` M. More precisely, as shown in Table 5, the median *DNMT1* (0.92±0.47) and *DNMT3A* (0.44±0.67) mRNA values in patients` M were reduced by 33 % and 77 %, respectively.

Table 5: Descriptive statistics of relative *DNMT1* and *DNMT3A* mRNA level.

Descriptive Statistics	Relative *DNMT1* mRNA level (n=144)		Relative *DNMT3A* mRNA level (n=143)	
	Donors M (n=96)	Patients M (n=48)	Donors M (n=95)	Patients M (n=48)
Average	2.34	0.84	2.87	0.64
Median	1.37	0.92	1.87	0.44
Standard deviation	4.43	0.47	4.24	0.67
Range	0.09-36.4	0.02-2.42	0.08-34.91	0.01-3.49

Through a correlation analysis (Figure 16), it could be determined in motile spermatozoa that both *DNMT1* and *DNMT3A* mRNA levels correlated significantly (strong positive) to each other ($p<0.001$, $r=0.671$, $n=143$). *DNMT1* and *DNMT3A* mRNA levels were not significantly correlated to clinical or spermiogram data of patients` and donors` M, such as age, sperm concentration, fertilization rate, pregnancy outcome, progressive and total motility.

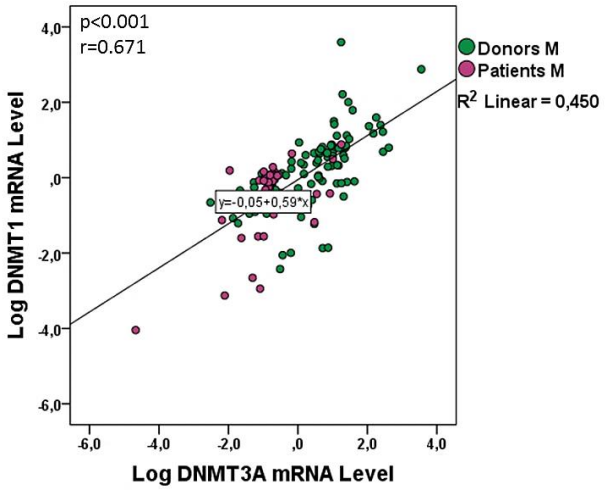

Figure 16: Significant positive correlation ($p<0.001$, $r=0.671$, $n=143$) between *DNMT1* and *DNMT3A* mRNA levels of donors`/patients` M (log scale).

Taken together, these data show that decreased mRNA levels of *DNMT1* and *DNMT3A* are characteristic for patients` motile sperm cells and can possibly influence their global DNA methylation status.

3.2 Analysis of the global DNA/RNA methylation & *L1* methylation states in motile and immotile human spermatozoa

In order to analyze possible influences of decreased DNA methyltransferase levels detected in patients` M, global DNA methylation and *L1* methylation were investigated in patients` M and donors` M as well as in immotile human spermatozoa of donors (donors` IM). In addition, 5-hmC and RNA methylation (m6A) were analyzed in the same samples.

3.2.1 5-mC / 5-hmC DNA and m6A RNA methylation in motile human spermatozoa

Total sperm DNA & RNA from 20 donors` M and 20 patients` M were extracted and their global methylation status was analyzed by ELISA (MethylFlashTM Global DNA Methylation ELISA Easy Kit, EpiQuik RNA Methylation Quantification Kit; Gentaur). Figure 17 shows the 5-mC DNA and m6A RNA methylation as box plots (green: donors` M, purple: patients` M).

5-hmC was analyzed using ELISA (MethylFlashTM Global DNA Hydroxymethylation ELISA Easy Kit, Gentaur) in 20 donors` M and 20 patients` M, and was absent (0.00 %) and thus not illustrated here.

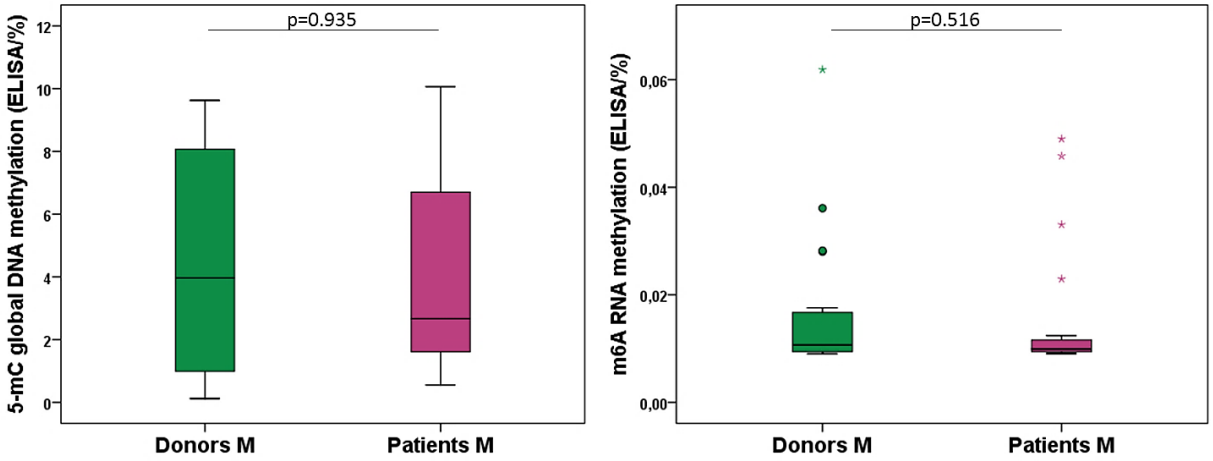

Figure 17: 5-mC DNA (left) and m6A RNA (right) methylation in donors` versus patients` M analyzed by ELISA. No significant differences in 5-mC DNA (p=0.935, n=40) and m6A RNA (p=0.516, n=40) methylation were found.

5-mC levels in patients` and donors` M did not differ significantly (p=0.935, n=40) from each other and ranged from 0.12 to 10.1 %. The methylation levels of m6A RNA were much lower and ranged from 0.01 to 0.06 % in patients` and donors` M and did not, as well, differ significantly between the two groups (p=0.516, n=40). In Table 6 the exact methylation values can be inspected.

Table 6: Descriptive statistics of 5-mC and m6A analyzes.

Descriptive Statistics	**5-mC global DNA methylation (Elisa/%, n=40)**		**m6A RNA methylation (Elisa/%, n=40)**	
	Donors M (n=20)	**Patients M (n=20)**	**Donors M (n=20)**	**Patients M (n=20)**
Average	4.52	3.97	0.02	0.02
Median	3.97	2.67	0.01	0.01
Standard deviation	3.68	3.00	0.01	0.01
Range	0.12-9.63	0.55-10.06	0.01-0.06	0.01-0.05

5mC DNA and m6A RNA methylation levels were not significantly correlated to clinical or spermiogram data of patients` and donors` M. Also, no significant correlation between DNA methyltransferases (*DNMT1* and *DNMT3A*) and global 5-mC DNA or m6A RNA methylation were found here in the cohorts.

The global DNA Methylation ELISA Easy Kit based findings showed here, that there are no differences in global DNA methylation levels between the motile sperm cells from healthy donors and subfertile patients. Also, RNA methylation levels were comparable in these two groups.

L1 is a retrotransposon that makes up to 17.0 % of the human genome and it was shown, that this element can serve as a surrogate measure for the global DNA methylation level.[73] For this reason, the *L1* methylation status in human spermatozoa was additionally investigated using two different methods, ELISA and pyrosequencing.

3.2.2 ELISA analyzes reveal that motile spermatozoa from healthy men possess higher *L1* methylation in comparison to that in subfertile men

Using ELISA for *L1* methylation analysis (Global DNA Methylation - *L1* Kit, Cat. No. 55017) total sperm DNAs extracted from 79 donors` M, 78 donors` IM and 48 patients` M were evaluated. In Figure 18 (left) the *L1* methylation levels of the cohorts (green: donors` M, orange: donors` IM, purple: patients` M) are shown as box plots.

For *L1* methylation analysis using pyrosequencing (*L1* pyrosequencing kit, Cat. No. 970012; levels shown in Figure 18, right) total sperm DNAs from 33 donors` M, 38 donors` IM and 48 patients` M were extracted and bisulfite treated (EZ DNA Methylation Kit).

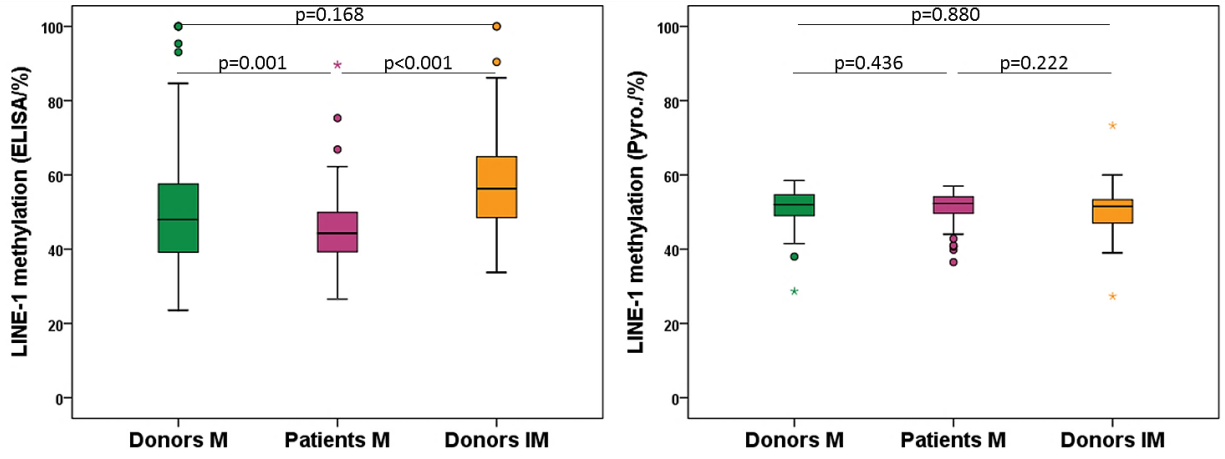

Figure 18: *L1* methylation of donors` M/IM and patients` M analyzed by ELISA (left) and pyrosequencing (right). No difference in *L1* methylation is measurable using pyrosequencing. Using ELISA, *L1* methylation is significantly decreased in patients` M compared to donors` M (p=0.001, n=127) and donors` IM (p<0.001, n=126). Between donors` M and IM no difference in *L1* methylation is measurable (p=0.168, n=157).

Evaluating the pyrosequencing results (Figure 18, right) no significant differences were found between the cohorts (all p>0.05). Median *L1* methylation of donors` M (52.0±6.22), donors` IM (51.5±7.06) and patients` M (52.3±4.67) of the three CpGs investigated by pyrosequencing are almost identical (Table 7).

By using the ELISA kit (Figure 18, left), *L1* methylation was found significantly decreased in patients` M compared to donors` M (p=0.001, n=127) and donors` IM (p<0.001, n=126). No significant difference in *L1* methylation was found between donors` M and IM (p=0.168, n=157). This different result is probably due to the higher number of analyzed CpGs (n=12) and a different L1 region considered. Evaluation of median values (Table 7) showed, that *L1* methylation was reduced in patients` M (44.3±12.5) by 7.7 % compared to donors` M (48.0±18.8) and by 21 % compared to donors` IM (56.3±13.5).

Table 7: Descriptive statistics of *L1* methylation analyzes.

Descriptive Statistics	***L1* methylation (Elisa/%; n=205)**			***L1* methylation (Pyro./%; n=118)**		
	Donors M (n=79)	**Donors IM (n=78)**	**Patients M (n=48)**	**Donors M (n=33)**	**Donors IM (n=38)**	**Patients M (n=47)**
Average	52.25	58.07	47.19	50.54	50.33	51.11
Median	47.96	56.32	44.29	52.00	51.50	52.33
Standard deviation	18.79	13.52	12.53	6.22	7.06	4.67
Range	23.55-100	33.73-100	26.53-89.73	28.67-58.50	27.33-73.33	36.50-57.00

L1 methylation levels, analyzed by pyrosequencing and ELISA, were not significantly correlated to clinical and spermiogram data of patients` and donors` M. A significant correlation of *L1* methylation levels to other genes (*DNMT1* and *DNMT3A*, Figure 19), 5-mC DNA and m6A RNA methylation was not found here.

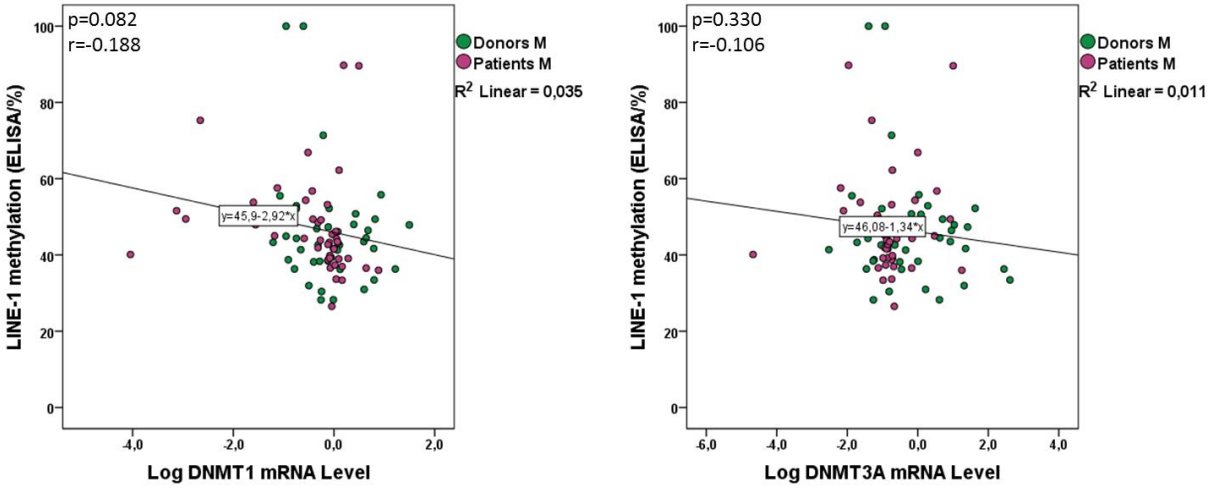

Figure 19: No significant correlation between *L1* methylation and *DNMT1* (p=0.082, r=-0.188, n=87; left) or *DNMT3A* (p=0.330, r=-0.106, n=87; right) mRNA levels of donors` and patients` M.

Overall, differences in global methylation could be detected in patients` M using *L1* ELISA. As next, *L1* mRNA levels were investigated in motile and immotile human spermatozoa, in order to examine if there are any differences.

3.2.3 Immotile spermatozoa possess high levels of *L1* mRNA

Total sperm RNAs from 58 donors` M, 50 donors` IM and 33 patients` M were extracted and reverse transcribed into cDNA. A specific PCR primer set for *L1* (Table 3) was used to quantify and compare the mRNA levels in donors` M and IM, and patients` M using RT-qPCR. Figure 20 displays the relative and logarithmic *L1* mRNA levels as box plots (green: donors` M, orange: donors` IM, purple: patients` M) for the cohorts after normalization to the housekeeping gene *β-Actin* (Table 3).

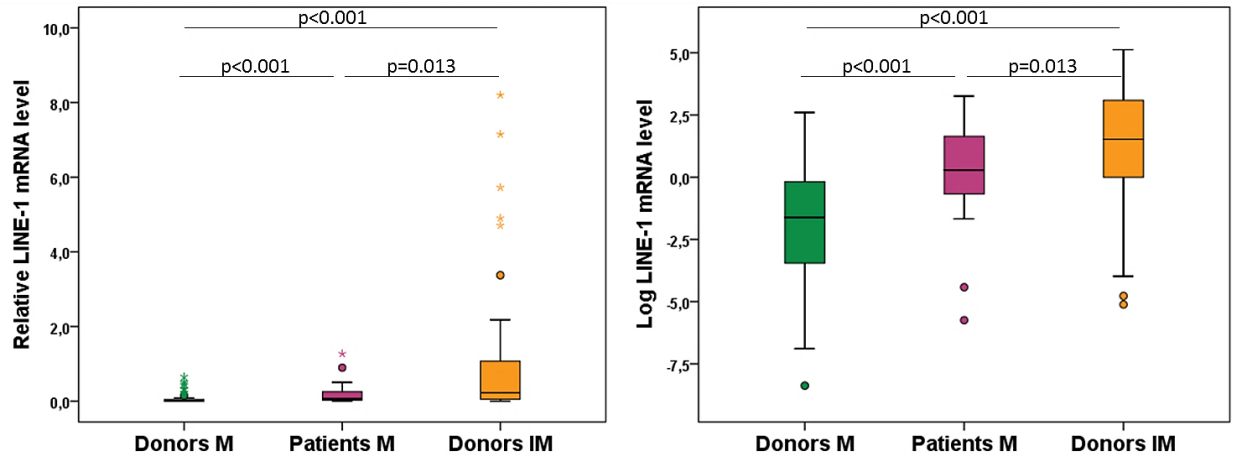

Figure 20: *L1* mRNA level of donors` M/IM and patients` M analyzed by RT-qPCR (left: relative scale 1:20; right: log scale). *L1* mRNA levels were at highest in donors` immotile sperms and are significantly increased compared to donors` (p<0.001, n=108) and patients` motile sperm fractions (p=0.013, n=83).

It was obvious, that *L1* mRNA levels were significantly increased in donors` IM compared to donor`s (p<0.001, n=108) and patients` M (p=0.013, n=83). Table 8 demonstrates that in donors` motile sperm the L1 mRNA levels were at lowest (0.19±3.08) and gradually increased in patients` motile sperm (1.33±5.61) and were at highest level in immotile sperm cells (4.59±38.5). This corresponds to 96 % and 71 % lower *L1* mRNA levels in donors` and patients` M, respectively. These observations provide a strong indication, that L1 is dysregulated (upregulated) in immotile sperms as well as in motile sperm of subfertile men.

Table 8: Descriptive statistics of relative *L1* mRNA level.

Descriptive Statistics	Relative *L1* mRNA level (n=141)		
	Donors M (n=58)	Donors IM (n=50)	Patients M (n=33)
Average	1.60	21.51	3.69
Median	0.19	4.59	1.33
Standard deviation	3.08	38.50	5.61
Range	0.00-13.49	0.01-168.04	0.00-26.06

It is well-known, that L1 in somatic cells are suppressed by DNA hypermethylation.[61,74,105] In agreement with this, a significant negative correlation between *L1*-mRNA and -methylation levels was found here in motile human spermatozoa (p<0.001, r=0.3681, n=91; Figure 21, left).

In addition, a highly significant positive correlation between the fertilization rate and *L1* methylation was found, exclusively in the patient subgroup showing a positive pregnancy (p=0.009, r=0.555, n=21; Figure 21, right).

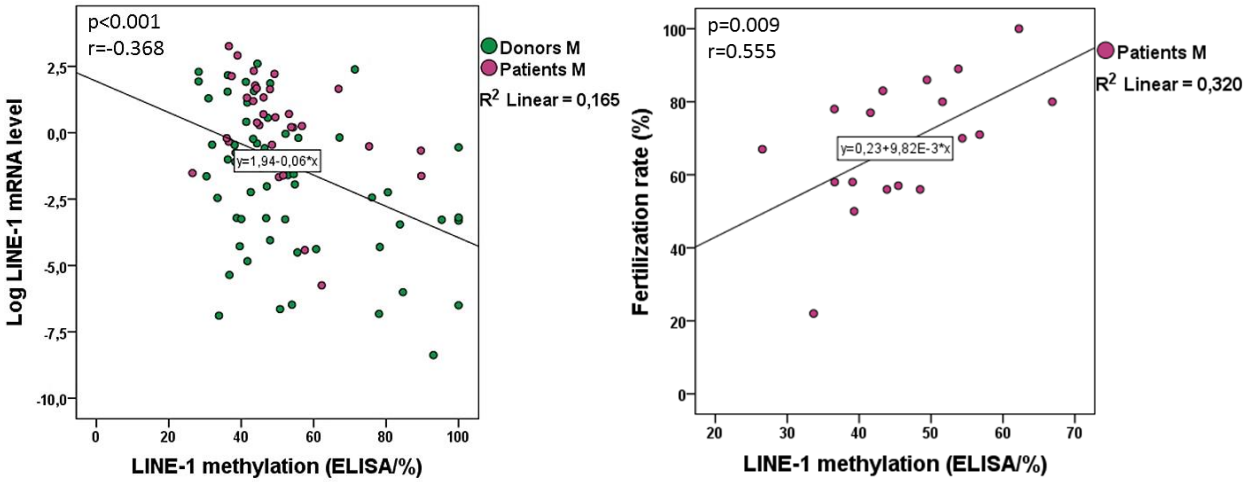

Figure 21: Significant negative correlation (p=0.008, r=-0.368, n=91) between *L1* methylation and mRNA levels in donors` and patients` M (left). Significant positive correlation (p=0.009, r=0.555, n=21) between *L1* methylation and fertilization rate in patients` M with a positive pregnancy (right).

L1 mRNA levels were not significantly correlated to other clinical and spermiogram data of patients` and donors` M such as age, sperm concentration, fertilization rate, pregnancy outcome, progressive and total motility. Also, no significant correlations of *L1* expression to expression of other genes (*DNMT1* and *DNMT3A*) were found. In donors` M, 5-mC DNA and *L1* methylation, analyzed by ELISA, were positively correlated to each other, but their correlation coefficient was very low (p=0.045, r=0.154, n=20).

All these findings suggest, that a targeted regulation of L1 elements is important for male fertility and ART outcome. For this reason, different epigenetic regulators of L1, well known from studies on somatic cells, were studied in human sperm cells and, moreover in healthy human testis tissues, in order to evaluate those factors relevant for L1 regulation in human spermatogenesis and in mature sperm.

3.3 *SIRT6* methylation and expression analyzes

Sirtuin 6 (SIRT6) is a histone deacetylase, which packages L1 elements into transcriptionally repressive heterochromatin in human dermal fibroblasts but fails with stress and age by for e. g. *SIRT6* promoter methylation and reduced expression.[89]

Here, for *SIRT6* methylation analysis using pyrosequencing (*SIRT6* pyrosequencing kit, Cat. No. 978746) total sperm DNA from 32 donors` M, 35 donors` IM and 47 patients` M were extracted and bisulfite treated (EZ DNA Methylation Kit). In Figure 22 the evaluated *SIRT6* methylation levels in the cohorts are displayed (green: donors` M, orange: donors` IM, purple: patients` M).

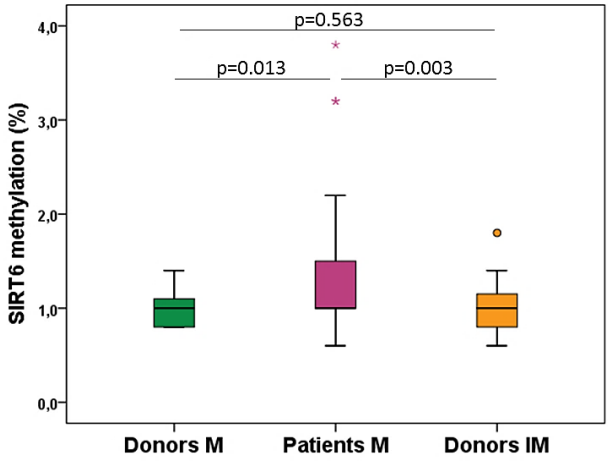

Figure 22: *SIRT6* methylation in donors` M and IM and patients` M was analyzed by pyrosequencing. *SIRT6* methylation was significantly increased in patients` M compared to donors` M and IM (p=0.003/p=0.013; n=79/n=82; respectively). Between donors` M and IM no difference was measured (p=0.563, n=67).

Patients' motile sperm possessed significantly increased *SIRT6* methylation (Table 9) in comparison to controls' motile (p=0.013, n=79) as well as immotile sperm (p=0.003, n=82). There was no difference in *SIRT6* methylation between donors` M and IM (p=0.563, n=67).

Table 9: Descriptive statistics of *SIRT6* methylation analyzed by pyrosequencing.

Descriptive Statistics	***SIRT6* methylation (Elisa/%, n=114)**		
	Donors M (n=32)	**Donors IM (n=35)**	**Patients M (n=47)**
Average	1.00	0.97	1.34
Median	1.00	1.00	1.00
Standard deviation	0.21	0.23	0.69
Range	0.80-1.40	0.60-1.80	0.60-3.80

In literature[91] it is described, that *SIRT6* methylation in lymphocytes increases with age. To check the situation in human sperm cells, *SIRT6* methylation was analyzed in correlation to age in the available samples (Figure 23). For all groups, no significant correlation between *SIRT6* methylation and age could be detected. Thus, it can be concluded that in sperm there is no age effect on *SIRT6* methylation.

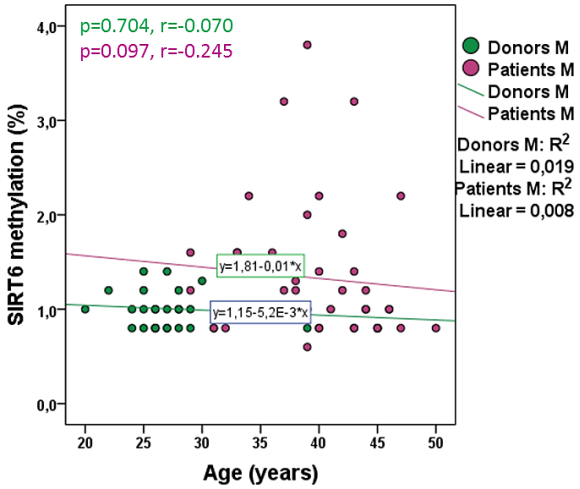

Figure 23: No significant correlation between *SIRT6* methylation and age in patients` M (p=0.097, n=47) and donors` M (p=0.704, n=32) was found.

It is tempting to speculate, if increased *SIRT6* methylation in patients` M decreased L1 packaging into silent heterochromatin and thus, led to L1 activation. Therefore, a correlation analysis between *SIRT6* methylation and *L1* mRNA level of patients` and donors` M was performed (Figure 24). No significant correlation was found, but the correlation directions were different between the cohorts.

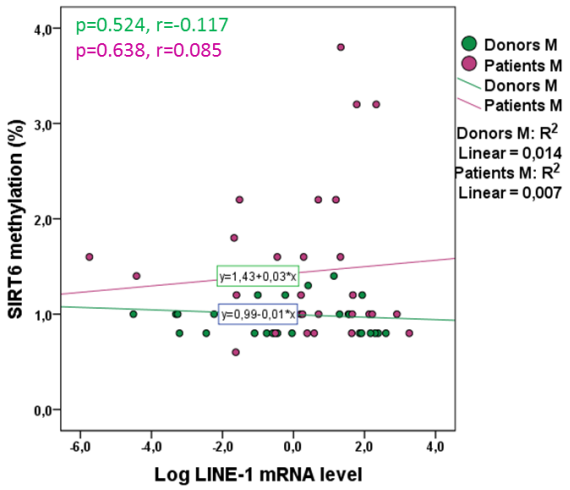

Figure 24: *SIRT6* methylation and *L1* mRNA level were not significantly correlated in patients` M (p=0.638, r=-0.085, n=33) and donors` M (p=0.524, r=-0.117, n=32).

SIRT6 mRNA and protein levels in human spermatozoa were analyzed as a next step, to see if these are connected with L1 regulation. Three different qPCR primer sets for *SIRT6* were taken from literature[99–101] (Table 3) to analyze *SIRT6* mRNA level in human spermatozoa. In five donors` M and LNCaP (human prostate cancer cell line used as positive control) the primer sets mentioned above were tested. In Figure 25 the agarose gels of the obtained PCR products for *SIRT6* analysis are shown.

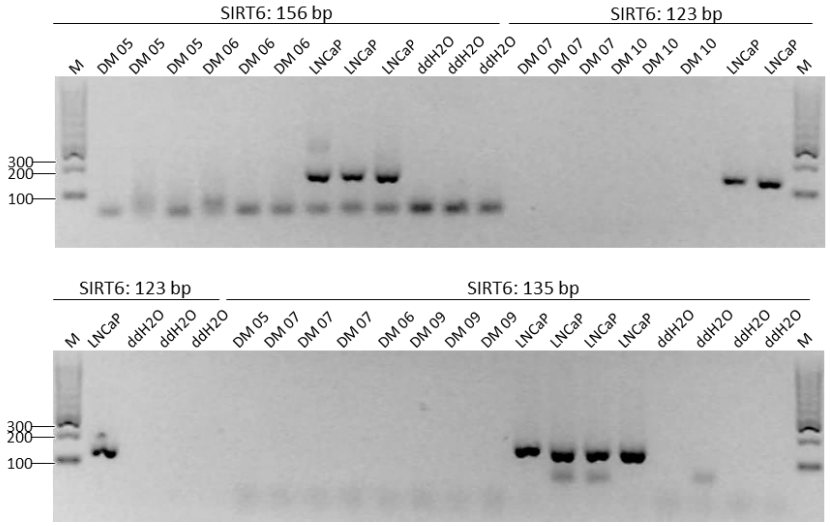

Figure 25: *SIRT6* mRNA analysis in donors` M using primers selected from published studies. SIRT6: 156 bp; Radak *et al*., 2011.[99] SIRT6: 123 bp; Wang *et al*., 2014.[100] SIRT6: 135 bp; Nagai *et al*., 2015.[101] All three qPCR primer sets worked well in positive controls (LNCaP, prostate cancer cell line). No PCR product bands could be amplified using indicated primer pairs in all five motile sperm samples.

The right PCR products were detected only in LNCaP cells, whereas in motile sperm samples *SIRT6* mRNA was absent. In the next step SIRT6 protein levels in motile human spermatozoa were analyzed by western blot using two different primary antibodies, to see if any *SIRT6* mRNA was translated during spermatogenesis and stored in mature sperm.

SIRT6 protein levels in donors` M could not be analyzed with western blot because of the weak performance of the used antibodies (Figure 26). Two primary antibodies against SIRT6 (ab62739 -no longer available at abcam, checked on February 5, 2019- and ab176345) were tested. Since no LNCaP protein extracts were available, those from HeLa were used as a positive control instead.

Ab62739 showed unspecific bands in the positive control HeLa (Figure 26, left, green band at 39 kDa), whereas ab176345 performed better (Figure 26, right, green band at 39 kDa). No SIRT6 was detected in all sperm samples.

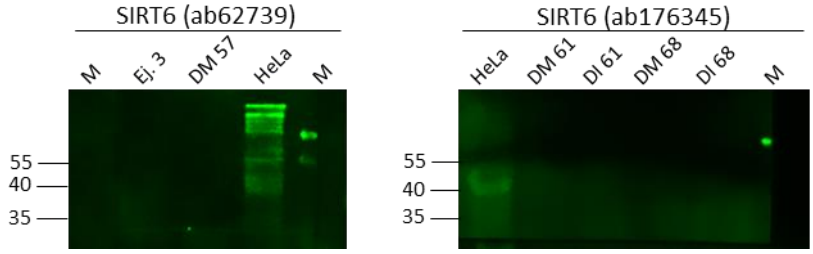

Figure 26: Western blot analysis using two SIRT6 primary antibodies on donors` M and HeLa cells (positive control). On the left picture ab62739 (SIRT6, 39 kDa, 1:2000, unspecific green bands in HeLa) and on the right picture ab176345 (SIRT6, 39 kDa, 1:500, green band in HeLa) was used as primary antibody against SIRT6. No bands in human sperm samples were detected using both antibodies (Ej. 3: whole ejaculate; DM: motile sperms; DI: immotile sperms).

To sum up, *SIRT6* methylation was increased in patients in comparison to fertile controls. No correlation between *SIRT6* methylation and age was found in human sperm. Regarding *SIRT6* expression, neither *SIRT6*-mRNA nor -protein could be detected in human sperm. The latter suggests, that SIRT6 is probably not expressed, at least during the last stages of human spermatogenesis. Also, neither significant correlations of *SIRT6* methylation to clinical and spermiogram data of patients` and donors` M nor to methylation (5-mC, m6A and *L1*) and mRNA (*DNMT1*, *DNMT3A* and *L1*) data previously obtained were found here.

3.4 Analyzes on *MORC2* mRNA in human sperm

MORC2 (microrchidia 2) is a chromatin regulator and suppresses L1 elements by silencing its transcription in human chronic myeloid leukemia K562 and human embryonic stem cells (hESC).[93] Total sperm RNA from 32 donors` M, 24 donors` IM and 46 patients` M were extracted and reverse transcribed into cDNA. For *MORC2* mRNA levels analysis a specific PCR primer set was designed (Table 3) and used to quantify and compare the levels in donors` M and IM and patients` M using RT-qPCR. Figure 27 displays the relative and logarithmic *MORC2* mRNA levels as box plots (green: donors` M, orange: donors` IM, purple: patients` M) for the cohorts after normalization to the housekeeping gene *β-Actin* (Table 3).

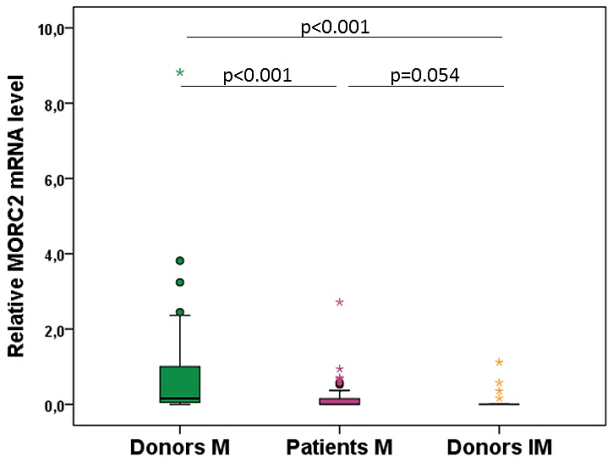

Figure 27: *MORC2* mRNA measured in donors` M and IM and patients` M. In healthy donors` M, *MORC2* mRNA levels were significantly increased compared to patients` M (p<0.001, n=78) and donors` IM (p<0.001, n=56).

Relative *MORC2* mRNA levels were significantly higher in donors` M compared to patients` M (p<0.001, n=78) and donors` IM (p<0.001, n=56). The relative *MORC2* mRNA was in 4 donors` M, 20 donors` IM and 26 patients` M not detectable and therefore set as zero. The logarithmic scale could not be used here as the log (0) is not defined. Table 10 summarizes the average and median relative values observed for *MORC2* mRNA.

Table 10: Descriptive statistics of relative *MORC2* mRNA level.

Descriptive Statistics	Relative *MORC2* mRNA level, inclusive zero values (n=102)			Relative *MORC2* mRNA level, exclusive zero values (n=52)		
	Donors M (n=32)	Donors IM (n=24)	Patients M (n=46)	Donors M (n=28)	Donors IM (n=4)	Patients M (n=20)
Average	0.95	0.09	0.19	1.09	0.55	0.44
Median	0.16	0.00	0.00	0.34	0.47	0.25
Standard deviation	1.76	0.26	0.45	1.84	0.41	0.61
Range	0.00-8.82	0.00-1.12	0.00-2.72	0.01-8.82	0.16-1.12	0.01-2.72

To conclude, 28/32 in donors` M (87.5 %) and only 20/46 (43.5 %) in patients` M and 4/24 donors` IM (16.7 %) had detectable levels of *MORC2* mRNA. Healthy donors' motile sperm fraction had stored significantly higher levels of *MORC2* mRNA. No significant correlation of *MORC2* expression to *L1* expression (Figure 28) and clinical and spermiogram data of patients` and donors` M were found here.

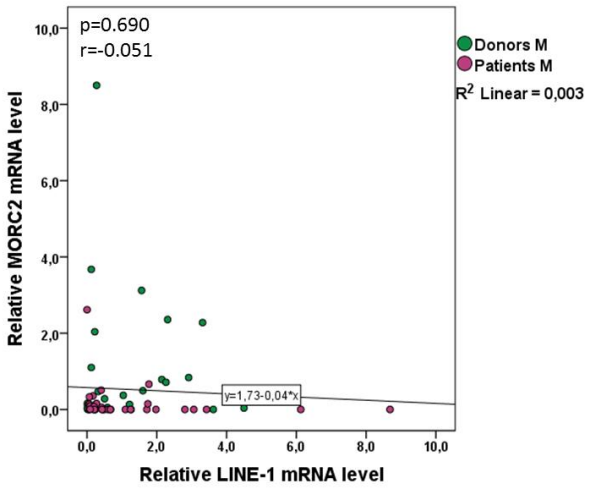

Figure 28: No significant correlation between *MORC2* and *LINE-1* mRNA levels in patients` M and donors` M (p=0.690, r=-0.51, n=63) was found.

3.5 YY1 expression analysis in human testis tissue

Human L1 elements contain a YY1 (Yin Yang 1) binding site at their 5`UTR, located on the antisense strand between position +13 and +21, and YY1 is known to regulate the human L1 transcription initiation.[60,88] Here, human testis tissue samples exhibiting normal spermatogenesis (obtained from patients with non-obstructive azoospermia for testicular sperm extraction) were investigated for YY1 expression (ab109237, 1:200).

Figure 29 shows that YY1 is exclusively expressed in Sertoli cells and no YY1 signal can be found in any spermatogenetic cell of the seminiferous epithelial cycle (I-V). Therefore, further experiments of YY1 in human spermatozoa were not performed.

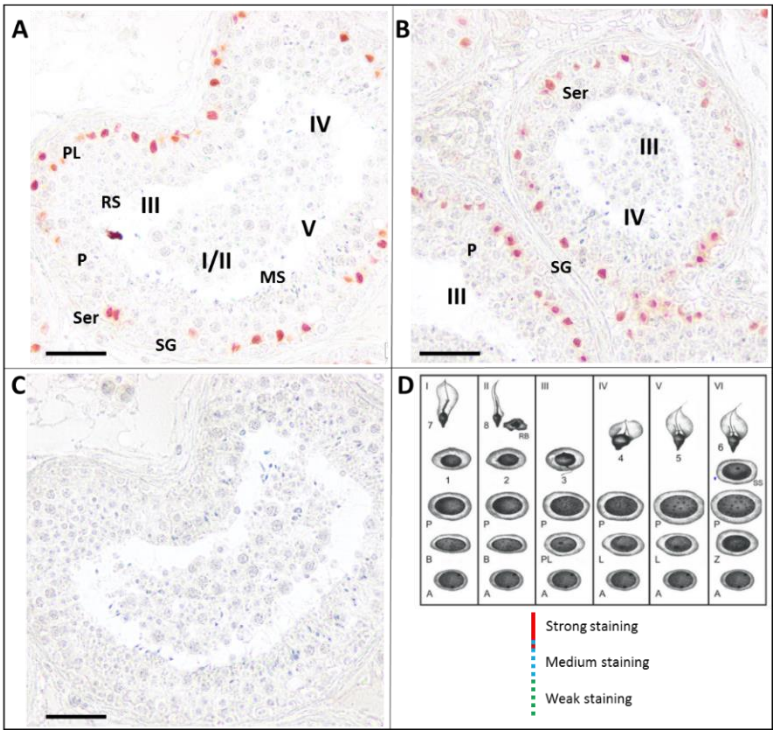

Figure 29: **A**-**C** show exemplary tubules with different stages of the seminiferous epithelial cycle (I-V), where YY1 (ab109237, 1:200) is only detectable in Sertoli cells. **C** represents the negative staining of serial section **A**. Magnification x40, Bar 50 µm. Sertoli cells = Ser; Spermatogonia = SG; Spermatocytes of the preleptotene stage = PL and pachytene stage = P; Round spermatids = RS; Maturing spermatids = MS. **D** shows a scheme[106] of the seminiferous epithelial cycle of man; modified from Clermont, 1963.[107]

3.6 Histone modifications & regulators associated with L1

Previously our group[34] showed that nucleosomes after protamine exchange are located in repetitive DNA elements, like L1 and SINEs. L1 elements were shown to be activated shortly after fertilization in the early mouse embryo and regulate global chromatin accessibility there.[62] The methylation status of histone 4 lysine 20 (H4K20me) has been identified as key player of the genomic integrity, playing distinct roles for DNA damage repair, DNA replication and chromatin compaction.[46] In 2016 a comprehensive study identified histone isoforms and post-translational modifications (PTHM) existing in mouse and human male germ cells.[42] On the H4 tail peptide encompassing amino acids 20-23, H4K20me2 was the most abundant PTHM (80.9 %) besides H4K20me3 (9.8 %) and H4K20me1 (7.9 %). The heterochromatin marker H4K20me3, and H4K20me2 and their regulators (histone methyltransferases KMT5A, KMT5B and KMT5C) were analyzed next, to see if they are associated with L1 regulation in spermatozoa.

3.6.1 IHC analyzes of H4K20me2 in human, mouse and bull testis samples

Healthy human testis tissues obtained for TESE, wildtype mouse and healthy bull testis tissues, all exhibiting normal spermatogenesis, were analyzed for H4K20me2 expression, using immunohistochemistry (IHC).

Figure 30 shows that H4K20me2 (ab9052, 1:100) is detectable in spermatogonia of stage I until step 4 elongating spermatids in man. The highest staining intensity for H4K20me2 can be observed in spermatogonia type B, then weaker in primary spermatocytes and again higher in elongating spermatids. In pachytene spermatocytes (III-V) and maturing spermatids (I/II/V) no H4K20me2 was present.

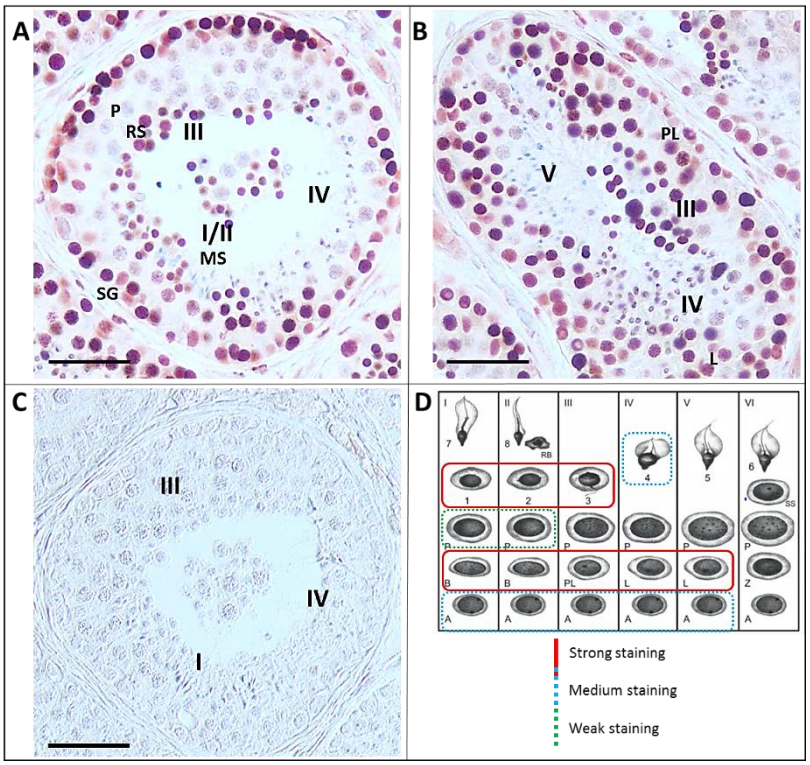

Figure 30: H4K20me2 is detectable in human SG of stage I until step 4 ES in man. In P (III-V) and MS (I/II/V) no H4K20me2 was present. **A**-**C** show exemplary tubules with different stages of the seminiferous epithelial cycle (I-V). **C** represents the negative staining of serial section **A**. Magnification x40, Bar 50 µm. Spermatogonia = SG; Spermatocytes of the preleptotene-/leptotene stage = PL/L and pachytene stage = P; Round spermatids = RS; Maturing spermatids = MS; Elongating Spermatids = ES. **D** shows a scheme[106] of the staining intensities of H4K20me2 in the seminiferous epithelial cycle of man; modified from Clermont, 1963.[107]

In mouse (Figure 31) high expression of H4K20me2 (ab9052, 1:100) could be detected in spermatogonia (stage II-VI), and less in preleptotene-/leptotene spermatocytes (VII-X), pachytene spermatocytes (stage VII-XI), round spermatids (stage I-VIII) and elongating spermatids (stage IX-XI). In maturing spermatids (stage I-VIII) no H4K20me2 was sighted.

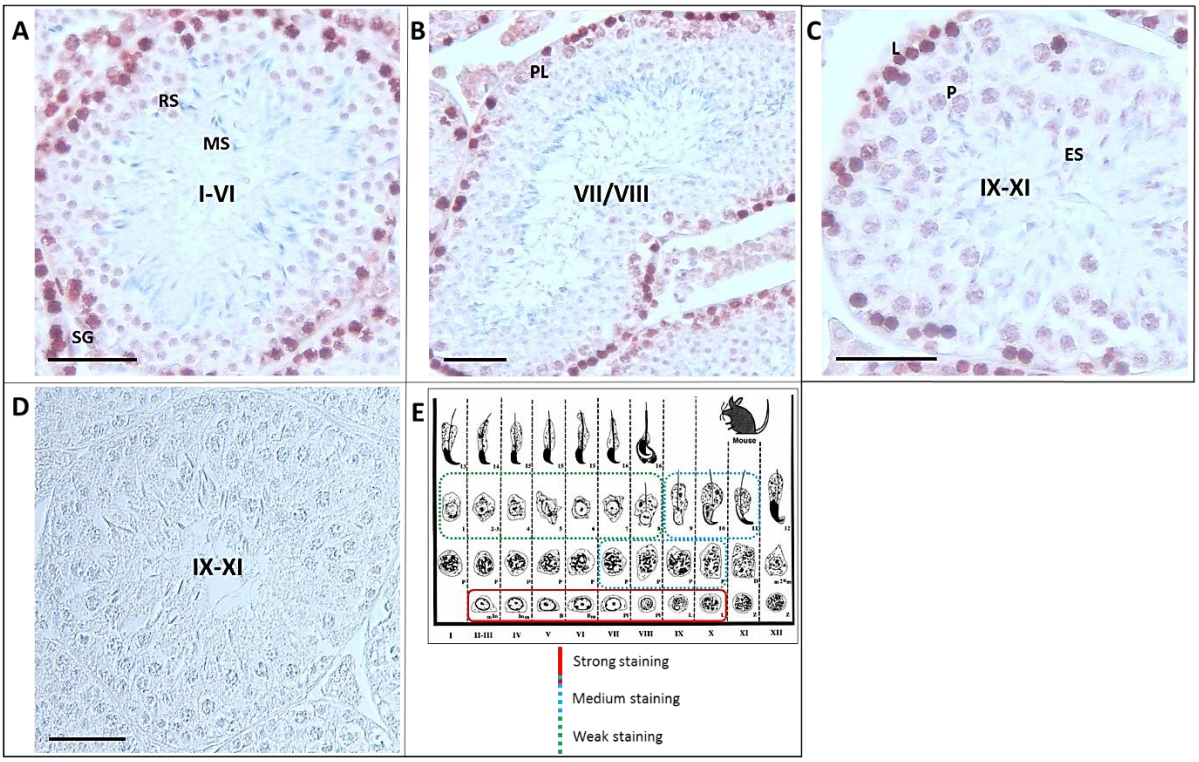

Figure 31: H4K20me2 is detectable in mouse SG (stage II-VI), PL/L (VII-X), RS (stage I-VIII), P (stage VII-XI) and ES (stage IX-XI) in mouse. Only in MS (stage I-VIII) no H4K20me2 was present. **A-D** show exemplary tubules with different stages of the seminiferous epithelial cycle. **D** represents the negative staining of a serial section **A**. Magnification x40, Bar 50 µm. Spermatogonia = SG; Spermatocytes of the preleptotene-/leptotene stage = PL/L and pachytene stage = P; Round spermatids = RS; Maturing spermatids = MS; Elongating Spermatids = ES. **E** shows a scheme[108] of the staining intensities of H4K20me2 in the 12 spermatogenetic stages of mouse; modified from Russell, 1990.[109]

Figure 32 presents the expression of H4K20me2 (ab9052, 1:100) in bull testis, which can be seen in spermatogonia (stage I-VI), preleptotene-/leptotene spermatocytes (VIII/IX), pachytene spermatocytes (stages II-IV), round spermatids (I-VII) and in elongating spermatids (stage VIII-X). Here, expression patterns of H4K20me2 were at highest in round and elongating spermatids. In pachytene spermatocytes (stages V-IX) and maturing spermatids (stage I-VI, XI-XIII) no H4K20me2 was detectable.

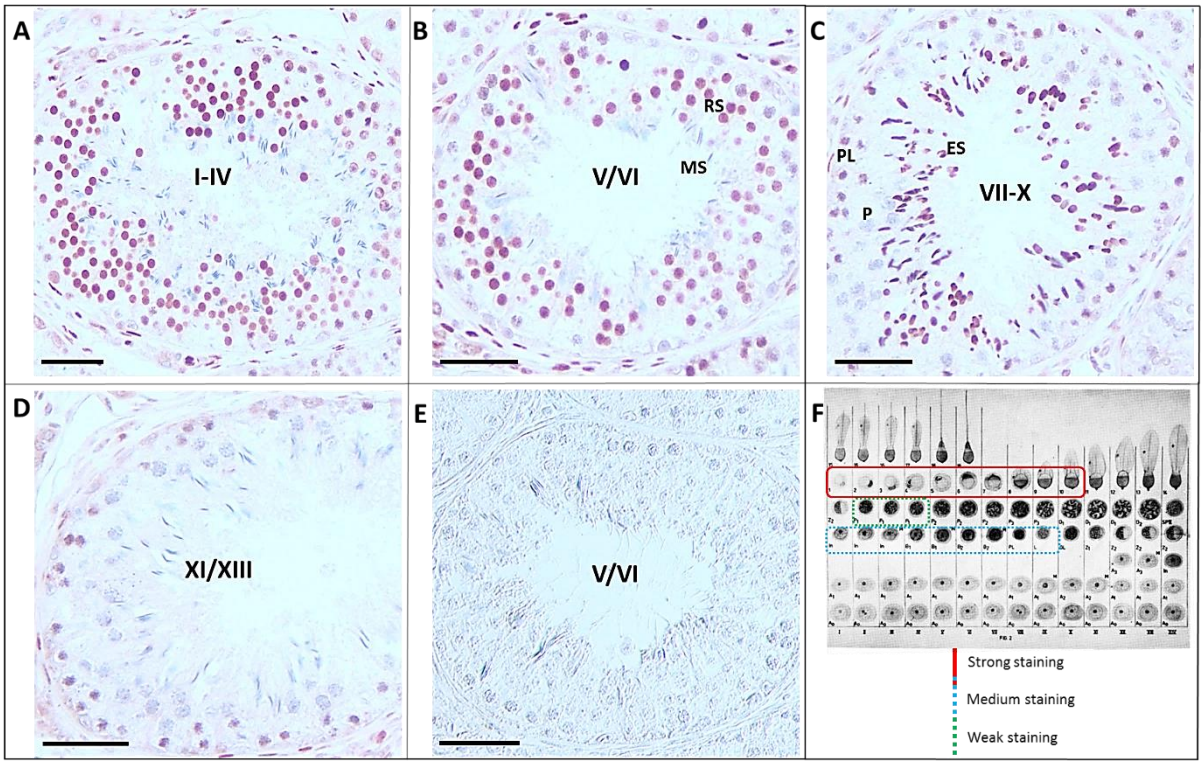

Figure 32: H4K20me2 is detectable in bull SG (stage I-VI), PL/L (VIII/IX), P (stages II-IV), RS (I-VII) and in ES (stage VIII-X) in bull. In maturing spermatids (stage I-VI, XI-XIII) no H4K20me2 was present. **A-E** show exemplary tubules with different stages of the seminiferous epithelial cycle (I-XIII). **E** represents the negative staining of serial section **B**. Magnification x20, Bar 50 µm. Spermatogonia = SG; Spermatocytes of the preleptotene-/leptotene stage = PL/L and pachytene stage = P; Round spermatids = RS; Maturing spermatids = MS; Elongating Spermatids = ES. **F** shows a scheme[110] of the staining intensities of H4K20me2 in the 14 spermatogenetic stages of bull.

In summary, H4K20me2 is ubiquitously expressed in human, mouse and bull testis and is highly abundant in spermatogonia, primary spermatocytes and round spermatids. In all three species no H4K20me2 expression could be detected in elongated/maturing spermatids. This is probably due to the mild decondensation step used here in this method, where sperm heads remain mostly intact.

To analyze if H4K20me2 is present in elongated/ maturing spermatids, immunocytochemical stainings and western blots were performed in motile human spermatozoa.

3.6.2 ICC staining & Western blot of H4K20me2 on human spermatozoa

Motile human sperm cells (donors` M), obtained by the swim-up method, were analyzed for H4K20me2 using immunocytochemistry (ICC) and western blot. Compared to the method used so far (IHC), ICC has an additional 2 h decondensation step to really crack the compact motile sperm heads for a staining. Figure 33 **A-D** shows ICC staining of two exemplary donors` M using H4K20me2 antibody (ab9052, 1:100), and in **E** western blot of two donors` M plus a whole ejaculate sample (Ej. 3) and HeLa as positive control are presented (ab9052, 1:500).

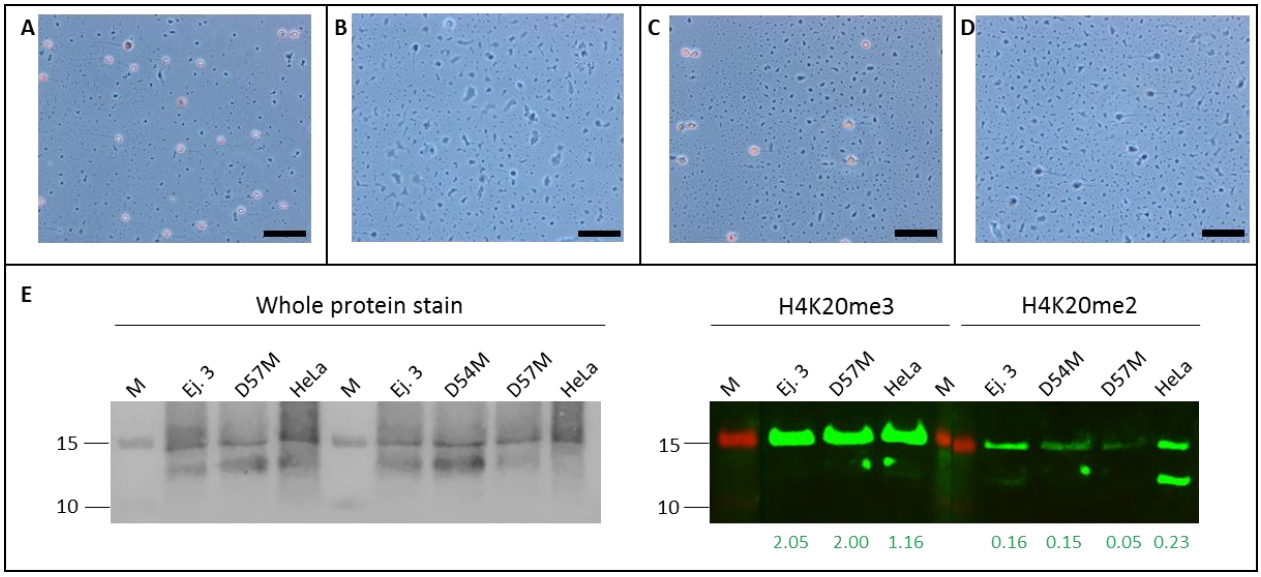

Figure 33: In two donors` M H4K20me2 could be detected (**A**: D52M, **B**: negative control of **A**, **C**: D58M, **D**: negative control of **C**). Magnification x40, Bar 50 µm. **E**: Left: whole protein extract after transfer to the membrane; Right: Western blot with H4K20me3 (ab9053, 1:500) and H4K20me2 (ab9053, 1:500) in total protein extracts (25µg/lane) of two donors` M, one whole ejaculate and HeLa cells (positive control). In all samples H4K20me3 (green bands, 13/15 kDa, lane 1-4) protein levels are 5.1-38.3-times higher than H4K20me2 (green bands, 13/15 kDa, lane 5-8) level.

When using ICC, the H4K20me2 retention in donors` M is clearly detectable (Figure 33, **A** and **C**, red staining). Western blot analyzes showed that the retention of H4K20me2 in motile sperm is 5.1-38.3-times lower compared to H4K20me3, after normalization to the whole protein content (Figure 33 **E**, right: green numbers under blot represent the enrichment factor).

Taken together, IHC, ICC and WB analyzes showed that H4K20me2 is present in all stages of human spermatogenesis as well as in human motile spermatozoa. In contrast to literature[42], the amount of H4K20me2 in mature sperm was considerably lower than that of H4K20me3.

3.6.3 IHC staining of H4K20me3 in human, mouse and bull testis samples

Healthy human testis tissues obtained for TESE, wildtype mouse and healthy bull testis tissues, all exhibiting normal spermatogenesis, were analyzed for H4K20me3, using IHC.

Figure 34 shows that H4K20me3 (ab9053, 1:100) is detectable in spermatogonia of stage I until step 4 elongating spermatids in man. The highest staining intensity for H4K20me3 can be observed in round spermatids, and gets weaker in primary spermatocytes and elongating spermatids. In pachytene spermatocytes (III-V) and maturing spermatids (I/II/V) no H4K20me3 was detectable.

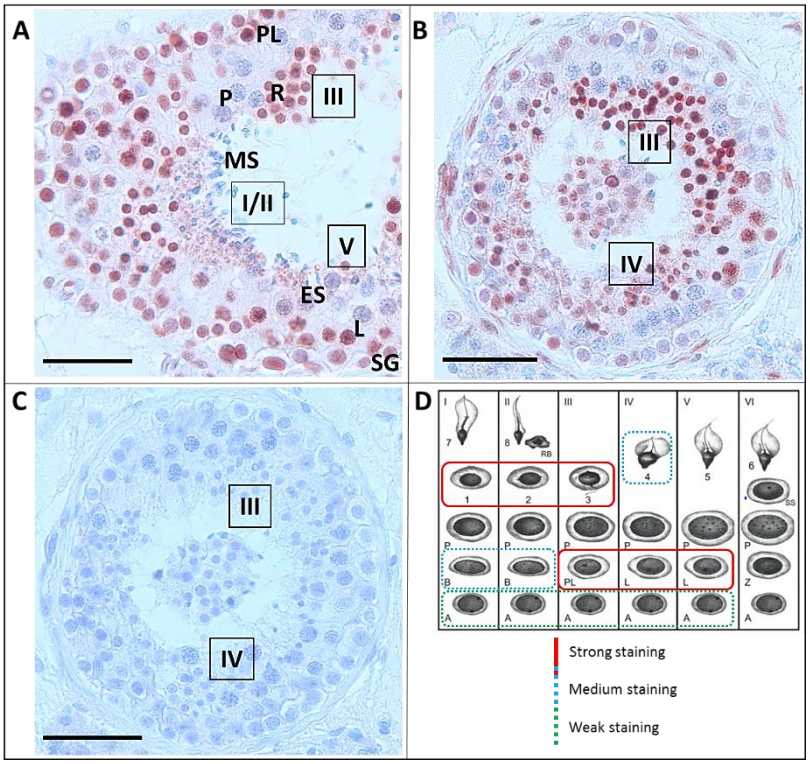

Figure 34: H4K20me3 is detectable in human SG of stage I until step 4 ES in man. In P (III-V) and MS (I/II/V) no H4K20me3 was present. **A**-**C** show exemplary tubules with different stages of the seminiferous epithelial cycle (I-V). **C** represents the negative staining of serial section **A**. Magnification x40, Bar 50 µm. Spermatogonia = SG; Spermatocytes of the preleptotene stage = PL, leptotene stage = L and pachytene stage = P; Round spermatids = RS; Maturing spermatids = MS; Elongating Spermatids = ES. **D** shows a scheme[106] of the staining intensities of H4K20me3 in the seminiferous epithelial cycle of man; modified from Clermont, 1963.[107]

In mouse (Figure 35) expression of H4K20me3 (ab9053, 1:100) can be detected at high levels in spermatogonia (stage II-VI), lesser in preleptotene-/leptotene spermatocytes (VII-X), pachytene spermatocytes (stage VII-XI), round spermatids (stage I-VIII), and again highly in elongating spermatids (stage IX-XI). In maturing spermatids (stage I-VIII) no H4K20me3 was detected.

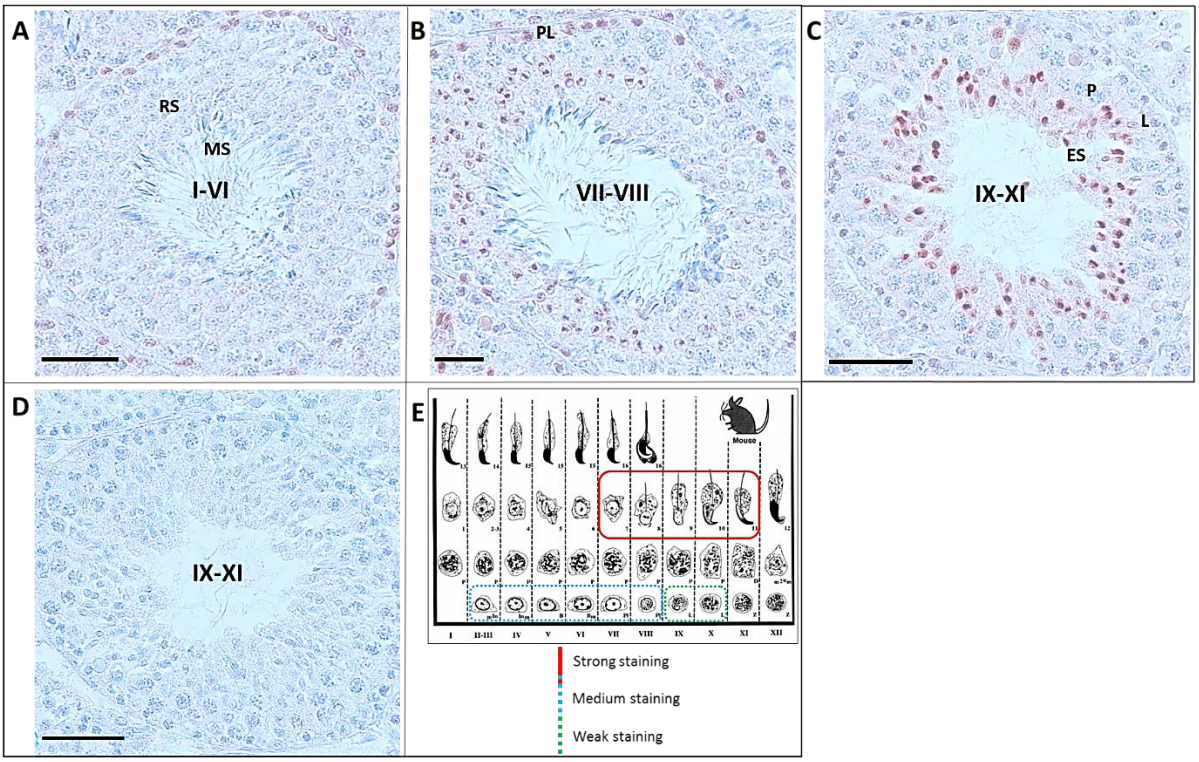

Figure 35: H4K20me3 is detectable in mouse SG (stage II-VI), PL/L (VII-X), RS (stage VII/VIII) and ES (stage IX-XI) in mouse. In P and MS (stage I-VIII) no H4K20me3 was present. **A**-**D** show exemplary tubules with different stages of the seminiferous epithelial cycle. **D** represents the negative staining of a serial section **A**. Magnification x40, Bar 50 µm. Spermatogonia = SG; Spermatocytes of the preleptotene stage = PL, leptotene stage = L and pachytene stage = P; Round spermatids = RS; Maturing spermatids = MS; Elongating Spermatids = ES. **E** shows a scheme[108] of the staining intensities of H4K20me3 in the 12 spermatogenetic stages of mouse; modified from Russell, 1990.[109]

Figure 36 presents the expression of H4K20me3 (ab9053, 1:100) in bull testis, which can be seen in spermatogonia (stage I-VI), preleptotene-/leptotene spermatocytes (VIII/IX), pachytene spermatocytes (stages II-IV), round spermatids (I-VII) and in elongating spermatids (stage VIII-X). Here, expression patterns of H4K20me3 were at highest in round and elongating spermatids. In pachytene spermatocytes (stages V-IX) and maturing spermatids (stage I-VI, XI-XIII) no H4K20me3 was detectable.

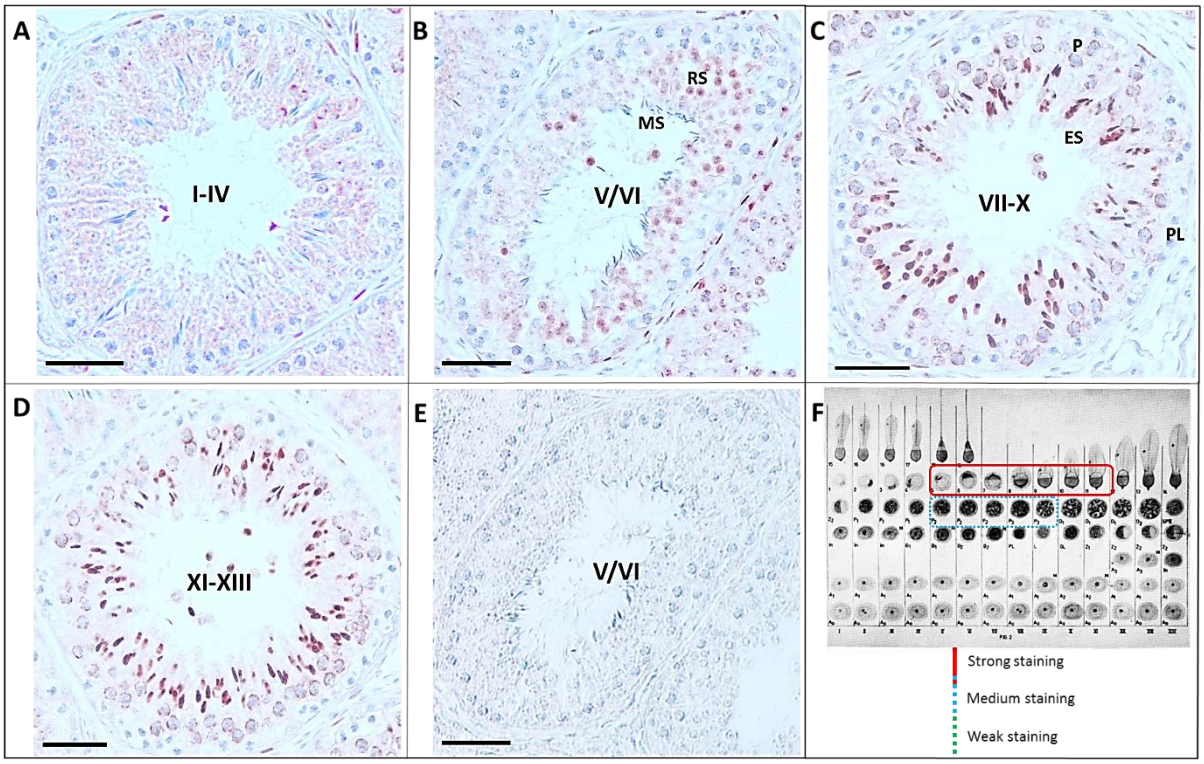

Figure 36: H4K20me3 is detectable in bull P (stages V-IX), RS (V-VII) and ES (stage VIII-X) in bull. In SG (stages I-VII) and MS (stage I-VI) no H4K20me3 was present. **A-E** show five exemplary tubules with different stages of the seminiferous epithelial cycle (I-XIII). **E** represents the negative staining of serial section **B**. Magnification x20, Bar 50 µm. Spermatogonia = SG; Spermatocytes of the preleptotene-/leptotene stage = PL/L and pachytene stage = P; Round spermatids = RS; Maturing spermatids = MS; Elongating Spermatids = ES. **F** shows a scheme[110] of the staining intensities of H4K20me2 in the 14 spermatogenetic stages of bull.

In summary, H4K20me3 is ubiquitously expressed in human, mouse and bull testis tissues and is most abundant in round and elongating spermatids. In comparison to H4K20me2, the expression peak of H4K20me3 is one to two stages later. In all three species no H4K20me3 expression can be detected in maturing spermatids. This is probably due to the mild decondensation step used here in this method, where sperm heads remain mostly intact. Thus, H4K20me3 was further analyzed in mature motile human spermatozoa using ICC and WB.

3.6.4 ICC staining & Western blot of H4K20me3 on human spermatozoa

Motile human sperm cells (donors` M), obtained by the swim-up method, were analyzed for H4K20me3 expression using ICC and WB. As mentioned before, ICC has an additional 2 h decondensation step, which is helpful to crack the motile sperm heads for a staining. Figure 37 **A-D** shows ICC staining of two exemplary samples (donors` M) using H4K20me3 antibody (ab9053, 1:100), and Figure 37 **E** shows western blot analyzes on 20 donors` M and 20 donors` IM (ab9053, 1:500) in order to compare the retention rates within each donor (green numbers under blots are evaluated enrichment scores).

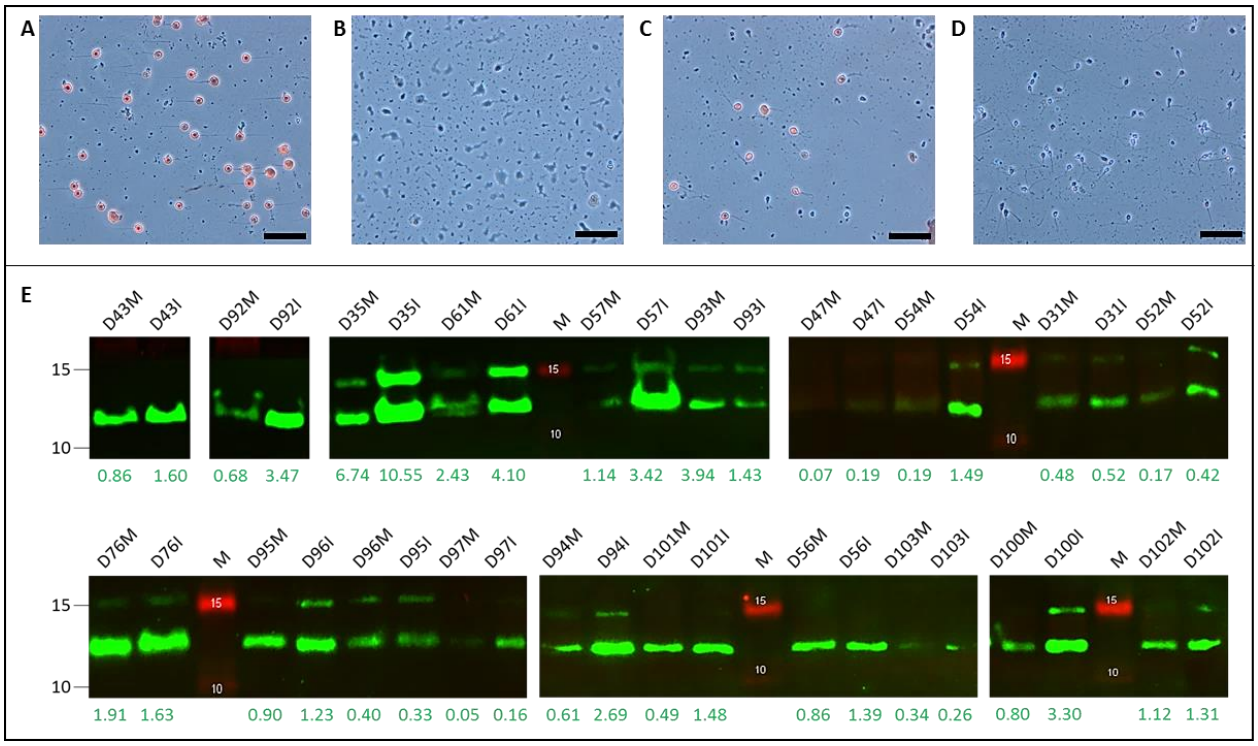

Figure 37: ICC and Western blot staining with H4K20me3 antibody in 20 donors` M and M, respectively. In two donors` M H4K20me3 was well detectable (**A**: D52M, **B**: negative ctrl of **A**, **C**: D58M, **D**: negative control of **C**). Magnification x40, Bar 50 µm. **E** Western blots with H4K20me3 in total protein extracts (25µg/lane) of 20 donors` M and same 20 donors` IM. Under each blot the signal intensity, normalized to the whole protein content for each donor, is noted in green. 16 of 20 donors showed higher amounts of H4K20me3 (13/15 kDa) in their immotile fractions (1.1-7.7-times more, see Table 11).

By using ICC, the H4K20me3 retention could be observed in mature spermatozoa (Figure 37, **A** and **C**, red staining), which was more intense compared to H4K20me2 signals (Figure 33).

Using western blot and blot quantification, it could be found that the retention of H4K20me3 in donors` immotile sperm was up to 7.7-times higher compared to motile ones (normalization to the whole protein content, Figure 37 **E**, see also Table 11). This means in 80 % (16/20) of the investigated samples H4K20me3 was enriched in donors` IM, which refers to the lower compactness of immotile human sperm heads.

Table 11: H4K20me3 analysis by western blot. The signal intensities of H4K20me3 for 20 donors` M (DM) and 20 donors` IM (DI) were calculated after normalization to their whole protein content. The enrichment factor was calculated by dividing the DI through the DM signal.

Donor-ID	DM signal	DI signal	Enrichment factor (DI/DM)
43	0.86	1.60	**1.87**
92	0.68	3.47	**5.10**
35	6.74	10.55	**1.57**
61	2.43	4.10	**1.69**
57	1.14	3.42	**3.00**
93	3.94	1.43	0.36
47	0.07	0.19	**2.71**
54	0.19	1.46	**7.68**
31	0.48	0.52	**1.08**
52	0.17	0.43	**2.53**
76	1.91	1.63	0.85
95	0.90	0.33	0.37
96	0.40	1.23	**3.08**
97	0.05	0.16	**3.20**
94	0.61	2.69	**4.41**
101	0.49	1.48	**3.02**
56	0.86	1.39	**1.62**
103	0.34	0.26	0.76
100	0.80	3.30	**4.13**
102	1.12	1.31	**1.17**

Taken together, these findings suggest that H4K20me3 is expressed in all spermatogenic stages, and is preserved in mature motile spermatozoa. Interestingly, immotile spermatozoa possessed often higher amounts of H4K20me3 probably reflecting an incomplete histone-to-protamine exchange and herewith a restriction in motility.

3.6.5 Analysis of histone methyltransferases KMT5A, KMT5B and KMT5C regulating H4K20

KMT5A, KMT5B and KMT5C, also known as SET8, SUV4-20H1 and SUV4-20H2, are histone methyltransferases for H4K20.[46] KMT5A is responsible for monomethylation (H4K20me1), KMT5C for trimethylation (H4K20me3) and KMT5B for both di-/trimethylation (H4K20me2/ H4K20me3). In order to analyze, whether KMT5s are dysregulated in subfertile men and immotile spermatozoa total sperm RNAs from 21 donors` M, 14 donors` IM and 31 patients` M were extracted and reverse transcribed into cDNA. For *KMT5A* and *KMT5B* mRNA levels analyzes specific qPCR primer sets (Table 3) were designed and used to compare their levels in donors` M and IM, and patients` M using RT-qPCR. Figure 38 illustrates the relative and logarithmic *KMT5A* and *KMT5B* mRNA levels as box plots (green: donors` M, orange: donors` IM, purple: patients` M) for the cohorts after normalization to the housekeeping gene *β-Actin* (Table 3).

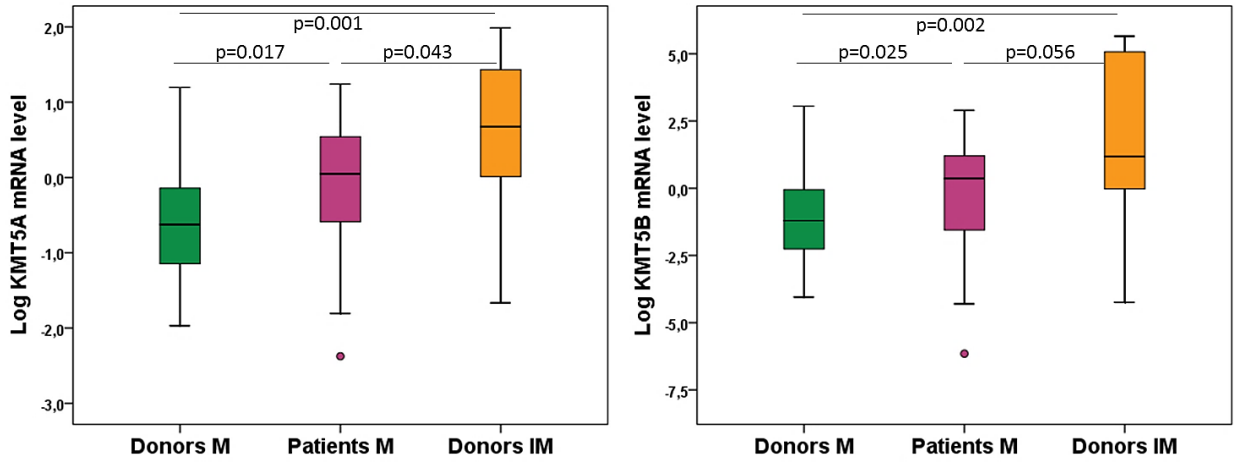

Figure 38: *KMT5A* and *KMT5B* mRNA levels in donors` M and IM, and patients` M (left: *KMT5A*; right: *KMT5B*; log scale 1:1, respectively). *KMT5A* mRNA levels were significantly increased in donors` IM compared to donors` M (p=0.001, n=35) and patients` M (p=0.043, n=45). In patients` M, *KMT5A* mRNA level were also significantly increased compared to donors` M (p=0.017, n=52). *KMT5B* mRNA levels were significantly decreased in donors` M compared to donors` IM (p=0.002, n=34) and patients` M (p=0.025, n=51). *KMT5B* mRNA level were increased in donors` IM compared to patients` M, but without significance (p=0.056, n=45).

Both *KMT5A* and *KMT5B* were significantly lower in donors` M compared to donors` IM (p=0.001/0.002, n=35/34, respectively) and patients` M (p=0.017/ 0.025, n=52/51, respectively). In Table 12 the exact values for *KMT5A* and *KMT5B* mRNA levels of the cohorts are listed. *KMT5A* mRNA levels were 96 % lower in donors` M (0.02±0.34) and 77 % lower in patients` M

(0.11±0.36) compared to immotile sperms (0.47±3.00). *KMT5B* mRNA levels were 88 % lower in donors` M (0.02±0.23) and 59 % lower in patients` M (0.07±0.17) compared to immotile sperms (0.17±4.80).

Table 12: Descriptive statistics of relative *KMT5A* and *KMT5B* mRNA level.

Descriptive Statistics	Relative *KMT5A* mRNA level (n=66)			Relative *KMT5B* mRNA level (n=65)		
	Donors M (n=21)	Donors IM (n=14)	Patients M (n=31)	Donors M (n=20)	Donors IM (n=14)	Patients M (n=31)
Average	0.12	1.87	0.25	0.07	2.91	0.12
Median	0.02	0.47	0.11	0.02	0.17	0.07
Standard deviation	0.34	3.00	0.36	0.23	4.80	0.17
Range	0.00-1.57	0.01-9.73	0.00-1.75	0.00-1.06	0.00-14.25	0.00-0.91

Next, the correlation between gene expression of KMT5s and *L1* methylation was examined. No significant correlation of *KMT5A* or *KMT5B* mRNA to *L1* methylation level in patients` M and donors` M was found (p=0.617/0.982, r=-0.072/0.003, n=51/50; respectively; Figure 39). Furthermore, no significant correlations between *KMT5A* and *KMT5B* mRNA levels with clinical and spermiogram data of patients` and donors` M were found.

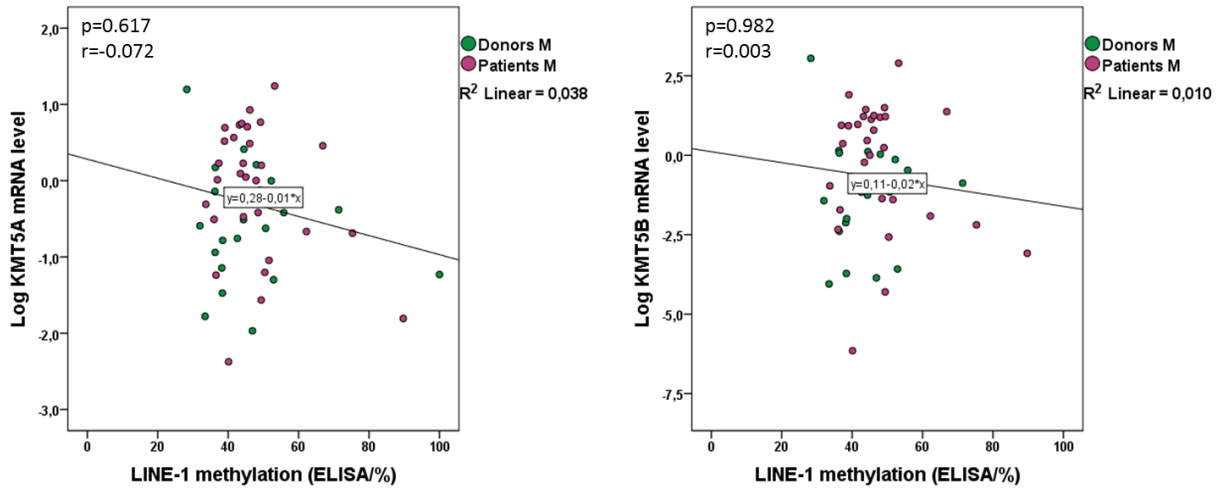

Figure 39: *KMT5A* (p=0.617, r=-0.072, n=51) and *KMT5B* (p=0.982, r=0.003, n=50) mRNA levels were not significantly correlated to *L1* methylation in patients` M and donors` M.

For *KMT5C* mRNA analysis three qPCR primer sets (Table 3) were designed. Figure 40 shows agarose gels of the PCR products generated with these qPCR primer sets in motile human sperm cells. With none of the designed primers *KMT5C* mRNA could be analyzed optimally, as only in few motile sperm samples (DM09, DM24, DM16, and DM25) the expected product sizes were amplified besides larger amounts of other PCR products. However, the primer sets worked well for positive controls (LNCaP, DU145 and PC3 cell lines) and showed the expected PCR products.

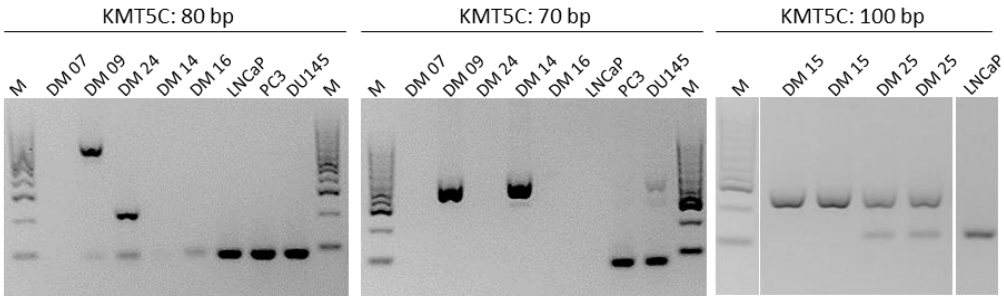

Figure 40: *KMT5C* mRNA analysis in donors` M and prostate cancer cell lines (LNCaP, PC3, DU145 used as positive controls). Three different qPCR primer sets (Table 3) for *KMT5C* mRNA analysis worked well in positive controls and showed the right PCR products (80/70/100 bp). Very weak or wrong product bands were observed in seven tested human sperm samples (DM = motile sperms).

According to the human protein atlas all three KMT5s are expressed in human testis tissue, showing higher values for KMT5A and KMT5B, and lowest for KMT5C.[111–113] To prove whether KMT5C protein, the main mediator of H4K20me3 in somatic cells[46], is present in motile spermatozoa, a western blot experiment was performed as next. KMT5A and KMT5B proteins were not investigated here, as these two histone methyltransferases primarily mediate H4K20me1 and H4K20me2, respectively. Figure 41 shows the results of KMT5C protein analysis (ab91224, 52 kDa, 1:50) in the positive control (HeLa) and in 12 donors` M and 12 donors` IM (50 µg protein loaded). KMT5C protein was not detectable in human sperm.

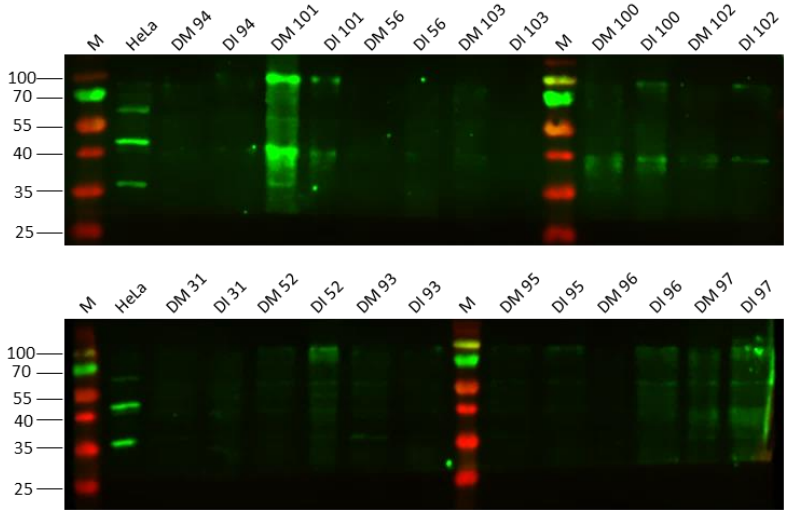

Figure 41: Western blot analysis using KMT5C primary antibody (ab91224, 1:50, expected size 52 kDa) on 12 donors` M and IM, and HeLa cells (positive control). None or wrong bands were visible in human sperm samples. In the positive control the right protein band (52 kDa) was detected besides two other protein bands.

To summarize the analysis of the histone methyltransferases of H4K20, both *KMT5A* and *KMT5B* mRNA levels were detectable in motile and immotile human spermatozoa. Thereby, significantly higher *KMT5A* and *KMT5B* mRNA levels were found in patients` motile and donors` immotile sperm cells compared to donors` motile. However, neither *KMT5C*-mRNA nor -protein could be detected in human spermatozoa.

3.7 ChIP-qPCR confirming H4K20me3 binding in gene regions evaluated by ChIP-sequencing

Chromatin immunoprecipitation followed by qPCR (ChIP-qPCR) was performed on motile and immotile sperm fractions of four healthy donors with H4K20me3 antibody (ab9053) and ChIP-IT High Sensitivity Kit (Active Motif, Cat. No. 53040) for intra- and inter-individual comparison of H4K20me3 enrichment. Based on recently generated ChIP-sequencing data from our group (Ozturk *et al*., 2019 in preparation), several genome/gene loci associating with H4K20me3 were found and, ChIP-qPCR primer sets were designed or taken from literature for some selected regions (Table 4). Promoter regions from five genes, namely *CXCL8*, *TNFSF13B*, *IFNW1*, *CST8*, and *L1* associated regions were analyzed. Two primer sets for L1 analyzes were designed, one covering the ORF1 (*L1*-OFR) and another covering the 5`UTR region (*L1*-5`UTR). Figure 42 shows exemplary for one donor sample (motile and immotile fractions) the ChIP-qPCR products amplified with all primer sets used here.

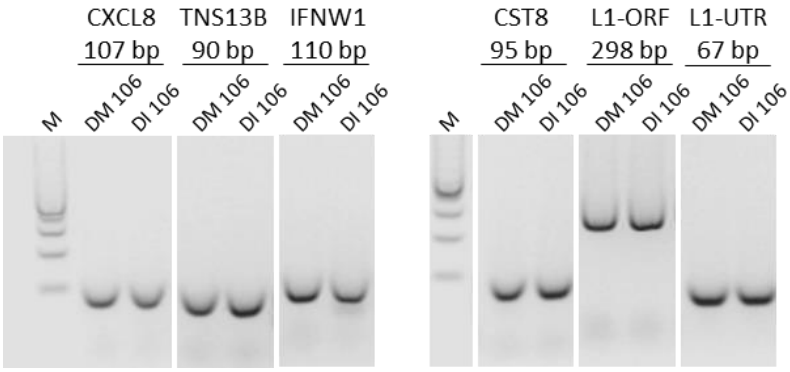

Figure 42: ChIP-qPCR products in motile and immotile sperm fractions of healthy donor number 106, obtained with the respective primer sets after ChIP with H4K20me3 antibody (ab9053). Gene names and expected PCR product sizes are shown on top. All primer sets amplify the right PCR products in human spermatozoa.

All ChIP-qPCR primers showed the expected PCR products in motile as well as immotile sperm cells. The relative binding of H4K20me3 was calculated using the ChIP-qPCR signals (CTs generated with H4K20me3-precipitated DNA and respective input DNAs). Then, relative binding

of H4K20me3 (80 % sample) was calculated as enrichments over the input signals (10 % sample; Table 13). The remaining 10 % of the samples were taken for a chromatin check.

Table 13: Relative enrichments of *CXCL8*, *TNSFS13B*, *IFNW1*, *CST8*, *L1*-ORF and *L1*-5`UTR in motile and immotile sperm fractions from four healthy men (2^-delta CT).

Sample ID	*CXCL8*	*TNSFS13B*	*IFNW1*	*CST8*	*L1*-ORF	*L1*-5`UTR
Donor M 98-H4K20me3	0,00	0,02	0,02	0,02	0,02	0,01
Donor I 98-H4K20me3	0,23	0,26	0,27	0,26	0,25	0,21
Donor M 106-H4K20me3	0,03	0,49	0,42	0,43	0,82	0,38
Donor I 106-H4K20me3	0,55	0,56	0,33	0,40	1,59	0,65
Donor M 107-H4K20me3	0,01	0,10	0,10	0,18	0,21	0,14
Donor I 107-H4K20me3	0,12	0,13	0,13	0,13	0,18	0,11
Donor M 113-H4K20me3	0,00	0,05	0,04	0,06	0,07	0,04
Donor I 113-H4K20me3	0,05	0,06	0,06	0,07	0,08	0,06

Figure 43 shows the box plots from ChIP-qPCR analyzes on motile and immotile sperm fractions from four healthy donors. Each sample was precipitated with H4K20me3 antibody and qPCRs for *CXCL8*, *TNSFS13B*, *IFNW1*, *CST8*, *L1*-ORF and *L1*-5`UTR were done in duplicates.

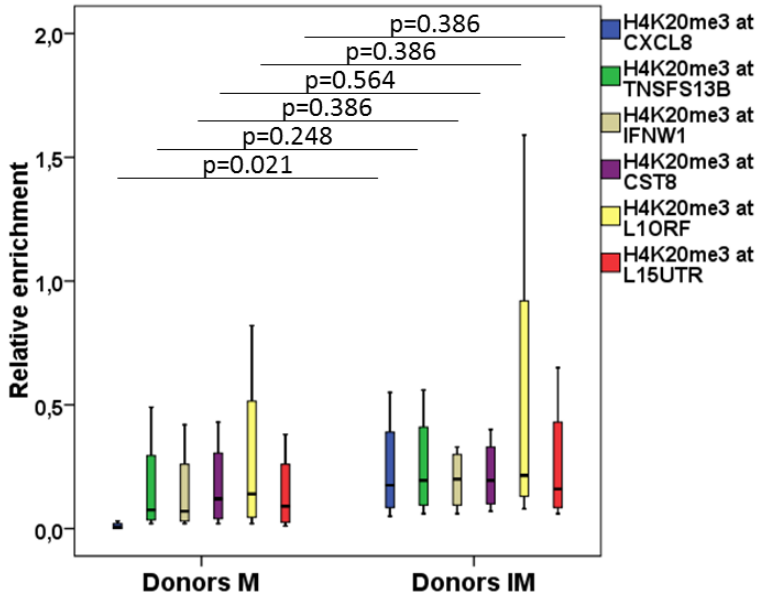

Figure 43: Relative enrichment of H4K20me3 over the input in *CXCL8*, *TNSFS13B*, *IFNW1*, *CST8*, *L1*-ORF and *L1*-*5*`UTR. The DNA of each gene could be found in motile and immotile sperm fractions. Binding of H4K20me3 in -*CXCL8* promoter was significantly higher among immotile sperms in comparison to motile ones (p=0.021).

All selected gene regions showed binding to H4K20me3 in varying degrees. Remarkably, H4K20me3 was significantly enriched at *CXCL8* in immotile sperm fractions compared to the motile ones (p=0.021, n=8). For the remaining four genes (*TNSFS13B*, *IFNW1*, *CST8* and *L1*) H4K20me3 was found at similar levels in motile and immotile sperms (p>0.05). In comparison to

L1-5`UTR an increased binding of H4K20me3 in *L1*-ORF was found in motile as well as in immotile sperms.

Tables 14 and 15 show the average values of H4K20me3 enrichment in five selected genes in human sperm samples (motile and immotile fractions). H4K20me3 was in average 24-times more enriched at *CXCL8* in immotile sperms in comparison to motile sperms. Interestingly, H4K20me3 was 1.9-times more enriched in *L1*-ORF than in *L1*-5'UTR in both motile and immotile sperms.

Table 14: Average values of H4K20me3 enrichment in motile sperm cells of healthy donors.

Descriptive Statistics	**H4K20me3 enrichment (ChIP-qPCR)**					
	Donors M (n=4)					
	CXCL8	***TNSFS13B***	***IFNW1***	***CST8***	***L1*-ORF**	***L1*-5`UTR**
Average	0.01	0.17	0.15	0.17	0.28	0.14
Median	0.01	0.08	0.07	0.12	0.14	0.09
Standard deviation	0.01	0.22	0.19	0.18	0.37	0.17
Range	0.00-0.03	0.02-0.49	0.02-0.42	0.02-0.43	0.02-0.82	0.01-0.38

Table 15: Average values of H4K20me3 enrichment in immotile sperm cells of healthy donors.

Descriptive Statistics	**H4K20me3 enrichment (ChIP-qPCR)**					
	Donors IM (n=4)					
	CXCL8	***TNSFS13B***	***IFNW1***	***CST8***	***L1*-ORF**	***L1*-5`UTR**
Average	0.24	0.25	0.20	0.22	0.53	0.26
Median	0.18	0.20	0.20	0.20	0.22	0.16
Standard deviation	0.22	0.22	0.12	0.15	0.71	0.27
Range	0.05-0.55	0.06-0.56	0.06-0.33	0.07-0.40	0.08-1.59	0.06-0.65

4. Discussion

Considering that more than one third of infertile men suffer from idiopathic infertility, more investigations are needed to uncover the causes of this type of infertility, so that differential diagnosis and potential treatment strategies can be developed. Aberrations in the sperm epigenome represent one of the possible causes for idiopathic male factor infertility/subfertility as it was frequently documented in literature.[31,36,72,114,115] Moreover, the sperm epigenome was found to be sensitive to environmental factors, diet and also to systemic diseases like obesity[9–11] - factors, which are handled as risk factors for male fertility.

During human spermiogenesis a histone-to-protamine exchange occurs after which around 3 % to 15 % of the histones still remain.[33,34,116] These histones and, respectively, their specific post-translational modification and genome-wide localization represent one of the main features of the sperm epigenome. Genome-wide studies using ChIP-seq revealed that histones stay in genes, which have a relevance for spermatogenesis and for development.[116–122] Our group and others have revealed that, viewed at the genome-wide scale, the majority of sperm histones and nucleosomes are located in gene-poor regions and are enriched in repetitive DNA elements like L1 and SINEs.[34,69] Also, independent studies have shown that epigenetic information in sperm chromatin was transferred to next generations and can regulate gene expression there.[123–125]

L1 elements are the only active retrotransposons and account for up to 17 % of the human genome.[57] L1 activity can impair genomic integrity by random insertion and lead to mutations and cause diseases like hemophilia A, colon cancer and X-linked Duchenne muscular distrophy.[56,126,127] In somatic cells, L1 is known to be regulated by CpG methylation, transcription factors and specific PTHMs, e. g. H4K20me3. The situation in mammalian sperm is still unknown.

In this thesis, epigenetic factors and regulators of L1 elements, known from studies on somatic cells, were investigated in human sperm cells to gain new insights about their suppression mechanisms and influences on spermatogenesis. In particular, motile spermatozoa of subfertile patients and of healthy fertile donors (healthy controls), as well as immotile spermatozoa from healthy donors (available only here) were studied. In addition, PTHMs were analyzed in testicular tissue samples from man, mouse and bull. These results should contribute to a better understanding of L1 regulation in spermatogenesis and mature sperm and their impact on male fertility.

4.1 Spermatozoa of subfertile patients possessed decreased *DNMT1* and *DNMT3A* mRNA levels

The best analyzed epigenetic factor, in sperm, is DNA methylation. Sperm cells have a unique and tailored DNA methylation pattern to ensure fertility and a proper embryo development.[27,128] Aberrations in global DNA methylation and imprinting genes are associated with poor sperm quality and male infertility.[31,77,78,128,129] DNA methylation is regulated by DNMTs, namely DNMT1/2/3A/3B or DNMT3L. During all stages of human and mouse spermatogenesis activities of DNMT1 and DNMT3A were found. Especially in spermatogonia type A, primary spermatocytes and round spermatids high *DNMT1/3A* expression was measured, while almost no activity was found in elongating spermatids.[26] In mice, knockout of *Dnmt3a* leads to decreased spermatogenesis through the maturation arrest at spermatogonia stage and mice embryos lacking *Dnmt3a* die after only one month.[23,26] Mutations and knockout of *Dnmt1* in mice cause global hypomethylation, retrotransposons reactivation and embryonic lethality at around day E9.[23,27]

Here, *DNMT1* and *DNMT3A* mRNA levels were measured in controls` and patients` motile spermatozoa. Both *DNMT1* and *DNMT3A* were significantly decreased in patients` M compared to controls` M and showed a significant positive correlation to each other. Lower global sperm DNA methylation was demonstrated in idiopathic infertile males, oligozoospermic men and low motility sperm samples.[21,130,131] Based on these findings and the results obtained here it can be presumed, that spermatozoa of subfertile patients are hypomethylated due to reduced DNMT levels. The lack of DNMTs in general could impair the progress and efficiency of the spermatogenic cycle in subfertile patients, as total sperm concentration and motility of this cohort was significantly reduced compared to those of healthy controls. Moreover, decreased *DNMT1* and *DNMT3A* mRNA levels could represent one reason for the subfertility of 26 of the 48 patients here, as they did not achieve a pregnancy through ART. But, the residual 22 subfertile patients were able to achieve a pregnancy despite low *DNMT1* and *DNMT/3A* mRNA levels. These observations emphasize the complex nature of molecular reasons of idiopathic male infertility. Another DNMT, namely DNMT3L, was shown to assist *de novo* methyltransferases like DNMT3A and DNMT3B, and *Dnmt3l* knockout mice developed azoospermia and infertility.[132,133] Therefore, further studies should involve DNMT3L in order to elucidate the role of DNA methylation on fertilizing capacity of human sperm.

4.2 Global DNA and RNA methylation status in human spermatozoa

The global DNA methylation in the human germline is strictly organized and occurs in two waves. Immediately after fertilization the first wave of active demethylation starts in the paternal pronucleus and is followed by passive demethylation of the female genome.[27,29] Reaching blastocyst stage, DNA methylation patterns become re-established until the second wave of demethylation occurs in PGCs. Finally, sex-specific *de novo* methylation starts to re-establish the sperm-/oocyte-specific methylomes.[29,30] Aberrant DNA methylation patterns in the sperm epigenome can negatively impact transcriptional gene regulation, genomic imprinting and embryonic development.[11,27,29] Moreover, idiopathic male infertility was associated with aberrant DNA methylation of imprinted loci.[130] This emphasizes the importance of the precise regulation of DNA methylation and demethylation patterns by its enzymes (DNMTs and TET1-3). Here, global DNA (5-mC, 5-hmC) and RNA (m6A) methylation levels were analyzed in spermatozoa of controls` and patients` motile spermatozoa to see if there are differences between the cohorts and if these influence the sperm quality. As L1 methylation was shown to serve as surrogate measure for global DNA methylation[73], the methylation level of L1 was also determined here.

4.2.1 Motile spermatozoa of healthy controls and subfertile patients did not differ in global DNA and RNA methylation levels

Mature human spermatozoa are transcriptionally inactive cells and most of their CpGs are highly methylated (90-96%).[22,27] Sperm hypermethylation is often observed in regions outside of gene promoters, more precisely in intergenic sequences and gene bodies, whereas sperm hypo-methylation is found at gene promoters, particularly of genes with developmental relevance.[31,132] In mouse and human, 5-hmC is highly abundant in neuronal tissues like the brain or spinal cord and ranges from 0.3-0.7 % and is lowest in liver and testis tissue ranging from 0.03-0.06 %.[134] Despite their transcriptional inactive state, mature human sperm cells carry a huge amount of RNAs, like mRNAs and non-coding RNAs, which in addition to DNMTs and TET enzymes also have the ability to mediate DNA methylation, as already proven in plants.[135,136] The most abundant RNA modification in eukaryotes is m6A (<80 %), which is involved in microRNA (miRNA) biogenesis and mRNA regulation.[137,138] In sperm RNA from asthenozoospermic patients, m6A content was significantly increased compared to healthy controls and was negatively correlated to sperm progressive motility.[139]

Measuring global 5-mC, 5-hmC DNA and m6A RNA methylation levels in motile spermatozoa of controls` and patients` no significant differences in 5-mC were found. 5-mC levels ranged from 0.12 to 10.1 %, whereby the average value in patients` was 3.97 % and in controls` 4.52 %. 5-hmC could not be detected in human sperm and m6A was almost identical between the groups (0.02 %).

Wang *et al*. evaluated the global 5-mC DNA methylation status in 24 human semen samples, by UPLC-MS/MS (ultra-performance liquid chromatography/tandem mass spectrometry)[140], which ranged from 3.79 % to 4.65 %, highly similar to the results obtained here. It is worth to note, that higher methylation (4.25 %) was observed in semen samples, where abnormal and dead sperm cells were removed by density gradient centrifugation. This reflects the findings obtained here, that 5-mC level in motile spermatozoa of healthy controls and subfertile patients, both purified with the swim-up technique, were ranging from 3.97-4.52 %. Guz *et al*. showed additionally that 5-mC DNA methylation levels in Percoll gradient purified spermatozoa of 91 men, measured by UPLC-MS/MS, range around 3.82 % ± 0.08 % and 5-hmC level are ranging around 0.80 % ± 0.17 %.[141] However, Jenkins *et al*. reported that 5-hmC DNA methylation levels in 30 human spermatozoa samples range from 0.00 % to 0.03 %,[142] which is comparable to the findings here. In that study the same ELISA kit was used for 5-hmC quantification as here, but the used DNA was higher concentrated and originated not only from motile but also from immotile sperm cells. The different sperm cell populations and higher amount of utilized DNA might be the reasons, why Jenkins *et al*. were able to measure at least 0.03 % 5-hmC in contrast to here (0.00 %).

To conclude, the results for global methylation in motile human spermatozoa obtained here are comparable to values reported in previous studies. 5-hmC methylation was not detectable here, apparently due to the low abundance of this DNA base in mature motile human spermatozoa and may be due to its detection limit using ELISA. No differences in global m6A RNA methylation level in the cohorts were analyzed here. This may be due to the fact that small differences between m6a RNA methylation levels in human sperm are not quantifiable by ELISA. Mass spectrometry could reveal such differences. The analysis of alternative RNA forms, like miRNAs and mRNAs, in mature human spermatozoa could be even more insightful. For example, in mice the injection of sperm-derived small non-coding RNAs into zygotes led a transmission of paternally acquired phenotypes to the offspring.[143] Also the analysis of m6A regulators in human sperm could be very insightful, as knockout of *Mettl3* (a catalysator of m6A formation), *Alkbh5* (an m6A eraser) and

Ythdc1 (an m6A reader), inhibited the spermatogenesis and, moreover, led to male infertility and also blocked oocyte development in mice.[144–146]

4.2.2 Lowest *L1* methylation was detectable in motile spermatozoa of subfertile patients using ELISA and *L1* mRNA was highest in immotile spermatozoa of healthy controls

DNA hypermethylation of L1 promoters was shown to be one suppression mechanism of L1 retrotransposition in somatic tissues.[74,147,148] In this thesis, *L1* methylation levels were determined in healthy controls` and patients` motile spermatozoa as well as in immotile sperm of healthy controls using two methods, pyrosequencing and ELISA.

Using pyrosequencing, no significant differences in *L1* methylation were found in the cohorts. *L1* methylation levels in patients` and controls` motile spermatozoa were ranging from 51.1 % to 50.5 %, respectively. Immotile spermatozoa of controls` showed *L1* methylation levels around 50.3 %. The use of ELISA technique (5-mC antibody against gDNA of interest, hybridized to a biotinylated L1 consensus probe) for *L1* methylation analysis revealed highly significant differences between the cohorts, showing highest values in immotile spermatozoa of controls` (58.1 %) and lower values in patients` and controls` motile spermatozoa (47.2 % and 52.3 %, respectively).

The difference to pyrosequencing is the detection and analysis of 12 CpG sites (instead of 3 CpGs in pyrosequencing) and analysis of another L1 genomic region. Notably, *L1* methylation levels in controls` motile and immotile spermatozoa were significantly increased compared to patients` motile spermatozoa. Moreover, analyzing the patient subgroup showing a positive pregnancy after ICSI, a significant correlation of *L1* methylation and fertilization rates was revealed. This suggests, that high *L1* methylation and, respectively, L1 suppression in sperm favors the proper fertilization and leads to embryo development and pregnancy. In contrast, in the patient subgroup showing a negative pregnancy, the correlation of fertilization rates and *L1* methylation was reversed and not significant, which implies that *L1* methylation needs to be strictly regulated to ensure fertilization. Furthermore, this fact could indicate that L1 activation in spermatogenesis leads to substandard sperm, due to its hypomethylation, and thus to failures in developmental program.

Various studies analyzed global sperm DNA methylation patterns, but found no differences in the methylation of *L1* between fertile and infertile patients.[31,78,149] However, Heyn *et al*. reported that L1 elements were hypomethylated in infertile patients,[150] and Pacheco *et al.* showed that most

CpGs (80 %) in low motility human sperm samples were also hypomethylated.[131] Furthermore, Hajj *et al*. demonstrated, that methylation of repetitive elements was significantly lower in sperm of infertile males compared to controls.[151] In accordance with these reports, significantly decreased *L1* methylation levels were found here in motile spermatozoa of subfertile patients.

L1 activation was shown in different tissues and diseases to cause mutations, genomic instability and cancer.[60,62,67] In order to see whether *L1* mRNA levels in sperm differ between the cohorts and between the motile and immotile sperm, and if *L1* mRNA is correlated to *L1* methylation, RT-qPCR was performed here using a published primer set from Muñoz-Lopez *et al*.[65] (Table 3). Highest *L1* mRNA levels were found in immotile spermatozoa of controls and motile spermatozoa of patients, which were both significantly increased in comparison to controls` motile spermatozoa. A correlation analysis between *L1*-methylation and -mRNA in motile human spermatozoa showed, that these are significantly negative correlated. This indicates that *L1* hypermethylation is associated with L1 inactivation in mature human spermatozoa and herewith confirms observations made in somatic cells.[61,74,105]

In terms of male germ cells and embryogenesis, Cheng *et al.* detected significantly increased *L1* transcripts in patients with hypospermatogenesis.[152] He *et al*. studied *L1*-methylation and -mRNA levels in human placentas from different gestational ages and found a significant decrease of *L1* methylation and increase of *L1* mRNA levels in third trimester placentas, showing evidence for a strict L1 regulation.[74] Belancio *et al*. analyzed somatic expression patterns of *L1* in human tissues and found the highest *L1* expression in the testis and lower in the prostate.[64] However, no significant correlations to clinical or semen parameters like age, sperm concentration, fertilization rate, pregnancy outcome, progressive and total motility were found for patients` as well as controls` motile spermatozoa.

In spermatogonia P-element-induced wimpy testis (Piwi) proteins were reported to repress L1 elements, whereby mutations in Piwi-interacting RNA (piRNA) pathways in mice were shown to induce L1 retrotransposition and result in defective sperm.[153,154] In human cryptorchidism, characterized by the absence of one or both testicles from the scrotum, impaired expression of Piwi pathway genes, like *PIWIL2* and *PIWIL4*, was related to derepression of L1 retrotransposons.[155] Moreover, in infertile men, suffering from spermatogenic failure and Sertoli cell-only syndrome, inactivation of *PIWIL2* and its processing factor *TDRD1* was associated with hypomethylation of L1 elements and reduced spermatogenesis.[150]

Possibly, in the subfertile patients` cohort analyzed in this thesis, Piwi pathways were dysregulated, which could explain the decreased *L1*-methylation and increased *L1*-mRNA levels measured here in comparison to healthy controls` motile spermatozoa. Recently, Giebler *et al.* have shown, that *PIWIL1* and *PIWIL2* mRNA expression can be measured in ejaculated spermatozoa of men and, that expression levels of these two genes were negatively associated with sperm count and progressive motility.[156] The measurement of *PIWIL1* and *PIWIL2* mRNA levels in subfertile patients` spermatozoa could provide information, if these genes were correlated with L1 expression in mature spermatozoa and contribute to male fertility and pregnancy outcome after ART.

Taken together all these findings suggest, that *L1* methylation is a critical factor for male fertility and can possibly be used as diagnostic marker. Future studies should consider *L1* methylation in subfertile patients, as this could provide information about their fertilization rates by using ARTs. Moreover, L1 dysregulation was traceable here in sperm of subfertile men and in immotile sperm of healthy controls, although it remains unclear how and why L1 became dysregulated. This implies, that L1 regulation is an important factor in spermatogenesis, and to shed more light on this issue, some selected L1 regulators known from somatic cells were analyzed in the current work, and these results are discussed below.

4.3 *SIRT6* was hypermethylated in motile spermatozoa of subfertile patients

SIRT6 was shown to package L1 elements into transcriptionally repressive heterochromatin in human dermal fibroblasts (HDF) but fails with stress and age.[89] SIRT6 modulation in mice dramatically influences aging and DNA repair processes.[90,91] Moreover, SIRT6 protein was detectable in the mouse nucleus of transitional spermatids and in the acrosome of mature spermatozoa, which implies a role for SIRT6 in spermiogenesis, the final step of spermatogenesis.[157]

SIRT6 promoter methylation increases with age in human lymphocytes and *SIRT6* mRNA levels in the brain of pigs decrease with age.[91,158] These findings indicate, that SIRT6 is epigenetically regulated by methylation. In this work, *SIRT6* promoter methylation, mRNA and protein levels in spermatozoa of healthy controls and subfertile patients were analyzed, to determine, whether SIRT6 is differentially regulated in these and possibly associated with L1 regulation.

Significantly elevated *SIRT6* methylation was observed in patients` motile spermatozoa compared to controls` motile and immotile spermatozoa. No significant correlations between *SIRT6* methylation, *L1*-methylation or -mRNA were found in the cohorts investigated here.

In sperm *SIRT6* methylation was not affected by age, which contradicts literature observations, but can be explained by the different cell types (human lymphocytes and human dermal fibroblasts), which were analyzed there.[89,91] *SIRT6* hypermethylation found in sperm of subfertile patients could indicate that lower amounts of *SIRT6* mRNA and protein are present and thus packaging of L1 into its silent heterochromatin state is decreased.

Using three different qPCR primer sets from literature[99–101] with proven functionality in positive controls *SIRT6* mRNA was analyzed in the cohorts. However, in none of the sperm samples *SIRT6* mRNA could be detected. Also, SIRT6 protein levels could not be detected in mature spermatozoa of healthy controls. However, two antibodies used here showed also poor performances in Western blot (ab176345 and ab62739, Abcam). According to the human protein atlas SIRT6 is highly present in human testis.[92] The antibody used there **(**HPA071776, Sigma) or mass spectrometric analyzes could further help to reveal if SIRT6 protein is abundant in human spermatozoa and regulates L1.

4.4 Increased *MORC2* mRNA levels in motile spermatozoa of healthy controls

MORC2 is widely expressed in human tissues, showing highest abundance in brain, placenta and testis.[159] Mutations of MORC2 are known to cause diseases, like spinal muscular atrophy and the Charcot-Marie-Tooth disease.[160,161] In euchromatic environment, MORC2 together with the HUSH-complex was shown to bind and repress full-length L1 elements, whereby single or double knockout of MORC2 and/or HUSH-complex in human chronic myeloid leukemia cells (K562) led to an upregulated expression of L1s.[93]

Here, *MORC2* mRNA levels were analyzed in spermatozoa of healthy controls and subfertile patients to see if *MORC2* mRNA levels were connected to L1 regulation in human spermatozoa and possibly influence sperm quality. Relative *MORC2* mRNA level were detectable in 20/46 (43.5 %) patients` motile spermatozoa, 28/32 (87.5 %) controls` motile and 4/24 (16.7 %) controls` immotile spermatozoa. Especially in motile spermatozoa of controls *MORC2* mRNA was enriched. Thereby it was striking, that in most immotile sperm samples of controls and motile sperm samples of patients no *MORC2* mRNA was present.

On the one hand, MORC2 might only repress L1 elements in euchromatic environment, as shown in hESC and K562 cells,[93] and not in heterochromatic environment, as in mature human spermatozoa. On the other hand, MORC2 regulation might be disturbed in controls` immotile and patients` motile spermatozoa, as all measured values in this two cohorts were close to zero.

In addition, no correlations of MORC2 expression to *L1*-mRNA, -methylation and clinical or semen parameters like age, sperm concentration, fertilization rate, pregnancy outcome, progressive and total motility were found in patients` as well as controls` spermatozoa.

In mice two paralogues of *Morc2* are present, namely *Morc2a* and *Morc2b*. Particular *Morc2b* was found to be essential for meiotic progression and fertility in both sexes.[162] By extending the control and patient cohorts here and using alternative analytical methods (e.g. Western blot and IHC), MORC2 protein could be investigated in human spermatozoa and testis tissue. In addition, exploring the roles of HUSH complex subunits MPP8 and TASOR in mature human spermatozoa could be helpful, as these mediate L1 repression in euchromatic environment together with MORC2.[93]

4.5 No YY1 expression in male germ cells

Human L1 elements were shown to possess a YY1 binding site at their 5`UTR and this site is required for accurate human L1 transcription initiation.[60,88] YY1 expression was examined in embryos and adult testes of mice and was found in Sertoli cells of 14.5 days old embryos and spermatogonia, spermatocytes and spermatids of 12-week-old adult mice.[163] Loss of YY1 in mouse spermatocytes was shown to induce global heterochromatin instability and DNA double-strand breaks.[164]

Here, YY1 expression was analyzed by IHC in healthy human testis tissues exhibiting normal spermatogenesis, obtained for TESE, to see if YY1 is expressed in human spermatogonial cells and potentially influences L1 regulation in mature spermatozoa. YY1 expression was exclusively found in Sertoli cells and not in any male germ cell of the seminiferous epithelial cycle.

As mentioned above, YY1 expression was identified in embryos and adult testes of mice.[163] Using IHC, YY1 expression was analyzed in 14.5 days old embryos and found in the nuclei of 86 % of Sertoli cells and in 38 % of gonocytes. In adult mouse testis, YY1 expression was found in Sertoli cells, spermatogonia, spermatocytes and spermatids but not in spermatozoa. Knockouts of YY1 in mice greatly slow down embryonic development and lead to its death around peri-implantation phase.[165] These findings agree with the results obtained here from human testis, that YY1 was strongly expressed in Sertoli cells and not in mature spermatozoa using the same method, antibody (ab109237) and antibody dilution (1:200). This shows that IHC was a good method to analyze YY1 expression in human testis tissue and that its appearance is specific to Sertoli cells.

The role of YY1 in human Sertoli cells and its influence on male fertility and embryo development should be further investigated. Since Sertoli cells provide sperm cells with nutrients during spermatogenesis, YY1 expression in these could ensure repression of L1 elements throughout spermatogenesis. Moreover, analysis of other transcription factors located on human L1 5`UTR, like RUN3 and SOX could be interesting, as studies in human cell lines showed, that these factors are also implicated in L1 repression.[60,86,88] Thus, these transcription factors could also have important roles for L1 regulation during human spermatogenesis and potentially influence male fertility.

4.6 H4K20me2 and H4K20me3 were present during human, bull and mouse spermatogenesis and in mature human spermatozoa, besides KMT5A and KMT5B, histone methyltransferases of H4K20

Our group and Carone *et al.* have previously shown that after histone-to-protamine exchange certain histones and nucleosomes, respectively, are retained in repetitive DNA elements, like L1 and SINEs and are potentially implicated in embryonic developmental processes.[34,69] H4K20me2 and H4K20me3 are two PTHMs, which are highly abundant in human spermatozoa (80.9 % and 9.8 %) on the H4 tail peptide encompassing aa 20-23.[42] H4K20me3 is a known repressor of L1 elements in somatic cells and H4K20me2 plays distinct roles for DNA damage repair signaling.[47,48,79] The exact establishment of H4K20 methylation states by methyltransferases KMT5A, KMT5B and KMT5C, and their erasure mechanisms are not fully understood. Studies focusing on the regulation of H4K20me2 and H4K20me3 retention patterns and their specific localization in mature spermatozoa were needed to understand their biological relevance for male fertility and embryonic development.

Therefore, H4K20me2 and H4K20me3 expression patterns were analyzed in the current study in healthy human testis tissue obtained for TESE, wildtype mouse and healthy bull testis tissue all exhibiting normal spermatogenesis. First, with IHC a general overview of their expression patterns was obtained. Second, protein abundances of H4K20me2 and H4K20me3 in mature motile and immotile human spermatozoa were analyzed by ICC and third, protein quantities of these PTHMs were determined by western blot for inter- and intra-individual retention pattern analysis. Further, recently identified genes/gene loci by our group to be enriched with H4K20me3 in human spermatozoa through ChIP-sequencing (Ozturk *et al*., 2019 in preparation), were analyzed by

ChIP-qPCR in four sperm samples of healthy volunteers (motile and immotile fractions) to prove their interactions to verify ChIP-sequencing results. Finally, mRNA levels of the respective histone methyltransferases (HMTs) of H4K20 (KMT5A, KMT5B and KMT5C) were analyzed in the cohorts by RT-qPCR.

4.6.1 H4K20me2 and H4K20me3 were present during human, bull and mouse spermatogenesis and were retained in mature human spermatozoa

In human, mouse and bull testis tissues H4K20me2 expression was at highest detectable in spermatogonia and, in round and elongating spermatids and weaker in primary spermatocytes. The expression patterns of H4K20me3 were similar to those of H4K20me2 in human, mouse and bull testis tissues, but showed its highest levels in round spermatids and elongating spermatids, confirming previous results achieved with LC/MS-MS (Luense *et al*., 2016)[42]. Neither H4K20me2 nor H4K20me3 were detectable in human pachytene spermatocytes, but that of mouse and bull. Using ICC, H4K20me2 and H4K20me3 presence was proven in mature human spermatozoa, whereby higher staining intensities for H4K20me3 were obtained.

The expression patterns of this two PTHM allow interpretations for their functions in spermatogenetic processes. Since H4K20me2 plays different roles in the open and active chromatin regions for signaling DNA damage repair and DNA replication, its presence during spermatogenesis can be assumed in highly replicative stages in euchromatic environment. This was proven here by the fact that H4K20me2 was most abundant in spermatogonia and decreasingly in spermatocytes.[46,79] In round and elongating spermatids, cell division no longer occurs but DNA damage can still arise during cell differentiation. That is why a decreasing H4K20me2 expression can be assumed and was found here in three different mammalian species. H4K20me3 is a hallmark of constitutive heterochromatin and is associated with transcriptional inactivation.[43–45] High expression of H4K20me3 was found in late spermatogenetic phases, where cell divisions have stopped and chromatin gets condensed in its heterochromatic state. Indeed, highest H4K20me3 expression was found in round spermatids and elongating spermatids and further its retention was proven in mature spermatozoa by ICC. These results were in accordance with investigations in mouse spermatogenesis, where H4K20me3 was the PTHM which showed the highest enrichment in the transition from round spermatids to elongating spermatids.[42]

To summarize, the localization of H4K20me2 and H4K20me3 here can be interpreted conclusively with respect to their literature properties in three mammalian species. Further localization and

interactions studies with other proteins, for instance involved in DNA damage repair (e. g. 53BPI) or heterochromatin formation (H3K9me3), are necessary to support the assumed roles of these PTHMs here.

4.6.2 H4K20me3 was highly abundant in mature spermatozoa and was localized in L1 elements

Levels of H4K20me2 and H4K20me3 were analyzed by western blot (WB) in healthy controls` motile and immotile spermatozoa. Western blot in controls` motile spermatozoa showed that H4K20me2 protein levels (Signal intensities: 0.05-0.23) were much lower than those of H4K20me3 (Signal intensities: 1.16-2.05). In 80 % of the cases (16/20) H4K20me3 was 1.1-7.7-times enriched in the immotile sperm fraction of controls in comparison to their motile fraction, suggesting a disturbed retention mechanism of H4K20me3 in immotile spermatozoa. The use of another H4K20me2 specific antibody should verify if H4K20me2 levels are indeed lower than H4K20me3, as Luense *et al*. revealed, by analyzing eight normozoospermic human semen samples using Nano-LC-MS/MS, that H4K20me2 levels were around times higher than H4K20me3.[42]

The differences in histone retention patterns obtained here compared to those described in literature can be explained by different methods used and by analysis of differently composed samples. In the current work, motile and immotile sperm cells of normozoospermic healthy controls, fulfilling the WHO criteria, were separated by the swim-up technique prior western blot analysis. In the study of Luense *et al.*, semen samples also fulfilled the WHO criteria, but no swim-up was performed, so that a mixture of motile and immotile sperm cells was examined.[42]

A study in 2018 of 31 sperm samples from men with abnormal and normal sperm parameters showed striking differences in the abundance of H4K20 and H3K9 methylation states.[40] Especially asthenoteratozoospermic samples (abnormal motility, forward progression and morphology) show a significant increase in H4K20me1, H3K9me1 and decrease in H4K20me2, H3K9me2/me3 methylation. Moreover, H3K9me3 and H4K20me3 are postulated to be transmitted by the spermatozoon into the zygote and regulate constitutive heterochromatin formation there.[124]

Our group identified through an MNase followed by genome-wide ChIP-sequencing (Ozturk *et al*., 2019 in preparation) the distribution pattern of H4K20me3 in fertile human sperm. Evaluated H4K20me3 binding sites were analyzed and confirmed in the current work by ChIP-qPCR in four human sperm samples (motile and immotile sperm fractions). H4K20me3 was found at *CXCL8*,

TNFSF13B, *IFNW1*, *CST8* and *L1* associated regions in mature spermatozoa of healthy controls. Two primer sets for L1 analyzes were designed, one covering the ORF1 (*L1*-OFR) and another covering the 5`UTR region (*L1*-5`UTR). In comparison to *L1*-5`UTR an increased binding of H4K20me3 in motile as well as in immotile sperms was found in *L1*-ORF. This can be explained by the higher proportion of truncated L1 elements in the human genome than of full-length L1 elements.[57]

Other studies have already shown that H4K20me3 is associated with L1 elements in different cells and tumor tissues, like CRCs (colorectal cancer cells), ES (embryonic stem cells), proliferating and senescent human cells.[81,166,167] Here, for the first time an association between L1 elements and H4K20me3 could be proven in human spermatozoa through two methods, ChIP-sequencing and ChIP-qPCR. These results suggest that H4K20me3 is involved in L1 element regulation in human sperm cells. As a negative control, a ChIP-qPCR primer set covering a gene region known to be not associated with H4K20me3, was not included here, results should be considered with caution. But since normalization was performed on the respective sample inputs and the H4K20me3-antibody (ab9053, abcam), used in both ChIP experiments, was already validated during ChIP-sequencing, it can be assumed that specific results were obtained with ChIP-qPCR.

To sum up, H4K20me2 and H4K20me3 were retained in human spermatozoa after protamine exchange. Five gene loci recently identified by our group through ChIP-sequencing (Ozturk *et al*., 2019 in preparation), were also found in ChIP-qPCR to be associated with H4K20me3 in human sperm. This proves the reliability of the ChIP-sequencing and -qPCR results. Moreover, a connection between L1 elements and H4K20me3 could be proven here in mature spermatozoa using ChIP methods. Future research should focus more in detail on the genes identified here to be associated with H4K20me3, a repressive heterochromatin marker. With respect to male fertility the biological relevance of these genes should be analyzed, especially the one of the *CXCL8*, which showed significantly higher H4K20me3 binding among immotile sperms in comparison to motile ones.

4.6.5 KMT5A and KMT5B were present in human spermatozoa, but not KMT5C

In mammalian cells, KMT5A, KMT5B and KMT5C are histone methyltransferases (HMTs) responsible for the cell cycle dependent mono-/di- and tri-methylation of H4K20, repectively.[46] KMT5B can generate both H4K20me2 and H4K20me3, with a higher preference for H4K20me1 as substrate.[51]

In mice, knockout of *Kmt5a* is associated with mitotic defects and inhibits chromatin condensation.[47,168] Double knockout of *Kmt5b*/*Kmt5c* leads to an almost complete removal of H4K20me2 and H4K20me3 in mice and induces growth retardation and perinatal death.[85,168] Studies of H4K20 HMTs in human sperm and their possible influences on male fertility and embryonic development are missing. Therefore, *KMT5A*, *KMT5B* and *KMT5C* mRNA levels were analyzed in spermatozoa of healthy controls and subfertile patients to see if these are present and possibly connected to above analyzed factors in human spermatozoa.

Controls` immotile and patients` motile spermatozoa showed a significant increase of *KMT5A* and *KMT5B* mRNA levels in comparison to controls` motile spermatozoa. Interestingly, significantly increased H4K20me3 protein levels were also detected in controls` immotile spermatozoa (patients` immotile were not available for WB studies). No significant correlation of *KMT5A* and *KMT5B* expressions to *L1* methylation or clinical and spermiogram parameters of patients` and controls` motile spermatozoa were found. *KMT5C* mRNA and protein levels were not detectable in mature human spermatozoa samples evaluated here. Thus, KMT5A and KMT5B seem to be the key players in the establishment of H4K20 methylation states in human sperm and should be investigated in future studies. As KMT5B mediates tri-methylation of H4K20 besides di-methylation, this HMT might establish these two states in a cell cycle specific manner in human spermatozoa, as already postulated by Jørgensen *et al.* in proliferating cells.[46]

Aberrant histone retention in sperm of infertile men, showing decreased semen parameters, asthenoteratozoospermic patients and sperm used for ARTs were reported.[36,40,169] In mouse embryos, combined or single knockout of *Kmt5b* and *Kmt5c* led to the loss of H4K20me2 and H4K20me3 and resulted in genomic instability, developmental arrest and perinatal death.[47,85] In the current work, spermatozoa of patients` motile and controls` immotile showed both decreased semen parameters as well as increased HMT levels (KMT5A and KMT5B) compared to motile controls. Additionally, increased H4K20me3 protein levels were found in controls` immotile spermatozoa. All these observations provide a strong indication, that histone retention mechanisms were disturbed in immotile sperms as well as in motile sperm of subfertile men. To understand the exact roles of the HMTs identified here in human spermatozoa, functional studies are required. Possibly, with the results of such studies, male sub- and infertility treatments can be improved.

5. Limitations

Several potential limitations of this thesis should be taken into account. Patients` spermatozoa were limited by their availability and their sperm concentration, so experiments were first established in controls` spermatozoa to save material for many examinations. Further studies on a larger patient and control cohort, ideally with high sperm concentrations, would be helpful to strengthen the results obtained here.

Mature human spermatozoa are transcriptionally inactive cells, but still carry e. g. mRNAs, which were regarded as remnants of spermatogenesis.[22,170] So, mRNA studies could provide evidences of transcriptional levels of selected genes during mammalian spermatogenesis. Since the functions of RNAs in mature spermatozoa are still not clear, the results obtained here about mRNA levels by RT-qPCR should be considered with caution. To ensure that only mRNAs were measured in this study and no gDNA contaminations were present, which could have led to misinterpretations of the results, all RNA samples were treated with DNase I prior cDNA synthesis and RT-qPCR. In addition, during PCR primer design, care was taken to design exon-spanning primers.

A further limitation in this thesis was, that the global DNA methylation state in human spermatozoa was examined by selected CpG island regions (determined by commercially available ELISA kits and Pyrosequencing sets), which represent only a small subset of all CpG sites. Genome-wide DNA methylation studies, like the ones of Pacheco *et al.*[131], Hajj *et al.*[151] and Sujit *et al.*[171], could expand the results achieved here.

Studies on L1 transcription factors and other regulators are limited to methylation, mRNA and/or protein analyzes in mature spermatozoa and testis tissues. As cell lines representing male germ cells are not available, further functional insights could be obtained from studies on stem cell or cancer cell cultures. So, the exact function of these factors in human spermatozoa remain unknown and need to be further investigated.

Protein extraction from controls` immotile and patients` motile spermatozoa worked better and gave more yield in comparison to the compact motile spermatozoa of the controls. Hence, protein extractions from controls` motile spermatozoa might not be sufficient to reflect their whole protein pattern. To always compare same protein amounts of different samples, protein concentrations were previously adjusted by nanodrop measurements. In addition, obtained Western blot signals were normalized to the total protein content transferred onto the membranes.

6. Summary

Previously we have shown in human sperm, that the majority of retained nucleosomes are enriched in repetitive DNA elements like L1 and SINEs. L1 is the only active retrotransposon and occupies about 17 % of the human genome. L1 activity can induce mutagenesis, genomic instability and tumor progression. Mechanisms specifically targeting L1 suppression in spermatozoa are still unknown. In somatic cells, L1 is known to be regulated by CpG methylation and, respectively DNA methyltransferases (*DNMT1* and *DNMT3A*), specific transcription factors (*YY1, SIRT6* and *MORC2*) and selected histone marks, predominantly H4K20me3. Recently, our group identified by genome-wide ChIP-sequencing, that H4K20me3 is highly enriched in L1 elements of human spermatozoa (Ozturk *et al*., 2019 in preparation). H4K20me3 together with H4K20me2 were shown to be the most abundant histone modifications in human spermatozoa (80.9 %, 9.8 %; respectively), whereby H4K20me3 was the one, which had the highest enrichment in transition from round to elongating spermatids. H4K20 methylation is mediated by specific histone methyltransferases, namely *KMT5A, KMT5B* and *KMT5C*.

The aim of this thesis was to gain insights about the epigenetic regulation of L1 in spermatozoa and to reveal its impact on male subfertility. Therefore, the methylation and mRNA of *L1* were analyzed in spermatozoa of fertile men and compared to those in subfertile patients, who underwent ART with their female partners. As female partners were inconspicuous, a male factor infertility/ subfertility was presumed. Moreover, based on insights from studies on somatic cells, known epigenetic modifiers and regulators of L1 were also analyzed in both groups. In order to have a cell model for inappropriate spermatogenesis and defective sperm, respectively, immotile spermatozoa obtained from semen of healthy donors were also included in this study (immotile sperm fraction was not available from patients). A description of the study design and main results are presented below:

Ejaculates from 97 healthy donors (motile and immotile sperm fractions), fulfilling normal sperm parameters according to WHO and 48 subfertile patients (motile sperm fraction), who underwent an ART, like ICSI or IVF, were collected and analyzed separately.

- Spermatozoa of subfertile patients possessed significantly decreased *DNMT1* and *DNMT3A* mRNA levels in comparison to healthy donors;
- Global DNA and RNA methylation levels did not differ in motile spermatozoa of healthy donors and subfertile patients;
- Significantly decreased *L1* methylation was detectable in motile spermatozoa of subfertile patients in comparison to healthy donors` motile and immotile spermatozoa. Among patients` and donors` motile spermatozoa, *L1*-mRNA and -methylation were significantly negative correlated. Moreover, in the patient subgroup showing a positive pregnancy after ICSI, a significant correlation of *L1* methylation and fertilization rate was revealed. Interestingly, immotile spermatozoa of healthy donors possessed significantly increased *L1* mRNA levels;
- *SIRT6,* a transcription factor which was shown to be epigenetically downregulated in aging human dermal fibroblasts was observed in human sperm cells. *SIRT6* promotor hyper-methylation was found in spermatozoa of subfertile patients. In sperm cells *SIRT6* methylation was not affected by age. Another L1 transcription factor, *MORC2*, was found at lowest at mRNA level in immotile spermatozoa of healthy donors. In contrast, the L1 transcription factor *YY1* was exclusively found in human Sertoli cells, but not in male germ cells;
- Repressors of L1, H4K20me2 and H4K20me3, were found to be ubiquitously expressed in human, mouse and bull testis tissues, whereby H4K20me2 signals were more intense in earlier spermatogenetic stages (spermatogonia/spermatocytes) and H4K20me3 in later stages (round/ elongating spermatids). In mature spermatozoa of healthy donors, H4K20me2 and H4K20me3 were retained in both motile and immotile ones. Comparison of H4K20me3 signals revealed their higher abundance in immotile spermatozoa. Genome-wide H4K20me3 binding sites, recently revealed by ChIP-sequencing in motile human spermatozoa, could be confirmed here for some selected genes (*L1*, *CXCL8*, *TNSFS13B*, *IFNW1* and *CST8*);
- The mRNAs of H4K20 methyltransferases, *KMT5A* and *KMT5B*, were found in motile and immotile human spermatozoa. In contrast, *KMT5C*-mRNA and -protein were undetectable in human spermatozoa.

This is one of the pioneer studies aiming to understand the epigenetic regulation of retrotransposable elements in human spermatogenesis and mature sperm cells, and to clarify if this impacts the capacity of sperm and the male fertility. It was obvious that motile and immotile spermatozoa from healthy men have huge differences in terms of *L1* methylation and *L1* mRNA levels, but also in terms of L1 regulation. Interestingly, motile spermatozoa from subfertile patients showed for some factors tendencies towards immotile sperms of healthy men. Moreover, a significant negative correlation of *L1* mRNA and *L1* methylation found among all motile spermatozoa, and the significant positive correlation of *L1* methylation with fertilization rates after ART emphasizes the impact of a proper L1 regulation in male fertility issues.

Future work is required to investigate the exact regulation mechanisms of retrotransposons in human spermatogenesis, address the impact of L1 dysregulation for sperm quality and post-fertilization events, and clarify how these all could help in praxis and benefit men with idiopathic infertility.

7. Zusammenfassung

Zuvor haben wir im menschlichen Spermium gezeigt, dass die Mehrheit der verbleibenden Nukleosomen an repetitiven DNA-Elementen wie L1 und SINEs angereicht ist. L1 ist das einzig aktive Retrotransposon und nimmt etwa 17 % des menschlichen Genoms ein. L1-Aktivitäten können zur Mutagenese, genomischen Instabilität und Tumorprogression beitragen. Mechanismen, die speziell auf die L1-Suppression bei Spermien abzielen, sind noch unbekannt. In somatischen Zellen ist bekannt, dass L1 durch CpG-Methylierung und jeweils durch DNA Methyltranferasen (*DNMT1* und *DNMT3A*), spezifische Transkriptionsfaktoren (*YY1, SIRT6, MORC2*) und bestimmte Histonmarkierungen, insbesondere H4K20me3 reguliert wird. Vor kurzem hat unsere Gruppe durch genomweite ChIP-Sequenzierung identifiziert, dass H4K20me3 in L1-Elementen von menschlichen Spermien hoch angereichert vorliegt. (Ozturk *et al*., 2019 in Vorbereitung). H4K20me3 zusammen mit H4K20me2 sind die am häufigsten vorkommenden Histonmodifikationen in menschlichen Spermien (80.9 %, 9.8 %; jeweils), wobei H4K20me3 diejenige war, welche die höchste Anreicherung im Übergang von runden zu elongierenden Spermien aufwies. Die H4K20-Methylierung wird durch spezifische Histonmethyltransferasen vermittelt, nämlich *KMT5A, KMT5B* und *KMT5C*.

Das Ziel dieser Arbeit war es, Erkenntnisse über die epigenetische Regulation von L1 in Spermien zu gewinnen und dessen Auswirkungen auf die männliche Subfertilität aufzuzeigen. Daher wurden die Methylierung und mRNA von *L1* in Spermien von fertilen Männern (gesunde Spender) analysiert und mit denen von subfertilen Patienten verglichen, die mit ihren weiblichen Partnern eine ART durchgeführt haben. Da die weiblichen Partner unauffällig waren, wurde von einem männlicher Faktor Unfruchtbarkeit/Subfertilität angenommen. Darüber hinaus wurden auf der Grundlage von Erkenntnissen aus Studien in somatischen Zellen in beiden Kohorten auch bekannte epigenetische Modifikatoren und Regulatoren von L1 analysiert. Um ein Zellmodell für eine unzureichende Spermatogenese bzw. defektes Sperma zu haben, wurden auch immotile Spermien aus Samen gesunder Spender in diese Studie einbezogen (immotile Spermienfraktion war von Patienten nicht verfügbar). Eine Beschreibung des Studiendesigns und die wichtigsten Ergebnisse werden im Folgenden dargestellt:

Ejakulate von 97 gesunden Donoren (motile und immotile Spermienfraktionen), die normale Spermienparameter nach WHO erfüllten und 48 subfertilen Patienten (motile Spermienfraktion),

die sich einer ART wie ICSI oder IVF unterzogen haben, wurden gesammelt und separat analysiert.

- Die Spermien subfertiler Patienten besaßen im Vergleich zu gesunden Spendern signifikant niedrigere *DNMT1*- und *DNMT3A*-mRNA-Spiegel;
- Die globalen DNA- und RNA-Methylierungswerte unterschieden sich nicht in motilen Spermien von gesunden Spendern und subfertilen Patienten;
- Im Vergleich zu den motilen und immotilen Spermien gesunder Spender war eine signifikant verminderte *L1*-Methylierung bei motilen Spermien subfertiler Patienten nachweisbar. Bei den motilen Spermien von Patienten und Spendern waren *L1*-mRNA und -Methylierung signifikant negativ korreliert. Darüber hinaus wurde in der Patientenuntergruppe, die eine positive Schwangerschaft nach ICSI zeigte, eine signifikante Korrelation von *L1*-Methylierung und Befruchtungsrate festgestellt. Interessanterweise besaßen immotile Spermien von gesunden Spendern signifikant erhöhte *L1*-mRNA-Spiegel;
- *SIRT6*, ein Transkriptionsfaktor, der sich als epigenetisch herunterreguliert bei alternden menschlichen dermalen Fibroblasten erwiesen hat, wurde in menschlichen Samenzellen untersucht. *SIRT6*-Promotor-Hypermethylierung wurde in Spermien von subfertilen Patienten gefunden. In Spermien wurde die *SIRT6*-Methylierung durch das Alter nicht beeinflusst. Ein weiterer L1-Transkriptionsfaktor, *MORC2*, wurde auf dem niedrigsten mRNA-Spiegel in immotilen Spermien gesunder Spender gefunden. Im Gegensatz dazu wurde der L1-Transkriptionsfaktor *YY1* ausschließlich in menschlichen Sertoli-Zellen gefunden, nicht aber in männlichen Keimzellen;
- L1-Repressoren, H4K20me2 und H4K20me3, waren im Hodengewebe von Menschen, Maus und Bulle allgegenwärtig exprimiert, wobei die H4K20me2-Signale in früheren spermatogenetischen Phasen (Spermatogonien/Spermatozyten) ausgeprägter waren und die von H4K20me3 in späteren Phasen (runde/elongierende Spermatozoen). Sowohl in motilen als auch in immotilen Spermien gesunder Spender wurden H4K20me2 und H4K20me3 einbehalten. Der Vergleich der H4K20me3-Signale zeigte eine höhere Anreicherung in immotilen Spermien. Genomweite H4K20me3-Bindungsstellen, die kürzlich durch ChIP-Sequenzierung in beweglichen menschlichen Spermien entdeckt wurden, konnten hier für einige ausgewählte Gene bestätigt werden (*L1*, *CXCL8*, *TNSFS13B*, *IFNW1* und *CST8*);

- Die mRNAs der H4K20-Methyltransferasen *KMT5A* und *KMT5B* wurden in motilen und immotilen menschlichen Spermien gefunden. Im Gegensatz dazu waren *KMT5C*-mRNA und -Protein in menschlichen Spermien nicht detektierbar.

Dies ist eine der Pionierstudien, die darauf abzielt, die epigenetische Regulation retrotransposabler Elemente in der menschlichen Spermatogenese und in reifen Samenzellen zu verstehen und zu klären, ob diese Auswirkungen auf die Spermienkapazität und die männliche Fruchtbarkeit haben. Es war offensichtlich, dass motile und immotile Spermien von gesunden Männern große Unterschiede in Bezug auf *L1*-Methylierung und *L1*-mRNA-Spiegel, aber auch in Bezug auf L1-Regulation aufweisen. Interessanterweise zeigten motile Spermien von subfertilen Patienten für einige Faktoren Tendenzen zu immotilen Spermien gesunder Männer. Darüber hinaus verdeutlicht die signifikant negative Korrelation von *L1*-mRNA und L1-Methylierung, die unter allen motilen Spermien gefunden wurde, und die signifikant positive Korrelation von *L1*-Methylierung und Befruchtungsrate nach ART die Auswirkungen einer korrekten L1-Regulierung bei männlichen Fruchtbarkeitsproblemen.

Zukünftige Arbeiten sind erforderlich, um die genauen Regulationsmechanismen von Retrotransposons in der menschlichen Spermatogenese, den Einfluss der L1-Dysregulation auf die Spermienqualität und die Ereignisse nach der Befruchtung zu untersuchen, und um zu klären, wie dies alles in der Praxis helfen und Männern mit idiopathischer Unfruchtbarkeit nützen könnte.

8. References

1. Cui, W. Mother or nothing: the agony of infertility. *Bull. World Health Organ.* **88,** 881–882 (2010).
2. Unfruchtbarkeit - Ist bei mir alles in Ordnung? - Kinderwunschzentrum am Innsbrucker Platz. Available at: https://www.kinderwunschpraxis-berlin.de/unfruchtbarkeit/. (Accessed: 14th November 2018)
3. Krausz, C. Male infertility: Pathogenesis and clinical diagnosis. *Best Pract. Res. Clin. Endocrinol. Metab.* **25,** 271–285 (2011).
4. Common causes of male infertility | Nordfertility clinic. Available at: http://www.nord fertility.com/en/articles/causes-of-male-infertility. (Accessed: 14th November 2018)
5. ICSI (Intrazytoplasmatische Spermieninjektion) - künstliche Befruchtung | familien planung.de. Available at: https://www.familienplanung.de/kinderwunsch/behandlung/icsi/ #&panel1-1. (Accessed: 14th November 2018)
6. ICSI Benefits and Risks - Attain Fertility | Attain Fertility. Available at: https://attainfertility.com/understanding-fertility/treatment-options/icsi/icsi-benefits-and-risks/. (Accessed: 14th November 2018)
7. Intracytoplasmic sperm injection (ICSI) for non-male factor infertility: a committee opinion. *Fertil. Steril.* **98,** 1395–1399 (2012).
8. Kreuzer, V. K., Kimmel, M., Schiffner, J., Czeromin, U. & Tandler-schneider, A. Possible Reasons for Discontinuation of Therapy : an Analysis of 571 071 Treatment Cycles From the German IVF Registry Mögliche Gründe für einen Therapieabbruch : eine Analyse von 571 071 Behandlungszyklen aus dem Deutschen IVF-Register. 984–990 (2018).
9. Schagdarsurengin, U. & Steger, K. Epigenetics in male reproduction: Effect of paternal diet on sperm quality and offspring health. *Nat. Rev. Urol.* **13,** 584–595 (2016).
10. Craig, J. R., Jenkins, T. G., Carrell, D. T. & Hotaling, J. M. Obesity, male infertility, and the sperm epigenome. *Fertil. Steril.* **107,** 848–859 (2017).
11. Donkin, I. & Barrès, R. Sperm epigenetics and influence of environmental factors. *Mol. Metab.* **14,** 1–11 (2018).
12. Steger, K., Paradowska, A., Weidner, W. Der Histon-Protamin-Austausch während der Spermiogenese : Mögliche Funktionen von Resthistonen. *Leb. Wiss. / Spitzenforsch. i. d. Urol.* **2,** 176–183 (2009).
13. Neto, F. T. L., Bach, P. V., Najari, B. B., Li, P. S. & Goldstein, M. Spermatogenesis in humans and its affecting factors. *Semin. Cell Dev. Biol.* **59,** 10–26 (2016).
14. Heller, C. G. & Clermont, Y. Spermatogenesis in man: An estimate of its duration. *Science (80-.).* **140,** 184–186 (1963).
15. Wu, H., Hauser, R., Krawetz, S. A. & Pilsner, J. R. Environmental Susceptibility of the Sperm Epigenome During Windows of Male Germ Cell Development. *Curr. Environ. Heal. reports* **2,** 356–366 (2015).

16. Soubry, A., Hoyo, C., Jirtle, R. L. & Murphy, S. K. A paternal environmental legacy: Evidence for epigenetic inheritance through the male germ line. *BioEssays* **36,** 359–371 (2014).

17. Schagdarsurengin, U., Paradowska, A. & Steger, K. Analysing the sperm epigenome: roles in early embryogenesis and assisted reproduction. *Nat. Rev. Urol.* **9,** 609–619 (2012).

18. Levine, H. *et al.* Temporal trends in sperm count : a systematic review and meta-regression analysis. **23,** 646–659 (2017).

19. Jurewicz, J. *et al.* Human Semen Quality, Sperm DNA Damage, and the Level of Reproductive Hormones in Relation to Urinary Concentrations of Parabens. *JOEM* **59,** 1034–1040 (2017).

20. Desdoits-Lethimonier, C. *et al.* Parallel assessment of the effects of bisphenol A and several of its analogs on the adult human testis. *Hum. Reprod.* **32,** 1465–1473 (2017).

21. Montjean, D. *et al.* Sperm global DNA methylation level: Association with semen parameters and genome integrity. *Andrology* **3,** (2015).

22. Champroux, A., Cocquet, J., Henry-Berger, J., Drevet, J. R. & Kocer, A. A Decade of Exploring the Mammalian Sperm Epigenome: Paternal Epigenetic and Transgenerational Inheritance. *Front. Cell Dev. Biol.* **6,** (2018).

23. Jin, B., Li, Y. & Robertson, K. D. DNA methylation: superior or subordinate in the epigenetic hierarchy? *Genes Cancer* **2,** 607–17 (2011).

24. Stewart, K. R., Veselovska, L. & Kelsey, G. Establishment and functions of DNA methylation in the germline. *Epigenomics* **8,** 1399–1413 (2016).

25. Ni, K. *et al.* TET enzymes are successively expressed during human spermatogenesis and their expression level is pivotal for male fertility. *Hum. Reprod.* **31,** 1411–1424 (2016).

26. Joana Marques, C. *et al.* DNA methylation imprinting marks and DNA methyltransferase expression in human spermatogenic cell stages. *Epigenetics* **6,** 1354–1361 (2011).

27. Jenkins, T. G. & Carrell, D. T. The sperm epigenome and potential implications for the developing embryo. *Reproduction* **143,** 727–734 (2012).

28. Uysal, F., Akkoyunlu, G. & Ozturk, S. DNA methyltransferases exhibit dynamic expression during spermatogenesis. *Reprod. Biomed. Online* **33,** 690–702 (2016).

29. Liu, H. *et al.* DNA methylation dynamics: Identification and functional annotation. *Brief. Funct. Genomics* **15,** 470–484 (2016).

30. Rajender, S., Avery, K. & Agarwal, A. Epigenetics, spermatogenesis and male infertility. *Mutat. Res. - Rev. Mutat. Res.* **727,** 62–71 (2011).

31. Urdinguio, R. G. *et al.* Aberrant DNA methylation patterns of spermatozoa in men with unexplained infertility. *Hum. Reprod.* **30,** 1014–1028 (2015).

32. Hammoud, S. S. *et al.* Chromatin and transcription transitions of mammalian adult germline stem cells and spermatogenesis. *Cell Stem Cell* **15,** 239–253 (2014).

33. Gatewood, J. M., Cook, G. R., Balhorn, R., Schmid, C. W. & Bradbury, E. M. Isolation of four core histones from human sperm chromatin representing a minor subset of somatic histones. *J. Biol. Chem.* **265,** 20662–20666 (1990).

34. Samans, B. *et al.* Uniformity of nucleosome preservation pattern in mammalian sperm and Its connection to repetitive DNA elements. *Dev. Cell* **30,** 23–35 (2014).

35. Denomme, M. M., McCallie, B. R., Parks, J. C., Schoolcraft, W. B. & Katz-Jaffe, M. G. Alterations in the sperm histone-retained epigenome are associated with unexplained male factor infertility and poor blastocyst development in donor oocyte IVF cycles. *Hum. Reprod.* **32,** 2443–2455 (2017).

36. Hammoud, S. S. *et al.* Genome-wide analysis identifies changes in histone retention and epigenetic modifications at developmental and imprinted gene loci in the sperm of infertile men. *Hum. Reprod.* **26,** 2558–2569 (2011).

37. Samanta, L., Swain, N., Ayaz, A., Venugopal, V. & Agarwal, A. Post-Translational Modifications in sperm Proteome: The Chemistry of Proteome diversifications in the Pathophysiology of male factor infertility. *Biochim. Biophys. Acta - Gen. Subj.* **1860,** 1450–1465 (2016).

38. Qian, M. X. *et al.* XAcetylation-mediated proteasomal degradation of core histones during DNA repair and spermatogenesis. *Cell* **153,** 1012 (2013).

39. Naaby-Hansen, S. *et al.* CABYR, a novel calcium-binding tyrosine phosphorylation-regulated fibrous sheath protein involved in capacitation. *Dev. Biol.* **242,** 236–254 (2002).

40. Schon, S. B. *et al.* Histone modification signatures in human sperm distinguish clinical abnormalities. *J. Assist. Reprod. Genet.* (2018). doi:10.1007/s10815-018-1354-7

41. Bracke, A., Peeters, K., Punjabi, U., Hoogewijs, D. & Dewilde, S. A search for molecular mechanisms underlying male idiopathic infertility. *Reprod. Biomed. Online* **36,** 327–339 (2018).

42. Luense, L. J. *et al.* Comprehensive analysis of histone post-translational modifications in mouse and human male germ cells. *Epigenetics Chromatin* **9,** 24 (2016).

43. Wei, G. *et al.* High-Resolution Profiling of Histone Methylations in the Human Genome. *Cell* **129,** 823–837 (2007).

44. Lehnertz, B. *et al.* Suv39h-Mediated Histone H3 Lysine 9 Methylation Directs DNA Methylation to Major Satellite Repeats at Pericentric Heterochromatin. **114,** 139–140 (2003).

45. Wongtawan, T., Taylor, J. E., Lawson, K. A., Wilmut, I. & Pennings, S. Histone H4K20me3 and HP1alpha are late heterochromatin markers in development, but present in undifferentiated embryonic stem cells. *J Cell Sci* **124,** 1878–1890 (2011).

46. Jørgensen, S., Schotta, G. & Sørensen, C. S. Histone H4 Lysine 20 methylation: Key player in epigenetic regulation of genomic integrity. *Nucleic Acids Res.* **41,** 2797–2806 (2013).

47. Schotta, G. *et al.* A chromatin-wide transition to H4K20 monomethylation impairs genome integrity and programmed DNA rearrangements in the mouse. 2048–2061 (2008). doi:10.1101/gad.476008.5

48. Wang, Z. *et al*. Combinatorial patterns of histone acetylations and methylations in the human genome. *Nat Genet.* **40,** 897–903 (2008).

49. Shi, X. L., Guo, Z. J., Wang, X. L., Liu, X. L. & Shi, G. F. SET8 expression is associated with overall survival in gastric cancer. *Genet. Mol. Res.* **14,** 15609–15615 (2015).

50. Horton, J. R. *et al.* Enzymatic and structural insights for substrate specificity of a family of jumonji histone lysine demethylases. *Nat Struct Mol Biol.* **17,** 38–43 (2010).

51. Pesavento, J. J., Yang, H., Kelleher, N. L. & Mizzen, C. A. Certain and Progressive Methylation of Histone H4 at Lysine 20 during the Cell Cycle. *Mol. Cell. Biol.* **28,** 468–486 (2007).

52. Stender, J. D. *et al.* Control of Pro-Inflammatory Gene Programs by Regulated Trimethylation and Demethylation of Histone H4K20. *Mol Cell.* **48,** 28–38 (2012).

53. Ozboyaci, M., Gursoy, A., Erman, B. & Keskin, O. Molecular recognition of H3/H4 histone tails by the tudor domains of JMJD2A: A comparative molecular dynamics simulations study. *PLoS One* **6,** (2011).

54. Lee, J., Thompson, J. R., Botuyan, M. V. & Mer, G. Distinct binding modes specify the recognition of methylated histones H3K4 and H4K20 by JMJD2A-tudor. *Nat. Struct. Mol. Biol.* **15,** 109–111 (2008).

55. cellectablog. Cancer, the Human Mobilome, and LINE-1 Retrotransposons | Cellecta, Inc. (2017). Available at: https://www.cellecta.com/cancer-human-mobilome-line-1-retrotrans-posons/. (Accessed: 20th February 2019)

56. Bodak, M., Yu, J. & Ciaudo, C. Regulation of LINE-1 in mammals. *Biomol. Concepts* **5,** 409–428 (2014).

57. Doucet, J. *et al.* RNase L restricts the mobility of engineered retrotransposons in cultured human cells. **42,** 3803–3820 (2014).

58. Castro-Diaz, N. *et al.* Evolutionally dynamic L1 regulation in embryonic stem cells. *Genes Dev.* **28,** 1397–1409 (2014).

59. Hamdorf, M. *et al.* miR-128 represses L1 retrotransposition by binding directly to L1 RNA. *Nat. Publ. Gr.* **22,** 824–831 (2015).

60. Rosser, J. M. & An, W. L1 expression and regulation in humans and rodents. *Front Biosci (Elite Ed)* **4,** 2203–2225 (2012).

61. Wanichnopparat, W., Suwanwongse, K., Pin-on, P., Aporntewan, C. & Mutirangura, A. Genes associated with the cis-regulatory functions of intragenic LINE-1 elements. *BMC Genomics* **14,** 1–9 (2013).

62. Jachowicz, J. W. *et al.* LINE-1 activation after fertilization regulates global chromatin accessibility in the early mouse embryo. *Nat. Genet.* **49,** 1502–1510 (2017).

63. Rodić, N. & Burns, K. H. Long Interspersed Element-1 (LINE-1): Passenger or Driver in Human Neoplasms? *PLoS Genet.* **9,** 1–5 (2013).

64. Belancio, V. P., Roy-Engel, A. M., Pochampally, R. R. & Deininger, P. Somatic expression of LINE-1 elements in human tissues. *Nucleic Acids Res.* **38,** 3909–3922 (2010).

65. Muñoz-Lopez, M., Garcia-Cañadas, M., Macia, A., Santiago, M. & Jose L., G.-P. Analysis of LINE-1 Expression in Human Pluripotent Cells. *Hum. Embryonic Stem Cells Handb.* **873,** 113–125 (2012).

66. Kano, H. *et al.* L1 retrotransposition occurs mainly in embryogenesis and creates somatic mosaicism. *Genes Dev.* **23,** 1303–1312 (2009).

67. Lee, E. *et al.* Landscape of Somatic Retrotransposition in Human Cancers. *Science (80-.).* **337,** 967–971 (2013).

68. Cheng, Y. S., Wee, S. K., Lin, T. Y. & Lin, Y. M. MAEL promoter hypermethylation is associated with de-repression of LINE-1 in human hypospermatogenesis. *Hum. Reprod.* **32,** 2373–2381 (2017).

69. Carone, B. R. *et al.* High-Resolution Mapping of Chromatin Packaging in Mouse Embryonic Stem Cells and Sperm. *Dev. Cell* **30,** 11–22 (2014).

70. Tunc, O. & Tremellen, K. Oxidative DNA damage impairs global sperm DNA methylation in infertile men. *J. Assist. Reprod. Genet.* **26,** 537–544 (2009).

71. Moskalev, E. A. *et al.* GHSR DNA hypermethylation is a common epigenetic alteration of high diagnostic value in a broad spectrum of cancers. *Oncotarget* **6,** 4418–4427 (2014).

72. Poplinski, A., Tüttelmann, F., Kanber, D., Horsthemke, B. & Gromoll, J. Idiopathic male infertility is strongly associated with aberrant methylation of MEST and IGF2/H19 ICR1. *Int. J. Androl.* **33,** 642–649 (2010).

73. Lisanti, S. *et al.* Comparison of methods for quantification of global DNA methylation in human cells and tissues. *PLoS One* **8,** 1–11 (2013).

74. He, Z. M. *et al.* Transition of LINE-1 DNA methylation status and altered expression in first and third trimester placentas. *PLoS One* **9,** 1–11 (2014).

75. Li, S. *et al.* Hypomethylation of LINE-1 elements in schizophrenia and bipolar disorder. *J. Psychiatr. Res.* **107,** 68–72 (2018).

76. Teneng, I., Montoya-Durango, D. E., Quertermous, J. L., Lacy, M. E. & Ramos, K. S. Reactivation of L1 retrotransposon by benzo(a)pyrene involves complex genetic and epigenetic regulation. *Epigenetics* **6,** 355–367 (2011).

77. Cui, X. *et al.* DNA methylation in spermatogenesis and male infertility. *Exp. Ther. Med.* **12,** 1973–1979 (2016).

78. Marques, C. J. *et al.* Abnormal methylation of imprinted genes in human sperm is associated with oligozoospermia. *Mol. Hum. Reprod.* **14,** 67–73 (2008).

79. Kuo, A. J. *et al.* The BAH domain of ORC1 links H4K20me2 to DNA replication licensing and Meier-Gorlin syndrome. *Nature* **484,** 115–9 (2012).

80. Fraga, M. F. *et al.* Loss of acetylation at Lys16 and trimethylation at Lys20 of histone H4 is a common hallmark of human cancer. *Nat. Genet.* **37,** 391–400 (2005).

81. Gezer, U. *et al.* Characterization of H3K9me3- and H4K20me3-associated circulating nucleosomal DNA by high-throughput sequencing in colorectal cancer. *Tumor Biol.* **34,** 329–336 (2013).

82. Castillo, J., Estanyol, J. M., Ballescá, J. L. & Oliva, R. Human sperm chromatin epigenetic potential: genomics, proteomics, and male infertility. *Asian J. Androl.* **17,** 601–9 (2015).

83. Vavouri, T. & Lehner, B. Chromatin organization in sperm may be the major functional consequence of base composition variation in the human genome. *PLoS Genet.* **7,** (2011).

84. Hatanaka, Y. *et al.* Histone chaperone CAF-1 mediates repressive histone modifications to protect preimplantation mouse embryos from endogenous retrotransposons. *Proc. Natl. Acad. Sci. U. S. A.* **112,** 14641–6 (2015).

85. Eid, A., Rodriguez-Terrones, D., Burton, A. & Torres-Padilla, M. E. SUV4-20 activity in the preimplantation mouse embryo controls timely replication. *Genes Dev.* **30,** 2513–2526 (2016).

86. Hulme, A. E., Kulpa, D. A., Perez, J. L. G. & Moran, J. V. The impact of LINE-1 retro transposition on the human genome. *Genomic Disord. Genomic Basis Dis.* 35–55 (2006). doi:10.1007/978-1-59745-039-3_3

87. Richardson, S. R. *et al.* The Influence of LINE-1 and SINE Retrotransposons on Mammalian Genomes. *Microbiol. Spectr.* **3,** MDNA3-0061-2014 (2015).

88. Athanikar, J. N., Badge, R. M. & Moran, J. V. A YY1-binding site is required for accurate human LINE-1 transcription initiation. *Nucleic Acids Res.* **32,** 3846–3855 (2004).

89. Botulinum, R. I. & Study, R. SIRT6 represses LINE1 retrotransposons by ribosylating KAP1 but this repression fails with stress and age. **4,** 139–148 (2014).

90. Kanfi, Y. *et al.* The sirtuin SIRT6 regulates lifespan in male mice. *Nature* **483,** 218–221 (2012).

91. Sahin, K., Yilmaz, S. & Gozukirmizi, N. Changes in human sirtuin 6 gene promoter methylation during aging. *Biomed. reports* **2,** 574–578 (2014).

92. Tissue expression of SIRT6 - Staining in testis - The Human Protein Atlas. Available at: https://www.proteinatlas.org/ENSG00000077463-SIRT6/tissue/testis. (Accessed: 24th February 2019)

93. Liu, N. *et al.* Selective silencing of euchromatic L1s revealed by genome-wide screens for L1 regulators. *Nature* **553,** 228–232 (2018).

94. Tchasovnikarova, I. A. *et al.* Hyperactivation of HUSH complex function by Charcot-Marie-Tooth disease mutation in MORC2. *Nat. Genet.* **49,** 1035–1044 (2017).

95. Nee, K. *et al.* MORC1 represses transposable elements in the mouse male germline. *Nat. Commun.* **5,** (2014).

96. Ni, K. Investigations on the role of DNA methylation governing enzymes (TET1–3, DNMT1 and DNMT3A) for male fertility and ART treatment. (2016).

97. Ostermeier, G. C. *et al.* Toward using stable spermatozoal RNAs for prognostic assessment of male factor fertility. **83,** (2005).

98. Platts, A. E. *et al.* Success and failure in human spermatogenesis as revealed by teratozoospermic RNAs. **16,** 763–773 (2017).

99. Radak, Z. *et al.* Age-dependent changes in 8-oxoguanine-DNA glycosylase activity are modulated by adaptive responses to physical exercise in human skeletal muscle. *Free Radic. Biol. Med.* **51,** 417–423 (2011).

100. Wang, D., Li, C. & Zhang, X. The Promoter Methylation Status and mRNA Expression Levels of *CTCF* and *SIRT6* in Sporadic Breast Cancer. *DNA Cell Biol.* **33,** 581–590 (2014).

101. Nagai, K. *et al.* Depletion of SIRT6 causes cellular senescence, DNA damage, and telomere dysfunction in human chondrocytes. *Osteoarthr. Cartil.* **23,** 1412–1420 (2015).

102. effect size - What are real strengths of association when using Pearson correlation? - Cross Validated. Available at: https://stats.stackexchange.com/questions/104892/what-are-real-strengths-of-association-when-using-pearson-correlation. (Accessed: 8th February 2019)

103. W15_Eli_Correlation, T-Test, Chi-Square Test | Mercure AACE 2013. Available at: https://mercureaace2013.wordpress.com/2013/05/19/w15_eli_correlation-t-test-chi-square-test/. (Accessed: 8th February 2019)

104. Montoya-Durango, D. E. *et al.* Epigenetic Control of Mammalian LINE-1 Retrotransposon by Retinoblastoma Proteins. **665,** 20–28 (2009).

105. Rangasamy, D. Distinctive patterns of epigenetic marks are associated with promoter regions of mouse LINE-1 and LTR retrotransposons. *Mob. DNA* **4,** 27 (2013).

106. Steger, K., Behr, R., Kleiner, I., Weinbauer, G. F. & Bergmann, M. Expression of activator of CREM in the testis (ACT) during normal and impaired spermatogenesis: Correlation with CREM expression. *Mol. Hum. Reprod.* **10,** 129–135 (2004).

107. Clermont, Y. The cycle of the seminiferous epithelium in man. *Am. J. Anat.* **112,** 35–51 (1963).

108. Guan, J. *Mammalian Sperm Flagella*. (2009).

109. D. Russell, L., Ettlin, R., P. Sinha Hikim, A. & D. Clegg, E. Histological and Histopathological Evaluation of The Testis. *Int. J. Androl.* **16,** 83 (1990).

110. Guraya, S. S. & Bilaspuri, G. S. Stages of seminiferous epithelial cycle and in the buffalo (Bos bubalus). *Gegenbaurs Morphol. Jahrb.* **122,** 147–161 (1976).

111. Tissue expression of KMT5A - Summary - The Human Protein Atlas. Available at: https://www.proteinatlas.org/ENSG00000183955-KMT5A/tissue. (Accessed: 5th April 2019)

112. Tissue expression of KMT5B - Summary - The Human Protein Atlas. Available at: https://www.proteinatlas.org/ENSG00000110066-KMT5B/tissue. (Accessed: 5th April 2019)

113. Tissue expression of KMT5C - Summary - The Human Protein Atlas. Available at: https://www.proteinatlas.org/ENSG00000133247-KMT5C/tissue. (Accessed: 5th April 2019)

114. Oliva, R. & Luís Ballescà, J. Altered histone retention and epigenetic modifications in the sperm of infertile men. *Asian J. Androl.* **14,** 239–240 (2012).

115. Jenkins, T. G. *et al.* Teratozoospermia and asthenozoospermia are associated with specific epigenetic signatures. *Andrology* **4,** 843–849 (2016).

116. Hammoud, S. S. *et al.* Distinctive chromatin in human sperm packages genes for embryo development. *Nature* **460,** 473–478 (2009).

117. Hisano, M. *et al.* Genome-wide chromatin analysis in mature mouse and human spermatozoa. *Nat. Protoc.* **8,** 2449–70 (2013).

118. Arpanahi, A. *et al.* Endonuclease-sensitive regions of human spermatozoal chromatin are highly enriched in promoter and CTCF binding sequences. *Genome Res.* **19,** 1338–1349 (2009).

119. Brykczynska, U. *et al.* Repressive and active histone methylation mark distinct promoters in human and mouse spermatozoa. *Nat. Struct. Mol. Biol.* **17,** 679–687 (2010).

120. Yoshida, K. *et al.* Mapping of histone-binding sites in histone replacement-completed spermatozoa. *Nat. Commun.* **9,** 1–11 (2018).

121. Okada, Y. & Yamaguchi, K. Epigenetic modifications and reprogramming in paternal pronucleus: sperm, preimplantation embryo, and beyond. *Cell. Mol. Life Sci.* **74,** 1957–1967 (2017).

122. Erkek, S. *et al.* Molecular determinants of nucleosome retention at CpG-rich sequences in mouse spermatozoa. *Nat. Struct. Mol. Biol.* **20,** 868–875 (2013).

123. Rando, O. J. Intergenerational transfer of epigenetic information in sperm. *Cold Spring Harb. Perspect. Med.* **6,** 1–13 (2016).

124. van de Werken, C. *et al.* Paternal heterochromatin formation in human embryos is H3K9/HP1 directed and primed by sperm-derived histone modifications. *Nat. Commun.* **5,** 5868 (2014).

125. van der Heijden, G. W. *et al.* Sperm-derived histones contribute to zygotic chromatin in humans. *BMC Dev. Biol.* **8,** 34 (2008).

126. Belancio, V. P., Hedges, D. J. & Deininger, P. Mammalian non-LTR retrotransposons: For better or worse, in sickness and in health. *Genome Res.* **18,** 343–358 (2008).

127. Beck, C. R., Garcia-Perez, J. L., Badge, R. M. & Moran, J. V. LINE-1 Elements in Structural Variation and Disease. *Annu Rev Genomics Hum Genet* **12,** 187–215 (2011).

128. Kuhtz, J. *et al.* Epigenetic heterogeneity of developmentally important genes in human sperm: Implications for assisted reproduction outcome. *Epigenetics* **9,** 1648–1658 (2015).

129. Kläver, R. *et al.* DNA methylation in spermatozoa as a prospective marker in andrology. *Andrology* **1,** 731–740 (2013).

130. Tang, Q. *et al.* Idiopathic male infertility is strongly associated with aberrant DNA methylation of imprinted loci in sperm: A case-control study. *Clin. Epigenetics* **10,** 1–10 (2018).

131. Pacheco, S. E. *et al.* Integrative DNA methylation and gene expression analyses identify DNA packaging and epigenetic regulatory genes associated with low motility sperm. *PLoS One* **6,** 1–10 (2011).

132. Niles, K. M., Chan, D., la Salle, S., Oakes, C. C. & Trasler, J. M. Critical period of nonpromoter DNA methylation acquisition during prenatal male germ cell development. *PLoS One* **6,** (2011).

133. Oakes, C. C., La Salle, S., Smiraglia, D. J., Robaire, B. & Trasler, J. M. A unique configuration of genome-wide DNA methylation patterns in the testis. *Proc. Natl. Acad. Sci.* **104,** 228–233 (2007).

134. Müller, M. *et al.* Tissue Distribution of 5-Hydroxymethylcytosine and Search for Active Demethylation Intermediates. *PLoS One* **5,** e15367 (2010).

135. Matzke, M. A. & Mosher, R. A. RNA-directed DNA methylation: An epigenetic pathway of increasing complexity. *Nat. Rev. Genet.* **15,** 394–408 (2014).

136. Hosken, D. J. & Hodgson, D. J. Why do sperm carry RNA? Relatedness, conflict, and control. *Trends Ecol. Evol.* **29,** 451–455 (2014).

137. EpiQuik m6A RNA Methylation Quantification Kit (Colorimetric) | EpiGentek. Available at: https://www.epigentek.com/catalog/epiquik-m6a-rna-methylation-quantification-kit-colorimetric-p-3646.html?currency=de. (Accessed: 27th February 2019)

138. Chen, X., Li, X., Guo, J., Zhang, P. & Zeng, W. The roles of microRNAs in regulation of mammalian spermatogenesis. *J. Anim. Sci. Biotechnol.* **8,** 1–8 (2017).

139. Yang, Y. *et al.* Increased N 6 -methyladenosine in Human Sperm RNA as a Risk Factor for Asthenozoospermia. *Sci. Rep.* **6,** 1–8 (2016).

140. Wang, X., Suo, Y., Yin, R., Shen, H. & Wang, H. Ultra-performance liquid chromatography/tandem mass spectrometry for accurate quantification of global DNA methylation in human sperms. *J. Chromatogr. B Anal. Technol. Biomed. Life Sci.* **879,** 1647–1652 (2011).

141. Guz, J., Gackowski, D., Foksinski, M., Rozalski, R. & Olinski, R. Comparison of the Absolute Level of Epigenetic Marks 5-Methylcytosine, 5-Hydroxymethylcytosine, and 5-Hydroxymethyluracil Between Human Leukocytes and Sperm1. *Biol. Reprod.* **91,** 1–5 (2014).

142. Jenkins, T. G., Aston, K. I., Cairns, B. R. & Carrell, D. T. Paternal aging and associated intraindividual alterations of global sperm 5-methylcytosine and 5-hydroxymethylcytosine levels. *J. Urol.* **191,** 1356 (2014).

143. Zhang, Y. *et al.* Dnmt2 mediates intergenerational transmission of paternally acquired metabolic disorders through sperm small non-coding RNAs. *Nat Cell Biol.* **20,** 535–540 (2018).

144. Xu, K. *et al.* Mettl3-mediated m 6 A regulates spermatogonial differentiation and meiosis initiation. *Cell Res.* **27,** 1100–1114 (2017).

145. Klukovich, R. *et al.* ALKBH5-dependent m6A demethylation controls splicing and stability of long 3′-UTR mRNAs in male germ cells. *Proc. Natl. Acad. Sci.* **115,** E325–E333 (2017).

146. Kasowitz, S. D. *et al.* Nuclear m6A reader YTHDC1 regulates alternative polyadenylation and splicing during mouse oocyte development. *PLoS Genet.* **14,** 1–28 (2018).

147. Steinhoff, C. & Schulz, W. A. Transcriptional regulation of the human LINE-1 retrotransposon L1.2B. *Mol. Genet. Genomics* **270,** 394–402 (2003).

148. Babushok, D. V. & Kazazian, H. H. J. Progress in Understanding the Biology of the Human Mutagen LINE-1. *Hum. Mutat.* **28,** 527–539 (2007).

149. Kobayashi, H. *et al.* Aberrant DNA methylation of imprinted loci in sperm from oligospermic patients. *Hum. Mol. Genet.* **16,** 2542–2551 (2007).

150. Heyn, H. *et al.* Epigenetic Disruption of the PIWI Pathway in Human Spermatogenic Disorders. *PLoS One* **7,** (2012).

151. El Hajj, N. *et al.* Methylation status of imprinted genes and repetitive elements in sperm DNA from infertile males. *Sex. Dev.* **5,** 60–69 (2011).

152. Cheng, Y.-S. S., Wee, S.-K. K., Lin, T.-Y. Y. & Lin, Y.-M. M. MAEL promoter hypermethylation is associated with de-repression of LINE-1 in human hypospermatogenesis. *Hum. Reprod.* **32,** 2373–2381 (2017).

153. Newkirk, S. J. *et al.* Intact piRNA pathway prevents L1 mobilization in male meiosis. *Proc. Natl. Acad. Sci.* **114,** E5635–E5644 (2017).

154. Carmell, M. A. *et al.* MIWI2 Is Essential for Spermatogenesis and Repression of Transposons in the Mouse Male Germline. *Dev. Cell* **12,** 503–514 (2007).

155. Hadziselimovic, F., Hadziselimovic, N. O., Demougin, P., Krey, G. & Oakeley, E. Piwi-pathway alteration induces LINE-1 transposon derepression and infertility development in cryptorchidism. *Sex. Dev.* **9,** 98–104 (2015).

156. Giebler, M., Greither, T., Müller, L., Mösinger, C. & Behre, H. M. Altered PIWI‐LIKE 1 and PIWI‐LIKE 2 mRNA expression in ejaculated spermatozoa of men with impaired sperm characteristics. 260–264 (2018). doi:10.4103/aja.aja

157. Palmer, N. O., Fullston, T., Mitchell, M., Setchell, B. P. & Lane, M. SIRT6 in mouse spermatogenesis is modulated by diet-induced obesity. *Reprod. Fertil. Dev.* **23,** 929 (2011).

158. Ren, Y. *et al.* Effect of breed on the expression of Sirtuins (Sirt1-7) and antioxidant capacity in porcine brain. *Animal* **7,** 1994–1998 (2013).

159. Tissue expression of MORC2 - Summary - The Human Protein Atlas. Available at: https://www.proteinatlas.org/ENSG00000133422-MORC2/tissue. (Accessed: 18th April 2019)

160. Albulym *et al.* MORC2 Mutations Cause Axonal Charcot–Marie–Tooth Disease With Pyramidal Signs. *Ann. Neurol.* **4,** 419–427 (2017).

161. Schottmann, G., Wagner, C., Seifert, F., Stenzel, W. & Schuelke, M. MORC2 mutation causes severe spinal muscular atrophy-phenotype, cerebellar atrophy, and diaphragmatic paralysis . *Brain* **139,** e70–e70 (2016).

162. Shi, B. *et al.* MORC2B is essential for meiotic progression and fertility. *PLoS Genet.* **14,** 1–21 (2018).

163. Kim, J. S., Chae, J. H., Cheon, Y. P. & Kim, C. G. Reciprocal localization of transcription factors YY1 and CP2c in spermatogonial stem cells and their putative roles during spermatogenesis. *Acta Histochem.* **118,** 685–692 (2016).

164. Wu, S., Hu, Y.-C., Liu, H. & Shi, Y. Loss of YY1 Impacts the Heterochromatic State and Meiotic Double-Strand Breaks during Mouse Spermatogenesis. *Mol. Cell. Biol.* **29,** 6245–6256 (2009).

165. Donohoe, M. E. *et al.* Targeted disruption of mouse Yin Yang 1 transcription factor results in peri-implantation lethality. *Mol. Cell. Biol.* **19,** 7237–44 (1999).

166. Kidder, B. L., Hu, G., Cui, K. & Zhao, K. SMYD5 regulates H4K20me3-marked heterochromatin to safeguard ES cell self-renewal and prevent spurious differentiation. *Epigenetics Chromatin* **10,** 1–20 (2017).

167. Nelson, D. M. *et al.* Mapping H4K20me3 onto the chromatin landscape of senescent cells indicates a function in control of cell senescence and tumor suppression through preservation of genetic and epigenetic stability. *Genome Biol.* **17,** 1–20 (2016).

168. Tsang, L. W. K., Hu, N. & Alan Underhill, D. Comparative analyses of SUV420H1 isoforms and SUV420H2 reveal differences in their cellular localization and effects on myogenic differentiation. *PLoS One* **5,** (2010).

169. Yu, B. *et al.* Epigenetic alterations in density selected human spermatozoa for assisted reproduction. *PLoS One* **10,** 1–16 (2015).

170. Lalancette, C., Miller, D., Li, Y. & Krawetz, S. A. Paternal Contributions: New Functional Insights For Spermatozoal RNA. *J Cell Biochem* **104,** 157–1579 (2008).

171. Sujit, K. M. *et al.* Genome-wide differential methylation analyses identifies methylation signatures of male infertility. *Hum. Reprod.* **33,** 2256–2267 (2018).

9. Supplementary Information

Whole protein stainings after protein transfer with the REVERT™ Total Protein Stain Kit were performed, for checking transfer efficiency and later normalization of western blots. The stainings for later H4K20me3 protein level analysis of 20 donors` M/IM are shown here in Figure 44 (corresponding western blots with H4K20me3 displayed in Figure 37 **E**).

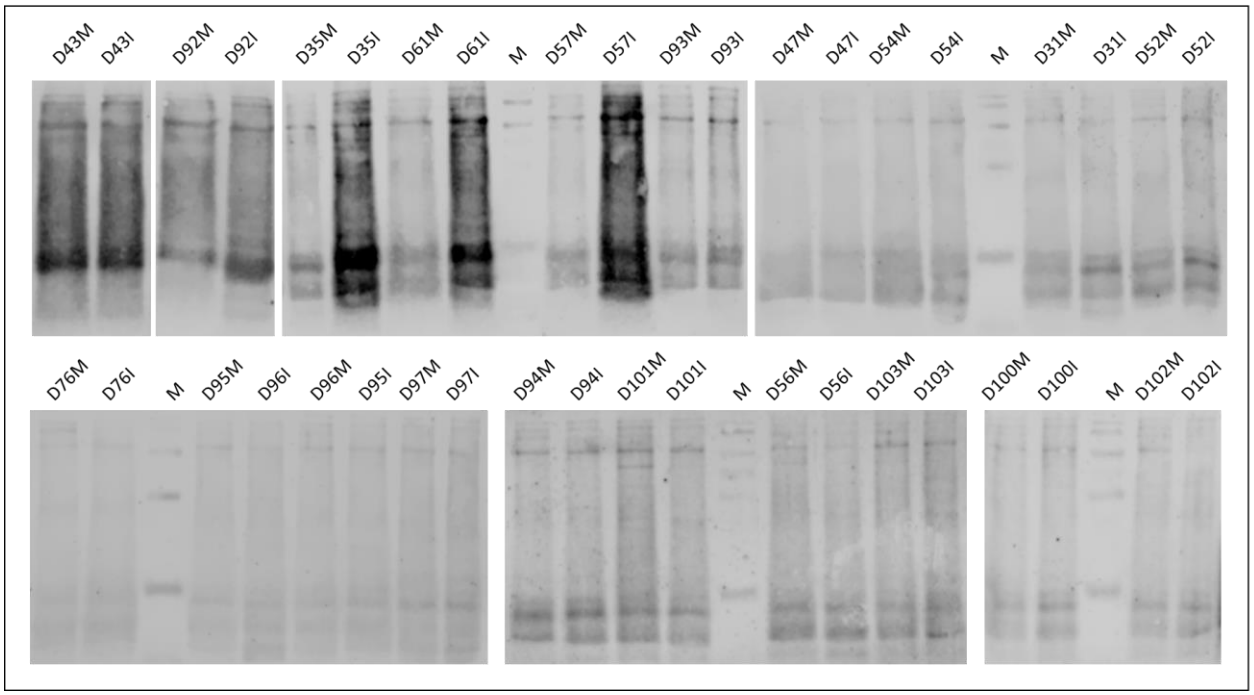

Figure 44: Whole protein stainings after protein transfer of 20 donors M/IM. The signal intensity for H4K20me3 in western blots (Fig. 37 **E**) was normalized to its whole protein content.

The normalization to the whole protein content of each sample is a much more stable method than normalization to individual house-keeping genes. In addition, uneven sample loads are eliminated with this normalization method and lead to an even more accurate comparison of protein signals between samples.

In the following Tables (16-21) methylation and mRNA values of all tested targets in the three cohorts (patients` M, donors` M/IM) are summarized.

Table 16: Summary of all values from methylation and mRNA analyzes in donors` M.

Type	ID	Fertiliza-tion rate	Outcome	5mC DNA meth.	m6A RNA meth.	L1 meth. pyroseq.	L1 meth. ELISA	L1 mRNA
Donor M	DFG-US-01	unknown	unknown					
Donor M	DFG-US-04	unknown	unknown					
Donor M	DFG-US-05	unknown	unknown					
Donor M	DFG-US-06	unknown	unknown					
Donor M	DFG-US-07	unknown	unknown					
Donor M	DFG-US-08	unknown	unknown					
Donor M	DFG-US-09	unknown	unknown				47,87	
Donor M	DFG-US-11	unknown	unknown					
Donor M	DFG-US-12	unknown	unknown					
Donor M	DFG-US-13	unknown	unknown					
Donor M	DFG-US-14	unknown	unknown					
Donor M	DFG-US-15	unknown	unknown					
Donor M	DFG-US-16	unknown	unknown					
Donor M	DFG-US-17	unknown	unknown					
Donor M	DFG-US-18	unknown	unknown					
Donor M	DFG-US-19	unknown	unknown					
Donor M	DFG-US-20	unknown	unknown					
Donor M	DFG-US-21	unknown	unknown					
Donor M	DFG-US-22	unknown	unknown					
Donor M	DFG-US-23	unknown	unknown					
Donor M	DFG-US-24	unknown	unknown				49,37	
Donor M	DFG-US-25	unknown	unknown				50,78	
Donor M	DFG-US-26	unknown	unknown				44,92	
Donor M	DFG-US-28	unknown	unknown					
Donor M	DFG-US-31	unknown	unknown			56,00	36,23	4,69
Donor M	DFG-US-33	unknown	unknown			53,33	71,38	10,86
Donor M	DFG-US-34	unknown	unknown			53,67	38,18	0,63
Donor M	DFG-US-35	unknown	unknown			55,00	48,00	6,43
Donor M	DFG-US-36	unknown	unknown			52,00	38,33	0,33
Donor M	DFG-US-37	unknown	unknown			50,17	50,64	0,41
Donor M	DFG-US-38	unknown	unknown	7,19	0,018	54,17	30,96	3,66
Donor M	DFG-US-39	unknown	unknown			58,50	52,23	0,96
Donor M	DFG-US-40	unknown	unknown	8,95	0,062	48,67	28,25	9,94
Donor M	DFG-US-41	unknown	unknown			52,33	47,33	1,75
Donor M	DFG-US-42	unknown	unknown	8,04	0,028	51,00	31,96	0,64
Donor M	DFG-US-43	unknown	unknown	7,89	0,011	51,83	100,00	0,04
Donor M	DFG-US-45	unknown	unknown	7,42	0,009	54,67	52,89	0,20
Donor M	DFG-US-46	unknown	unknown			49,50	33,44	0,09
Donor M	DFG-US-47	unknown	unknown	9,63	0,009	50,00	100,00	0,58
Donor M	DFG-US-48	unknown	unknown	8,47	0,016	41,50	55,51	0,01
Donor M	DFG-US-50	unknown	unknown			45,67	52,14	0,04
Donor M	DFG-US-51	unknown	unknown	1,88	0,010	44,33	44,35	0,67
Donor M	DFG-US-52	unknown	unknown	0,54	0,010	38,00	42,59	0,37
Donor M	DFG-US-53	unknown	unknown	6,00	0,009	49,00	55,78	0,82
Donor M	DFG-US-54	unknown	unknown	0,12	0,015	57,67	43,51	4,80
Donor M	DFG-US-55	unknown	unknown			56,00	46,88	0,04
Donor M	DFG-US-56	unknown	unknown	0,59	0,028	41,67	36,30	0,37
Donor M	DFG-US-57	unknown	unknown	0,59	0,036	51,67	38,73	0,04
Donor M	DFG-US-58	unknown	unknown	0,74	0,010	54,67	43,29	0,79
Donor M	DFG-US-59	unknown	unknown					

Type	ID	Log (L1 mRNA)	DNMT1 mRNA	Log (DNMT1 mRNA)	DNMT3A mRNA	Log (DNMT3A mRNA)	SIRT6 meth. pyroseq.	MORC2 mRNA
Donor M	DFG-US-01		16,73	2,82				
Donor M	DFG-US-04		17,75	2,88	34,91	3,55		
Donor M	DFG-US-05		4,04	1,40	10,80	2,38		
Donor M	DFG-US-06		1,99	0,69	11,60	2,45		
Donor M	DFG-US-07		3,92	1,37	7,72	2,04		
Donor M	DFG-US-08		3,06	1,12	4,08	1,41		
Donor M	DFG-US-09		4,46	1,50	2,81	1,03		
Donor M	DFG-US-11		1,11	0,10	1,19	0,17		
Donor M	DFG-US-12		1,41	0,35	1,18	0,16		
Donor M	DFG-US-13		0,86	-0,15	3,07	1,12		
Donor M	DFG-US-14		6,00	1,79	4,83	1,58		
Donor M	DFG-US-15		2,79	1,03	4,37	1,47		
Donor M	DFG-US-16		3,24	1,17	8,77	2,17		
Donor M	DFG-US-17		36,40	3,59	3,46	1,24		
Donor M	DFG-US-18		1,27	0,24	0,83	-0,19		
Donor M	DFG-US-19		1,06	0,06	1,81	0,59		
Donor M	DFG-US-20		7,42	2,00	4,26	1,45		
Donor M	DFG-US-21		3,04	1,11	3,07	1,12		
Donor M	DFG-US-22		0,91	-0,09	2,02	0,71		
Donor M	DFG-US-23		4,93	1,60	9,53	2,25		
Donor M	DFG-US-24		2,26	0,82	2,02	0,71		
Donor M	DFG-US-25		1,54	0,43	0,83	-0,18		
Donor M	DFG-US-26		0,39	-0,95	0,41	-0,90		
Donor M	DFG-US-28		1,48	0,39	1,71	0,54		
Donor M	DFG-US-31	1,55	1,13	0,12	0,63	-0,46	1,00	9,37
Donor M	DFG-US-33	2,39	0,81	-0,21	0,47	-0,74	0,80	0,00
Donor M	DFG-US-34	-0,46	0,67	-0,40	0,60	-0,51	1,00	0,27
Donor M	DFG-US-35	1,86	1,48	0,39	1,09	0,09	0,80	2,36
Donor M	DFG-US-36	-1,10	0,75	-0,28	1,01	0,01	0,80	0,19
Donor M	DFG-US-37	-0,89	0,35	-1,04	1,09	0,09	-1,00	0,14
Donor M	DFG-US-38	1,30	1,82	0,60	1,25	0,22	1,00	0,40
Donor M	DFG-US-39	-0,04	0,91	-0,10	5,09	1,63	0,80	1,41
Donor M	DFG-US-40	2,30	0,99	-0,01	1,85	0,61	0,80	6,83
Donor M	DFG-US-41	0,56	0,89	-0,11	4,11	1,41	-1,00	0,16
Donor M	DFG-US-42	-0,45	0,61	-0,50	3,73	1,32	0,80	0,23
Donor M	DFG-US-43	-3,31	0,39	-0,95	0,25	-1,40	1,00	0,48
Donor M	DFG-US-45	-1,60	0,47	-0,75	1,33	0,29	1,00	0,00
Donor M	DFG-US-46	-2,46	2,22	0,80	13,66	2,61	0,80	0,00
Donor M	DFG-US-47	-0,55	0,54	-0,61	0,40	-0,93	1,00	0,00
Donor M	DFG-US-48	-4,51	0,34	-1,07	0,15	-1,87	1,00	
Donor M	DFG-US-50	-3,26	0,47	-0,75	0,36	-1,02	1,00	0,04
Donor M	DFG-US-51	-0,40	0,47	-0,75	0,24	-1,41	1,40	6,12
Donor M	DFG-US-52	-1,01	1,11	0,11	0,35	-1,04	1,20	3,30
Donor M	DFG-US-53	-0,19	2,54	0,93	1,03	0,03	1,00	25,50
Donor M	DFG-US-54	1,57	1,81	0,59	2,52	0,92	1,00	1,48
Donor M	DFG-US-55	-3,22	0,71	-0,34	0,19	-1,67	-1,00	0,31
Donor M	DFG-US-56	-1,01	3,38	1,22	11,53	2,45	1,40	11,02
Donor M	DFG-US-57	-3,21	0,40	-0,91	0,29	-1,24	0,80	0,11
Donor M	DFG-US-58	-0,23	0,30	-1,21	0,18	-1,72	1,20	0,42
Donor M	DFG-US-59		9,13	2,21	3,61	1,28	-1,00	3,80

Type	ID	Log (MORC2 mRNA)	KMT5A mRNA	Log (KMT5A mRNA)	KMT5B mRNA	Log (KMT5B mRNA)
Donor M	DFG-US-01					
Donor M	DFG-US-04					
Donor M	DFG-US-05					
Donor M	DFG-US-06					
Donor M	DFG-US-07					
Donor M	DFG-US-08					
Donor M	DFG-US-09					
Donor M	DFG-US-11					
Donor M	DFG-US-12					
Donor M	DFG-US-13					
Donor M	DFG-US-14					
Donor M	DFG-US-15					
Donor M	DFG-US-16					
Donor M	DFG-US-17					
Donor M	DFG-US-18					
Donor M	DFG-US-19					
Donor M	DFG-US-20					
Donor M	DFG-US-21					
Donor M	DFG-US-22					
Donor M	DFG-US-23					
Donor M	DFG-US-24					
Donor M	DFG-US-25					
Donor M	DFG-US-26					
Donor M	DFG-US-28					
Donor M	DFG-US-31	2,24	0,72	-0,14	1,16	0,15
Donor M	DFG-US-33		0,41	-0,38	0,42	-0,88
Donor M	DFG-US-34	-1,30	0,07	-1,14	0,12	-2,12
Donor M	DFG-US-35	0,86	1,62	0,21	1,03	0,03
Donor M	DFG-US-36	-1,64	0,03	-1,47	0,02	-3,72
Donor M	DFG-US-37	-1,98	0,24	-0,62	0,31	-1,16
Donor M	DFG-US-38	-0,92				
Donor M	DFG-US-39	0,34	1,00	0,00	0,87	-0,14
Donor M	DFG-US-40	1,92	15,73	1,20	21,11	3,05
Donor M	DFG-US-41	-1,86				
Donor M	DFG-US-42	-1,45	0,26	-0,59	0,24	-1,43
Donor M	DFG-US-43	-0,74				
Donor M	DFG-US-45		0,05	-1,30	0,03	-3,58
Donor M	DFG-US-46		0,02	-1,78	0,02	-4,05
Donor M	DFG-US-47		0,06	-1,23		
Donor M	DFG-US-48					
Donor M	DFG-US-50	-3,27				
Donor M	DFG-US-51	1,81	0,31	-0,51	0,29	-1,25
Donor M	DFG-US-52	1,19	0,17	-0,76	0,31	-1,16
Donor M	DFG-US-53	3,24	0,38	-0,42	0,62	-0,47
Donor M	DFG-US-54	0,39				
Donor M	DFG-US-55	-1,18	0,01	-1,97	0,02	-3,86
Donor M	DFG-US-56	2,40	0,11	-0,94	0,09	-2,39
Donor M	DFG-US-57	-2,17				
Donor M	DFG-US-58	-0,86				
Donor M	DFG-US-59	1,34	0,17	-0,76	0,22	-1,51

Type	ID	Fertiliza-tion rate	Outcome	5mC DNA meth.	m6A RNA meth.	L1 meth. pyroseq.	L1 meth. ELISA	L1 mRNA
Donor M	DFG-US-60	unknown	unknown	1,34	0,009	54,67	36,32	8,74
Donor M	DFG-US-61	unknown	unknown	1,94	0,009	28,67	41,28	6,79
Donor M	DFG-US-62	unknown	unknown	8,46	0,012	54,00	42,63	0,11
Donor M	DFG-US-63	unknown	unknown	8,10	0,010	50,00	44,46	13,49
Donor M	DFG-US-64	unknown	unknown	1,27	0,009	46,33	38,43	0,47
Donor M	DFG-US-65	unknown	unknown				41,67	3,12
Donor M	DFG-US-66	unknown	unknown			53,67	28,22	6,93
Donor M	DFG-US-68	unknown	unknown	1,25	0,011	57,33	41,39	1,51
Donor M	DFG-US-69	unknown	unknown			52,00	46,44	0,56
Donor M	DFG-US-70	unknown	unknown			-2,00	30,41	0,19
Donor M	DFG-US-75	unknown	unknown				39,58	0,01
Donor M	DFG-US-76	unknown	unknown				41,71	0,01
Donor M	DFG-US-78	unknown	unknown				47,06	0,13
Donor M	DFG-US-79	unknown	unknown				36,74	0,00
Donor M	DFG-US-80	unknown	unknown				54,47	0,21
Donor M	DFG-US-81	unknown	unknown				40,01	0,04
Donor M	DFG-US-82	unknown	unknown				78,05	0,00
Donor M	DFG-US-83	unknown	unknown				100,00	0,00
Donor M	DFG-US-84	unknown	unknown				95,36	0,04
Donor M	DFG-US-85	unknown	unknown				78,26	0,01
Donor M	DFG-US-86	unknown	unknown				93,07	0,00
Donor M	DFG-US-87	unknown	unknown				50,73	0,00
Donor M	DFG-US-88	unknown	unknown				100,00	0,04
Donor M	DFG-US-90	unknown	unknown				80,48	0,11
Donor M	DFG-US-91	unknown	unknown				84,65	0,00
Donor M	DFG-US-92	unknown	unknown				47,96	0,02
Donor M	DFG-US-93	unknown	unknown				76,10	0,09
Donor M	DFG-US-95	unknown	unknown				67,14	0,84
Donor M	DFG-US-96	unknown	unknown				60,69	0,01
Donor M	DFG-US-97	unknown	unknown				54,61	
Donor M	DFG-US-98	unknown	unknown				54,80	0,14
Donor M	DFG-US-100	unknown	unknown				83,83	0,03
Donor M	DFG-US-101	unknown	unknown				57,22	
Donor M	DFG-US-102	unknown	unknown				57,01	
Donor M	DFG-US-103	unknown	unknown				60,38	
Donor M	DFG-US-105	unknown	unknown				49,99	
Donor M	DFG-US-106	unknown	unknown				57,89	
Donor M	DFG-US-107	unknown	unknown				55,94	
Donor M	DFG-US-108	unknown	unknown				37,06	
Donor M	DFG-US-109	unknown	unknown				29,84	
Donor M	DFG-US-110	unknown	unknown				47,30	
Donor M	DFG-US-111	unknown	unknown				32,43	
Donor M	DFG-US-112	unknown	unknown				27,06	
Donor M	DFG-US-113	unknown	unknown				52,95	
Donor M	DFG-US-114	unknown	unknown				61,90	
Donor M	DFG-US-115	unknown	unknown				58,24	

Type	ID	Log (L1 mRNA)	DNMT1 mRNA	Log (DNMT1 mRNA)	DNMT3A mRNA	Log (DNMT3A mRNA)	SIRT6 meth. pyroseq.	MORC2 mRNA
Donor M	DFG-US-60	2,17	0,46	-0,78	0,23	-1,46	0,80	2,51
Donor M	DFG-US-61	1,91	1,07	0,07	0,71	-0,34	0,80	2,14
Donor M	DFG-US-62	-2,24	0,73	-0,32	0,52	-0,65	1,00	
Donor M	DFG-US-63	2,60	1,89	0,64	1,87	0,63	0,80	0,12
Donor M	DFG-US-64	-0,75	0,89	-0,12	0,28	-1,27	0,80	0,26
Donor M	DFG-US-65	1,14	2,20	0,79	3,88	1,36	1,40	1,11
Donor M	DFG-US-66	1,94	0,77	-0,26	0,28	-1,26	1,20	7,07
Donor M	DFG-US-68	0,41	0,52	-0,66	0,08	-2,52	1,30	0,84
Donor M	DFG-US-69	-0,58	1,96	0,68	2,60	0,95	0,80	
Donor M	DFG-US-70	-1,64	0,78	-0,25	0,44	-0,81	1,40	
Donor M	DFG-US-75	-4,28						
Donor M	DFG-US-76	-4,84						
Donor M	DFG-US-78	-2,02						
Donor M	DFG-US-79	-5,36						
Donor M	DFG-US-80	-1,56						
Donor M	DFG-US-81	-3,25						
Donor M	DFG-US-82	-6,82						
Donor M	DFG-US-83	-6,50						
Donor M	DFG-US-84	-3,28						
Donor M	DFG-US-85	-4,30						
Donor M	DFG-US-86	-8,38						
Donor M	DFG-US-87	-6,64						
Donor M	DFG-US-88	-3,20						
Donor M	DFG-US-90	-2,24						
Donor M	DFG-US-91	-6,01						
Donor M	DFG-US-92	-4,05						
Donor M	DFG-US-93	-2,44						
Donor M	DFG-US-95	-0,18						
Donor M	DFG-US-96	-4,38						
Donor M	DFG-US-97							
Donor M	DFG-US-98	-1,94						
Donor M	DFG-US-100	-3,46						
Donor M	DFG-US-101							
Donor M	DFG-US-102							
Donor M	DFG-US-103							
Donor M	DFG-US-105							
Donor M	DFG-US-106							
Donor M	DFG-US-107							
Donor M	DFG-US-108							
Donor M	DFG-US-109							
Donor M	DFG-US-110							
Donor M	DFG-US-111							
Donor M	DFG-US-112							
Donor M	DFG-US-113							
Donor M	DFG-US-114							
Donor M	DFG-US-115							

Type	ID	Log (MORC2 mRNA)	KMT5A mRNA	Log (KMT5A mRNA)	KMT5B mRNA	Log (KMT5B mRNA)
Donor M	DFG-US-60	0,92	1,49	0,17	1,07	0,07
Donor M	DFG-US-61	0,76				
Donor M	DFG-US-62					
Donor M	DFG-US-63	-2,16	2,58	0,41	1,12	0,11
Donor M	DFG-US-64	-1,34	0,16	-0,78	0,14	-1,99
Donor M	DFG-US-65	0,11				
Donor M	DFG-US-66	1,96				
Donor M	DFG-US-68	-0,18				

Table 17: Summary of the values of further DNMT1/3A mRNA analyzes to enlarge the cohort of donors` M.

Type	ID	DNMT1 mRNA	Log (DNMT1 mRNA)	DNMT3A mRNA	Log (DNMT3A mRNA)
Donor M	ZP5G-01	2,25	0,81	3,23	1,17
Donor M	ZP5G-02	1,91	0,65	2,73	1,00
Donor M	ZP5G-03	1,74	0,55	2,35	0,85
Donor M	ZP5G-04	1,92	0,65	1,59	0,46
Donor M	ZP5G-05	1,81	0,60	3,70	1,31
Donor M	ZP5G-07	2,00	0,69	1,83	0,61
Donor M	ZP5G-09	1,58	0,46	1,78	0,58
Donor M	ZP5G-10	1,38	0,32	3,23	1,17
Donor M	ZP5G-11	2,32	0,84	4,01	1,39
Donor M	ZP5G-13	2,41	0,88	2,63	0,97
Donor M	ZP5G-14	2,35	0,86	2,64	0,97
Donor M	ZP5G-15	2,19	0,78	3,23	1,17
Donor M	ZP5G-16	2,35	0,85	2,57	0,95
Donor M	ZP5G-18	1,96	0,67	2,29	0,83
Donor M	ZP5G-19	2,13	0,76	1,93	0,66
Donor M	ZP5G-20	1,36	0,31	2,63	0,97
Donor M	ZP5G-22	1,78	0,58	2,72	1,00
Donor M	ZP5G-23	1,34	0,29	2,37	0,86
Donor M	ZP5G-24	4,13	1,42	2,85	1,05
Donor M	ZP5G-25	1,03	0,03	1,79	0,58
Donor M	ZP5G-26	1,93	0,66	2,32	0,84
Donor M	ZP5G-27	0,29	-1,23	1,60	0,47
Donor M	ZP5G-28	0,44	-0,83	0,32	-1,14
Donor M	ZP5G-30	0,55	-0,59	1,49	0,40
Donor M	ZP5G-31	0,14	-2,00	0,81	-0,20
Donor M	ZP5G-32	0,13	-2,06	0,64	-0,44
Donor M	ZP5G-34	1,66	0,51	3,82	1,34
Donor M	ZP5G-35	0,09	-2,42	0,60	-0,51
Donor M	ZP5G-37	0,15	-1,87	2,04	0,71
Donor M	ZP5G-38	0,47	-0,76	1,01	0,01
Donor M	ZP5G-40	1,39	0,33	3,09	1,13
Donor M	ZP5G-41	0,43	-0,84	1,21	0,19
Donor M	ZP5G-42	0,16	-1,86	2,39	0,87
Donor M	ZP5G-43	0,62	-0,48	0,84	-0,17
Donor M	ZP5G-45	0,85	-0,16	1,46	0,38
Donor M	ZP5G-46	0,86	-0,15	3,50	1,25

Table 18: Summary of all values from methylation and mRNA analyzes in patients` M.

Type	ID	Fertiliza-tion rate	Outcome	5mC DNA meth.	m6A RNA meth.	L1 meth. pyroseq.	L1 meth. ELISA	L1 mRNA
Patient M	P01	0,60	negative			53,67	50,40	0,19
Patient M	P02	0,67	positive			55,00	26,53	0,22
Patient M	P03	0,60	negative	4,24	0,011	53,00	89,73	0,20
Patient M	P04	0,70	positive			44,00	54,34	1,22
Patient M	P05	0,69	negative	8,40	0,009	55,33	47,92	5,15
Patient M	P06	0,50	negative			36,50	89,60	0,51
Patient M	P07	0,78	positive			51,67	36,55	0,71
Patient M	P08	0,89	positive	2,37	0,012	47,00	53,79	1,24
Patient M	P09	1,00	negative	10,06	0,049	53,00	45,01	1,33
Patient M	P10	0,60	negative			39,83	35,99	0,82
Patient M	P11	0,50	negative			52,33	49,37	0,26
Patient M	P12	0,67	positive			52,33	44,33	1,47
Patient M	P13	0,76	negative	7,67	0,009	54,33	57,56	0,01
Patient M	P14	0,60	negative			51,33	40,11	
Patient M	P15	0,80	positive	8,34	0,046	52,33	51,59	0,20
Patient M	P16	0,67	positive			50,00	49,03	
Patient M	P17	0,50	negative			55,33	75,30	0,60
Patient M	P18	0,86	positive	5,48	0,033	52,67	49,43	1,79
Patient M	P19	0,80	positive	7,50	0,023	51,67	66,86	5,23
Patient M	P20	0,71	positive	5,90	0,010	55,83	56,76	1,29
Patient M	P21	0,58	positive	1,41	0,011	53,00	36,59	26,06
Patient M	P22	unknown	negative			41,00	36,95	
Patient M	P23	0,22	negative			47,67	33,66	
Patient M	P24	1,00	positive	0,71	0,010	50,67	62,22	0,00
Patient M	P25	1,00	negative	2,76	0,011	52,00	53,19	2,03
Patient M	P26	0,83	negative			52,67	38,96	18,38
Patient M	P27	0,75	negative	2,62	0,010	54,67	46,12	2,01
Patient M	P28	0,58	positive			50,00	39,08	
Patient M	P29	0,57	negative			55,33	43,19	
Patient M	P30	0,56	positive	0,55	0,009	49,00	48,48	0,63
Patient M	P31	unknown	negative			52,00	38,71	
Patient M	P32	0,38	negative			56,33	45,34	
Patient M	P33	0,83	positive	0,90	0,010	40,67	43,30	3,30
Patient M	P34	0,86	negative			56,67	37,34	8,42
Patient M	P35	0,56	positive	2,52	0,009	49,33	43,86	5,93
Patient M	P36	0,79	negative			42,83	41,66	
Patient M	P37	0,57	positive			54,00	45,44	0,26
Patient M	P38	0,69	positive			53,67	46,16	3,79
Patient M	P39	0,50	positive			55,00	39,30	
Patient M	P40	1,00	negative	1,57	0,010	53,67	49,19	9,18
Patient M	P41	0,67	negative			57,00	39,81	
Patient M	P42	0,55	negative			54,67	41,87	
Patient M	P43	0,80	negative	1,65	0,010	49,00	44,25	5,32
Patient M	P44	0,77	positive	2,13	0,009	50,67	41,57	3,75
Patient M	P45	unknown	positive				42,75	
Patient M	P46	0,64	negative			49,33	39,19	
Patient M	P47	0,79	negative			52,00	33,38	
Patient M	P48	0,53	negative	2,71	0,009	52,00	43,46	10,28

Type	ID	Log (L1 mRNA)	DNMT1 mRNA	Log (DNMT1 mRNA)	DNMT3A mRNA	Log (DNMT3A mRNA)	SIRT6 meth. pyroseq.	MORC2 mRNA
Patient M	P01	-1,67	0,21	-1,56	0,32	-1,15	1,80	0,42
Patient M	P02	-1,52	0,96	-0,04	0,51	-0,67	2,20	0,08
Patient M	P03	-1,63	1,21	0,19	0,14	-1,96	0,60	0,20
Patient M	P04	0,20	0,57	-0,56	0,93	-0,08	1,00	1,52
Patient M	P05	1,64	0,21	-1,56	0,37	-0,98	0,80	
Patient M	P06	-0,67	1,64	0,49	2,73	1,00	1,00	1,07
Patient M	P07	-0,34	1,89	0,64	0,84	-0,17	1,40	
Patient M	P08	0,21	0,20	-1,60	0,20	-1,63	1,20	0,18
Patient M	P09	0,29	0,31	-1,18	1,61	0,47	1,60	
Patient M	P10	-0,20	2,42	0,88	3,49	1,25	1,00	0,47
Patient M	P11	-1,33	0,66	-0,42	2,51	0,92	1,00	0,28
Patient M	P12	0,38	0,55	-0,59	0,85	-0,16	0,80	
Patient M	P13	-4,42	0,32	-1,13	0,11	-2,19	1,40	
Patient M	P14		0,02	-4,04	0,01	-4,67	1,00	0,07
Patient M	P15	-1,60	0,04	-3,13	0,12	-2,11	1,20	0,98
Patient M	P16		0,38	-0,97	0,50	-0,70	1,20	2,05
Patient M	P17	-0,51	0,07	-2,66	0,27	-1,31	0,80	0,22
Patient M	P18	0,58	0,05	-2,94	0,34	-1,09	0,80	
Patient M	P19	1,65	0,60	-0,52	1,00	0,00	1,00	0,44
Patient M	P20	0,25	0,65	-0,43	1,72	0,54	1,00	
Patient M	P21	3,26	0,93	-0,07	0,33	-1,12	0,80	
Patient M	P22		1,18	0,16	0,50	-0,68	1,40	1,90
Patient M	P23		1,04	0,04	0,48	-0,74	2,00	
Patient M	P24	-5,75	1,11	0,10	0,49	-0,72	1,60	7,85
Patient M	P25	0,71	0,88	-0,13	0,48	-0,74	1,00	
Patient M	P26	2,91	1,10	0,09	0,48	-0,74	1,00	
Patient M	P27	0,70	1,08	0,08	0,58	-0,55	2,20	
Patient M	P28		1,32	0,28	0,49	-0,72	1,00	
Patient M	P29		1,08	0,08	0,43	-0,84	0,80	
Patient M	P30	-0,46	0,73	-0,32	0,44	-0,82	1,60	
Patient M	P31		0,89	-0,12	0,48	-0,74	0,80	1,66
Patient M	P32		0,99	-0,01	0,38	-0,96	0,80	
Patient M	P33	1,19	0,91	-0,09	0,44	-0,82	2,20	
Patient M	P34	2,13	1,02	0,02	0,40	-0,91	1,00	
Patient M	P35	1,78	0,76	-0,27	0,41	-0,89	3,20	
Patient M	P36		0,99	-0,01	0,43	-0,84	0,80	
Patient M	P37	-1,33	0,96	-0,04	0,44	-0,82	1,40	0,02
Patient M	P38	1,33	1,04	0,03	0,48	-0,74	3,80	
Patient M	P39		0,95	-0,05	0,43	-0,84	1,30	2,73
Patient M	P40	2,22	0,77	-0,26	0,43	-0,84	1,00	
Patient M	P41		0,92	-0,08	0,49	-0,72	0,80	
Patient M	P42		0,73	-0,32	0,39	-0,94	1,00	
Patient M	P43	1,67	1,05	0,05	0,55	-0,60	1,20	1,99
Patient M	P44	1,32	1,00	0,00	0,41	-0,89	1,60	
Patient M	P45		0,89	-0,12	0,43	-0,84	1,20	
Patient M	P46		0,92	-0,08	0,37	-0,98		1,02
Patient M	P47		1,18	0,16	0,37	-0,98	1,40	
Patient M	P48	2,33	1,07	0,07	0,45	-0,80	3,20	

Type	ID	Log (MORC2 mRNA)	KMT5A mRNA	Log (KMT5A mRNA)	KMT5B mRNA	Log (KMT5B mRNA)
Patient M	P01	-0,87	0,06	-1,20	0,08	-2,57
Patient M	P02	-2,48				
Patient M	P03	-1,63	0,02	-1,81	0,05	-3,08
Patient M	P04	0,42				
Patient M	P05		1,00	0,00	3,31	1,20
Patient M	P06	0,06				
Patient M	P07		0,06	-1,24	0,18	-1,72
Patient M	P08	-1,71				
Patient M	P09		1,11	0,05	1,00	0,00
Patient M	P10	-0,76	0,31	-0,51	0,10	-2,33
Patient M	P11	-1,27	0,03	-1,57	0,01	-4,30
Patient M	P12		0,34	-0,47	0,36	-1,02
Patient M	P13					
Patient M	P14	-2,60	0,00	-2,37	0,00	-6,15
Patient M	P15	-0,02	0,09	-1,04	0,25	-1,40
Patient M	P16	0,72	0,75	-0,12	1,27	0,24
Patient M	P17	-1,52	0,21	-0,69	0,11	-2,19
Patient M	P18		1,59	0,20	3,38	1,22
Patient M	P19	-0,82	2,87	0,46	3,94	1,37
Patient M	P20					
Patient M	P21					
Patient M	P22	0,64	1,03	0,01	2,57	0,94
Patient M	P23		0,49	-0,31	0,38	-0,96
Patient M	P24	2,06	0,22	-0,67	0,15	-1,91
Patient M	P25		17,45	1,24	18,13	2,90
Patient M	P26		3,29	0,52	2,53	0,93
Patient M	P27		3,06	0,49	2,20	0,79
Patient M	P28		4,94	0,69	6,70	1,90
Patient M	P29		5,39	0,73	3,39	1,22
Patient M	P30		0,38	-0,42	0,26	-1,37
Patient M	P31	0,50				
Patient M	P32					
Patient M	P33					
Patient M	P34		1,69	0,23	1,44	0,36
Patient M	P35		5,62	0,75	4,21	1,44
Patient M	P36					
Patient M	P37	-3,93	5,08	0,71	3,11	1,13
Patient M	P38		8,46	0,93	3,48	1,25
Patient M	P39	1,00				
Patient M	P40		5,84	0,77	4,47	1,50
Patient M	P41					
Patient M	P42					
Patient M	P43	0,69	1,69	0,23	1,59	0,46
Patient M	P44		3,67	0,56	2,64	0,97
Patient M	P45					
Patient M	P46	0,02				
Patient M	P47					
Patient M	P48		1,24	0,09	0,80	-0,23

Table 19: Summary of all values from methylation and mRNA analyzes in donors` IM.

Type	ID	Fertiliza-tion rate	Outcome	L1 meth. pyroseq.	L1 meth. ELISA	L1 mRNA	Log (L1 mRNA)	SIRT6 meth. pyroseq.
Donor IM	DFG-US-30	unknown	unknown	51,67	53,47	2,79	1,03	1,00
Donor IM	DFG-US-31	unknown	unknown	52,00	40,63	2,88	1,06	1,20
Donor IM	DFG-US-32	unknown	unknown	51,00	48,78	4,78	1,57	0,80
Donor IM	DFG-US-33	unknown	unknown	51,33	54,25	15,67	2,75	0,80
Donor IM	DFG-US-34	unknown	unknown	51,67	44,17	23,37	3,15	
Donor IM	DFG-US-35	unknown	unknown	54,33	66,13	0,95	-0,05	0,80
Donor IM	DFG-US-36	unknown	unknown	50,33	50,23	0,02	-3,98	1,00
Donor IM	DFG-US-37	unknown	unknown	47,00	71,98	0,01	-5,12	
Donor IM	DFG-US-38	unknown	unknown	51,00	61,04	0,92	-0,08	0,80
Donor IM	DFG-US-39	unknown	unknown	56,33	56,74	2,19	0,79	0,80
Donor IM	DFG-US-40	unknown	unknown	46,67	50,41	0,01	-4,77	1,20
Donor IM	DFG-US-41	unknown	unknown	52,00	60,41	1,12	0,11	1,20
Donor IM	DFG-US-42	unknown	unknown	49,33	50,83	23,48	3,16	1,00
Donor IM	DFG-US-43	unknown	unknown	73,33	58,91	69,12	4,24	0,80
Donor IM	DFG-US-44	unknown	unknown	53,33	47,89	21,93	3,09	
Donor IM	DFG-US-45	unknown	unknown	49,67	100,00	96,44	4,57	1,00
Donor IM	DFG-US-46	unknown	unknown	51,00	63,29	168,04	5,12	1,00
Donor IM	DFG-US-47	unknown	unknown	51,67	82,23			0,60
Donor IM	DFG-US-48	unknown	unknown	41,67	65,55	100,47	4,61	0,80
Donor IM	DFG-US-49	unknown	unknown	60,00	46,00	17,83	2,88	0,80
Donor IM	DFG-US-50	unknown	unknown	44,00	47,60			1,20
Donor IM	DFG-US-51	unknown	unknown	42,00	65,62			0,80
Donor IM	DFG-US-52	unknown	unknown	39,00	65,03	18,56	2,92	1,20
Donor IM	DFG-US-53	unknown	unknown	47,00	45,08			1,80
Donor IM	DFG-US-54	unknown	unknown	54,33	47,49	117,29	4,76	1,00
Donor IM	DFG-US-55	unknown	unknown	53,33	66,74	10,90	2,39	1,00
Donor IM	DFG-US-56	unknown	unknown	41,67	57,94	15,38	2,73	0,80
Donor IM	DFG-US-57	unknown	unknown	50,67	57,01	19,39	2,96	0,80
Donor IM	DFG-US-58	unknown	unknown	54,33	58,30			
Donor IM	DFG-US-60	unknown	unknown	53,67	64,95			0,80
Donor IM	DFG-US-61	unknown	unknown	27,33	60,51	26,60	3,28	0,80
Donor IM	DFG-US-62	unknown	unknown	51,67	49,56			1,20
Donor IM	DFG-US-63	unknown	unknown	49,67	55,82			0,80
Donor IM	DFG-US-64	unknown	unknown	42,00	50,86			1,00
Donor IM	DFG-US-65	unknown	unknown	53,33	55,99			1,20
Donor IM	DFG-US-66	unknown	unknown	53,67	50,83	5,65	1,73	0,80
Donor IM	DFG-US-68	unknown	unknown	57,33	41,86			1,10
Donor IM	DFG-US-69	unknown	unknown	52,00	55,86	1,00	0,00	1,40
Donor IM	DFG-US-70	unknown	unknown		59,16			0,80

Type	ID	MORC2 mRNA	Log (MORC2 mRNA)	KMT5A mRNA	Log (KMT5A mRNA)	KMT5B mRNA	Log (KMT5B mRNA)
Donor IM	DFG-US-30	3,23	1,17	2,23	0,35	2,60	0,96
Donor IM	DFG-US-31	0,48	-0,74	5,10	0,71	5,54	1,71
Donor IM	DFG-US-32			4,98	0,70	5,98	1,79
Donor IM	DFG-US-33			0,02	-1,67	0,01	-4,24
Donor IM	DFG-US-34			1,03	0,01	0,98	-0,02
Donor IM	DFG-US-35						
Donor IM	DFG-US-36			4,50	0,65	2,11	0,75
Donor IM	DFG-US-37	1,67	0,51	0,32	-0,49	0,26	-1,36
Donor IM	DFG-US-38			0,69	-0,16	0,33	-1,10
Donor IM	DFG-US-39			4,99	0,70	4,04	1,40
Donor IM	DFG-US-40	1,03	0,03	1,61	0,21	1,12	0,11
Donor IM	DFG-US-41						
Donor IM	DFG-US-42						
Donor IM	DFG-US-43			51,09	1,71		
Donor IM	DFG-US-44					160,90	5,08
Donor IM	DFG-US-45			97,34	1,99	285,04	5,65
Donor IM	DFG-US-46			60,76	1,78	159,79	5,07
Donor IM	DFG-US-47						
Donor IM	DFG-US-48						
Donor IM	DFG-US-49						
Donor IM	DFG-US-50						
Donor IM	DFG-US-51						
Donor IM	DFG-US-52			27,00	1,43	186,11	5,23
Donor IM	DFG-US-53						
Donor IM	DFG-US-54						
Donor IM	DFG-US-55						
Donor IM	DFG-US-56						
Donor IM	DFG-US-57						
Donor IM	DFG-US-58						
Donor IM	DFG-US-60						
Donor IM	DFG-US-61						
Donor IM	DFG-US-62						
Donor IM	DFG-US-63						
Donor IM	DFG-US-64						
Donor IM	DFG-US-65						
Donor IM	DFG-US-66						
Donor IM	DFG-US-68						
Donor IM	DFG-US-69						
Donor IM	DFG-US-70						

Type	ID	Fertiliza-tion rate	Outcome	L1 meth. ELISA	L1 mRNA	Log (L1 mRNA)
Donor IM	DFG-US-73	unknown	unknown	90,42	0,04	-3,14
Donor IM	DFG-US-74	unknown	unknown	60,66	12,68	2,54
Donor IM	DFG-US-75	unknown	unknown	86,16	2,53	0,93
Donor IM	DFG-US-76	unknown	unknown	59,92	44,63	3,80
Donor IM	DFG-US-78	unknown	unknown	58,82	32,34	3,48
Donor IM	DFG-US-79	unknown	unknown	74,59	2,09	0,74
Donor IM	DFG-US-80	unknown	unknown	76,83	4,41	1,48
Donor IM	DFG-US-81	unknown	unknown	80,76	0,22	-1,50
Donor IM	DFG-US-82	unknown	unknown	46,77	7,34	1,99
Donor IM	DFG-US-83	unknown	unknown	58,10	146,53	4,99
Donor IM	DFG-US-84	unknown	unknown	48,83	1,43	0,36
Donor IM	DFG-US-85	unknown	unknown	56,64	8,52	2,14
Donor IM	DFG-US-86	unknown	unknown	50,15	1,99	0,69
Donor IM	DFG-US-87	unknown	unknown	48,47	12,55	2,53
Donor IM	DFG-US-88	unknown	unknown	62,66	24,08	3,18
Donor IM	DFG-US-90	unknown	unknown	63,05	0,15	-1,88
Donor IM	DFG-US-91	unknown	unknown	69,12	1,87	0,62
Donor IM	DFG-US-92	unknown	unknown	50,35	0,12	-2,11
Donor IM	DFG-US-93	unknown	unknown	63,75		
Donor IM	DFG-US-94	unknown	unknown	45,10		
Donor IM	DFG-US-95	unknown	unknown	49,47	1,01	0,01
Donor IM	DFG-US-96	unknown	unknown	47,30	0,39	-0,95
Donor IM	DFG-US-97	unknown	unknown	51,87	0,11	-2,23
Donor IM	DFG-US-98	unknown	unknown	100,00	0,97	-0,03
Donor IM	DFG-US-100	unknown	unknown	65,37	2,50	0,91
Donor IM	DFG-US-101	unknown	unknown	47,69		
Donor IM	DFG-US-102	unknown	unknown	52,97		
Donor IM	DFG-US-103	unknown	unknown	54,00		
Donor IM	DFG-US-104	unknown	unknown	33,73		
Donor IM	DFG-US-105	unknown	unknown	-1,00		
Donor IM	DFG-US-106	unknown	unknown	85,81		
Donor IM	DFG-US-107	unknown	unknown	36,71		
Donor IM	DFG-US-108	unknown	unknown	37,15		
Donor IM	DFG-US-109	unknown	unknown	46,77		
Donor IM	DFG-US-110	unknown	unknown	43,09		
Donor IM	DFG-US-111	unknown	unknown	70,37		
Donor IM	DFG-US-112	unknown	unknown	62,70		
Donor IM	DFG-US-113	unknown	unknown	72,38		
Donor IM	DFG-US-114	unknown	unknown	45,14		
Donor IM	DFG-US-115	unknown	unknown	46,83		

Table 20: Clinical data of patients` M.

Type	ID	Age man	Sperm concentration (Mio/ml)	Total sperm concentration (Mio)	Progressive motility (%)	Total motility (%)	Morphology (%)
Patient M	P01	42	13	20,8	28	48	0
Patient M	P02	47	4	14,8	18	39	0
Patient M	P03	39	11	64,9	29	55	0
Patient M	P04	37	18,4	31,28	23	50	0
Patient M	P05	50	36	136,8	28	46	0
Patient M	P06	41	3,2	18,24	41	59	0
Patient M	P07	32	2,4	9,12	12	32	0
Patient M	P08	29	46,6	219,02	40	71	4
Patient M	P09	33	48	110,4	43	67	4
Patient M	P10	43	3,2	10,24	14	25	0
Patient M	P11	38	10,2	55,08	13	30	0
Patient M	P12	43	6,5	22,75	54	66	0
Patient M	P13	38	2,5	5,75	31	52	0
Patient M	P14	38	8	5,12	16	52	0
Patient M	P15	45	219	394,2	60	82	5
Patient M	P16	37	126	491,4	60	82	6
Patient M	P17	47	4,3	22,36	40	61	0
Patient M	P18	32	33	135,3	26	53	0
Patient M	P19	47	57	68,4	26	46	0
Patient M	P20	37	10,8	30,24	24	35	1
Patient M	P21	45	17,7	157,53	53	76	0
Patient M	P22	31	4,8	15,84	26	51	0
Patient M	P23	39	1,2	6,84	9	30	0
Patient M	P24	30	84	310,8	41	63	1
Patient M	P25	38	31	213,9	55	82	0
Patient M	P26	37	34	268,6	30	60	0
Patient M	P27	35	23	85,1	59	81	0
Patient M	P28	46	25	87,5	51	75	0
Patient M	P29		11,6	85,84	43	58	0
Patient M	P30	36	78	163,8	31	61	2
Patient M	P31	40	58	63,8	59	77	0
Patient M	P32	44	155	294,5	36	70	0
Patient M	P33	40	10,1	36,36	34	56	0
Patient M	P34	43	11	71,5	43	66	0
Patient M	P35	43	45	585	60	83	0
Patient M	P36	45	68,4	177,84	34	64	0
Patient M	P37	40	63,9	166,14	54	80	0
Patient M	P38	39	14	51,8	60	79	0
Patient M	P39	38	81	186,3	41	72	0
Patient M	P40	33	21	52,5	31	61	2
Patient M	P41	40	17,7	72,57	38	53	0
Patient M	P42	35	15	130,5	62	83	0
Patient M	P43	38	19	72,2	42	74	0
Patient M	P44	33	11,6	27,84	46	62	0
Patient M	P45	42	3,4	8,16	26	51	0
Patient M	P46	31	44	233,2	47	72	0
Patient M	P47	43	49	176,4	45	70	0
Patient M	P48	37	16	75,2	39	59	0

Table 21: Clinical data of female partners from patients` M. Nd = not detectable.

ID	Age woman	BMI	FSH	MTHFR677 polymorphism	Anti-Müllerian hormone	Vitamin D	Vitamin B12	Folate	Estradiol	Fertilization rate
P01	31	22	175	normal	2.9	29.9	939	19	2899	60
P02	36	22	187	normo	1,2	32	319		1734	67
P03	36	24	137	normo	nd	nd	nd	nd	5085	60
P04	33		100		nd	nd	nd	nd	1368	70
P05	40	22	225	hetero	1.5	29	1026	20	5154	69
P06	28	22	187	normo	3.0	26.6	491	0.8	4745	50
P07	31	20	175	hetero	2.3	34,8	460	19,5	2675	78
P08	31	22	150	normo	1.2	nd	656	20	3562	89
P09	30	22	18	normo	1.5	33	491	20	2235	100
P10	45	21	225	hetero	0,9	32	983	20	1276	60
P11	35	23	200	hetero	nd	nd	nd	nd	3240	50
P12	40	25	225	normo	0.2	32	500	20	1823	67
P13	38	23	183	normo	nd	nd	nd	nd	2889	76
P14	35	24		hetero	5,4	17,5	593	4,7	3203	60
P15	28	20	132	hetero	7.3	34.2	872	20	2090	80
P16	38	22	150		2.5	36.8	489	17.8	2893	67
P17	41	23	225	hetero	0,7	21.2	800	20	2152	50
P18	30	22	175	hetero	2,6	19.9	679	20	2902	86
P19	33	21	225	hetero	0.5	nd	794	15.4	2142	80
P20	36	23	75	normo	2.1	nd	583	13	3006	71
P21	43	21	150	normo	3.2	42	583	17.9	6387	58
P22	31	22	125	hetero	3.4	23.9	600	20	220.8	
P23	36	25	200	normo					1875	22
P24	33	26	225	normo	0.5	nd	252	11	1434	100
P25	34	35	225		0,5	nd	nd	nd	1772	100
P26	35	23	225	hetero	nd	29	1112	16	1566	83
P27	37	22	225	normo	0.9	21	451	20	5850	75
P28	34		150	hetero	4.7	49.6	426	11.1	3241	58
P29	33	26	132	homo	7.4	23.5	410	13.0	1757	57
P30	33	22	175	hetero	2.0	nd	1376	20	2710	56
P31	38	24	100	normo	0,7	36,3	753	20		
P32	37	22	225	hetero	1.3	19.7	476	8.4	4101	38
P33	39	22	225	normo		21	416	7.9	1572	
P34	37	24	200	hetero	0,5	19	523		1060	38
P35	40	20	225	hetero	0.6	24.4	377	20	1433	56
P36	43	24	175	normo	3.0	22.7	407	20	3345	79
P37	37	22	225	hetero	0,6	nd	nd	nd	2394	57
P38	37	21	225	hetero	1.7	60	397	20	4884	69
P39	35	23	132	normo	3,8	25.2	786	20	1380	50
P40	37	22		hetero	3.7	28	479	16.2	1629	100
P41	33	22	225	hetero	nd	nd	nd	nd	5198	67
P42	37	26,6	150	normo	4.0	21,2	485	16,8	2244	55
P43	35	21	150	normo	0.7	13	413	19	3609	80
P44	32	21	150	homo	2.8	nd	271		1602	77
P45	36	20	225	hetero	1,0	26,4	426	16,4		0
P46	28	24	50	normo	nd	nd	nd	nd	3970	64
P47	44	24	200	hetero	0,8	17,2	615	20	3895	79
P48	27	20	125	hetero	3.1	34	403	17	1506	53

10. List of abbreviations

APS	Ammonium persulfate
ART	Assisted reproductive technologies
bp	Base pair
BSA	Bovine serum albumin
ChIP	Chromatin immunoprecipitation
kDa	Kilo dalton
ddH_2O	Destilled water
DEPC	Diethypyrocarbonate
DNA	Desoxyribonucleic acid
DNase I	Desoxyribonuclease I
DNMT	DNA methyltransferase
dNTP	2'-deoxynucleoside-5'-triphosphate
DTT	Dithiolthreitol
EDTA	Ethylenediaminetetraacetic acid
EtOH	Ethanol
FWD	Forward primer
GAPDH	Glyceraldehyde 3-phosphate dehydrogenase
h	Hour
HeLa	Human cervix carcinoma cell line (from **He**nrietta **La**cks)
hESC	Human embryonic stem cells
H_2O_2	Hydrogen peroxide
HCl	Hydrochloric acid
HDF	Human dermal fibroblasts
HSA	Human serum albumin
HTF	Human tubal fluid
ICC	Immunocytochemistry
ICSI	Intracytoplasmic sperm injection
IHC	Immunohistochemistry
Immot. / IM	Immotile (sperm cells)
IVF	In vitro fertilization

L1/L1	Long interspersed nuclear element 1
M	Molar (mol/L)
MeOH	Methanol
mg	Milligram
min	Minute
mio	Million
L	Milliliter
LIS	Lithium 3,5-diiodosalicylate
mot. / M	Motile (sperm cells)
NaAc	Sodium acetate
NaCl	Sodium chloride
NaOH	Sodium hydroxide
nm	Nanometer
NP-40	Nonyl phenoxypolyethoxylethanol
n.s.	Not significant
PBS	Phosphate buffered saline
PFA	Paraformaldehyde
PMSF	Phenylmethylsulfonyl fluoride
PVDF	Polyvinylidene difluoride
REV	Reverse primer
RNA	Ribonucleic acid
RNAse I	Ribonuclease I
RT	Room temperature
RT-qPCR	Real time-quantitative polymerase chain reaction
s	Second
SINE	Short interspersed nuclear element
SDS-PAGE	Sodium dodecyl sulfate polyacrylamide gel electrophoresis
TEMED	Tetramethylethylenediamine
V	Volt
WB	Western blot
WHO	World Health Organization (guidelines)
x	Time(s)

11. Acknowledgements

First of all, I would like to thank my supervisor Prof. Dr. rer. nat. Undraga Schagdarsurengin for the opportunity to write a doctoral thesis on such an interesting topic in her working group. Thank you very much for your constant help and support during the preparation of my doctoral thesis. It was very nice that you allowed me to take part in conferences, courses and career trainings in addition to my doctoral thesis. Without your guidance I would not have been able to develop personally and professionally as I am now.

I would also like to deeply thank my co-supervisor Prof. Dr. med. vet. Christine Wrenzycki for the opportunity to do a laboratory internship in her working group. I really enjoyed my time there and got to know new methods, like the IVF in bovines. I also thank PD Dr. med. Nina Rogenhofer for kindly providing the patient samples and Prof. Dr. rer. nat. Klaus Steger for his help during IHC analysis. Thanks also a lot to Prof. Dr. med. Hans-Christian Schuppe and all the technicians from our department, foremost Tania and Kerstin, for collecting and andrological analysis of the semen samples from healthy donors.

Furthermore, I would like to extremely thank the whole working group for the gorgeous working atmosphere and the students, Sina, Tamara and Frauke for their great support in the project. I have always felt very comfortable and especially the lunch breaks would not have been nearly so beautiful without you, Conni, Tatjana, Magnus, Laura, Deborah and Barbara. My special thanks go to Dr. rer. nat. Nihan Ozturk, who has been working in the same project and gave me very good instructions and valuable tips all the time.

Last but not least, I would like to thank the DFG for funding the project I have been participating in and the Giessen Graduate School for Life Sciences and the PhD programs of the JLU for offering interesting seminars, workshops and conferences.

Finally, I would like to thank my family and boyfriend for having always supported and encouraged me during my thesis. Vielen lieben Dank Mama, Papa und Alexandra für eure Unterstützung und Ermutigung während meines gesamten Studiums und insbesondere der Zeit als Doktorandin! Marc, dir möchte ich nochmal ganz besonders für dein Verständnis, deine Hilfe und Liebe danken.

12. List of own publications

12.1 Publications & Articles

- U. Schagdarsurengin, L. M. Teuchert, C. Hagenkötter, N. Nesheim, T. Dansranjavin, H.-C. Schuppe, S. Gies, A. Pilatz, W. Weidner, F. M. E. Wagenlehner. Chronic Prostatitis Affects Male Reproductive Health and Is Associated with Systemic and Local Epigenetic Inactivation of C-X-C Motif Chemokine 12 Receptor C-X-C Chemokine Receptor Type 4. *Urol Int*, *98*, 89-101, **2017**.

- S. Gies, N. Öztürk, K. Ni, N. Rogenhofer, K. Steger, C. Wrenzycki, U. Schagdarsurengin, Idiopathic male infertility: The role of sperm epigenetics and nucleosome preservation, *Reproduction in Domestic Animals, Vol. 52, Suppl. 1*, 1-64, **2017**.

- S. Gies, N. Öztürk, S. W. Kürschner, K. Steger, H.-C. Schuppe, K. Ni, N. Rogenhofer, U. Schagdarsurengin, Association between sperm epigenetics and male subfertility: retrotransposon suppression and nucleosome preservation pattern, *Reproduction in Domestic Animals, Vol. 53, Suppl. 1*, 1-48, **2018**.

12.2 Conference abstracts, presentations and prices

- International Giessen Graduate Centre for the Life Sciences (GGL) annual congress (Sep. 2016, Giessen). Nucleosome preservation in human sperm: an epigenetic program to ensure the healthy reproduction of men. [Poster]

- 50th Annual Conference of Physiology and Pathology of Reproduction and 42nd Mutual Conference on Veterinary and Human Reproductive Medicine (Feb. 2017, München). Idiopathic male infertility: The role of sperm epigenetics and nucleosome preservation. [Presentation]

- International GGL annual congress (Sep. 2017, Giessen). Epigenetic reasons for male factor infertility: the role of nucleosome preservation in sperm chromatin and DNA methylation. [Poster]

- 1. Science Day (Nov. 2017, Giessen). Epigenetic reasons for male factor infertility: the role of nucleosome preservation in sperm chromatin and DNA methylation. [Poster]
- 9. Symposium Urologische Forschung der Deutschen Gesellschaft für Urologie (Nov. 2017, Freiburg). Male subfertility: the role of nucleosome preservation and retrotransposon suppression in sperm epigenetics. [Presentation]
- 10th Meeting of the EAU Section of Andrological Urology (ESAU17, Nov. 2017, Malmö, Sweden). Male subfertility: the role of DNA methylation and nucleosome preservation in sperm epigenetics. [**Poster, 1st poster price**]
- 7. DVR-Kongress (Dez. 2017, München). Idiopathic male infertility: L1 suppression and nucleosome preservation patterns in human sperm. [Poster]
- 51th Annual Conference of Physiology and Pathology of Reproduction and 43nd Mutual Conference on Veterinary and Human Reproductive Medicine (Feb. 2018, Hannover). Association between sperm epigenetics and male subfertility: Retrotransposon suppression and nucleosome preservation patterns. [Presentation, **3rd abstract price**]
- International Giessen Graduate Centre for the Life Sciences (GGL) annual congress (Sep. 2018, Giessen). Sperm epigenetics: L1 elements and preserved nucleosomes in male subfertility. [Poster]
- 2. Science Day (Nov. 2017, Giessen). Sperm epigenetics: L1 elements and preserved nucleosomes in male subfertility. [Poster]
- 30. Jahrestagung der Deutschen Gesellschaft für Urologie e.V. (Dez. 2018, Giessen). Untersuchungen zu L1 Retrotransposons in Spermien von fertilen und subfertilen Männern. [Presentation]

13. Declaration of honour

I declare that I have completed this dissertation single-handedly without the unauthorized help of a second party and only with the assistance acknowledged therein. I have appropriately acknowledged and referenced all text passages that are derived literally from or are based on the content of published or unpublished work of others, and all information that relates to verbal communications. I have abided by the principles of good scientific conduct laid down in the charter of the Justus Liebig University of Giessen in carrying out the investigations described in the dissertation.

Ich erkläre: Ich habe die vorgelegte Dissertation selbständig, ohne unerlaubte fremde Hilfe und nur mit den Hilfen angefertigt, die ich in der Dissertation angegeben habe. Alle Textstellen, die wörtlich oder sinngemäß aus veröffentlichten oder nicht veröffentlichten Schriften entnommen sind, und alle Angaben, die auf mündlichen Auskünften beruhen, sind als solche kenntlich gemacht. Bei den von mir durchgeführten und in der Dissertation erwähnten Untersuchungen habe ich die Grundsätze guter wissenschaftlicher Praxis, wie sie in der „Satzung der Justus-Liebig-Universität Gießen zur Sicherung guter wissenschaftlicher Praxis“ niedergelegt sind, eingehalten.

Giessen, May 2019

X

Sabrina Gies